# Spectroscopic and Theoretical Investigations of Vibrational Frequencies in Binary Unsaturated Transition−Metal Carbonyl Cations, Neutrals, and Anions

**ARTICLE** *in* CHEMICAL REVIEWS · JULY 2001

Impact Factor: 46.57 · DOI: 10.1021/cr990102b · Source: PubMed

# Spectroscopic and Theoretical Investigations of Vibrational Frequencies in Binary Unsaturated Transition-Metal Carbonyl Cations, Neutrals, and Anions

Mingfei Zhou

*Department of Chemistry, Laser Chemistry Institute, Fudan University, Shanghai 200433, P. R. China*

Lester Andrews*

*Department of Chemistry, University of Virginia, Charlottesville, Virginia 22904-4319*

Charles W. Bauschlicher, Jr.

*Mail Stop 230-3, NASA Ames Research Center, Moffett Field, California 94035*

*Received August 18, 2000*

## *Contents*



## *I. Introduction*

Transition-metal carbonyl complexes, $M(CO)_x$, are cornerstones of modern coordination chemistry and organometallic chemistry.[1] Coordinatively unsaturated transition-metal carbonyls are building blocks of stable organometallic complexes and can be exceedingly reactive and engage in a wide variety of chemical processes. Carbon monoxide activation and reduction by transition-metal atoms are important in a great many industrial processes such as hydroformylation, alcohol synthesis, and acid synthesis.[2,3] Furthermore, metal carbonyls are often considered as models for CO binding to the metal surface,[4] and they play important roles in catalysis and synthesis[5,6] and as a ligand in the formation of long-lived complexes in the gas phase.[7] Since the first report[8] of nickel tetracarbonyl $Ni(CO)_4$ in 1890, the synthesis, detection, structural characterization, and reactivities of these species have been the subject of intensive studies and are still important components of modern transition-metal chemistry.

The matrix-isolation technique has provided valuable spectroscopic information on coordinatively unsaturated metal carbonyls; much of what is known about the structure of these species comes from matrix-isolation studies of their infrared spectra. Despite the development of supersonic jet high-resolution spectroscopy, matrix isolation remains a powerful technique for spectroscopic study of unsaturated transition-metal carbonyls. Matrix isolation spectroscopic study has a number of advantages for

10.1021/cr990102b CCC: $36.00 
Published on Web 06/13/2001

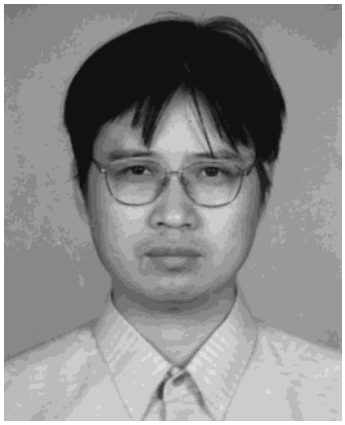

Mingfei Zhou was born in Zhejiang province, P. R. China, in 1968. He was educated at Fudan University, where he received his Ph.D. degree in Chemistry in 1995 in the group of Qizong Qin. He worked from 1997 to 1999 in the group of Lester Andrews at the University of Virginia as a postdoctoral fellow. Since 1999 he has been a faculty member at Fudan University. He is the author of over 50 publications on molecular spectroscopy.

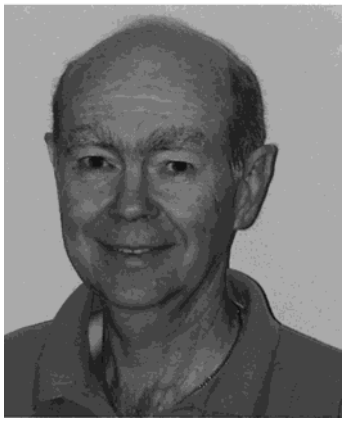

Lester Andrews was born in Lincolnton, NC, on Jan. 31, 1942. He earned his B.S. degree in Chemical Engineering from Mississippi State University in 1963 and his Ph.D. degree in Physical Chemistry from the University of California, Berkeley, in 1966. Dr. Andrews joined the faculty of the University of Virginia in 1966, where he has been active in matrix-isolation spectroscopy, publishing over 500 research papers on novel chemical species.

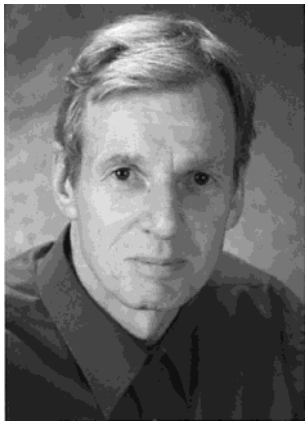

Charles W. Bauschlicher, Jr. is a Senior Computational Chemist at the NASA Ames Research Center. He received his B.S. degree in 1972 from SUNY at Stony Brook and his Ph.D degree in 1976 from UC Berkeley. After postdoctoral research at Battelle, he joined NASA in 1977 and became a permanent staff member in 1982. His research interests include transition-metal-containing species, astrochemistry, thermochemistry, and nanotechnology.

investigating unsaturated transition-metal carbonyls, especially for carbonyl ions. As the unsaturated transition-metal carbonyl species are extremely reactive and photolabile, fast and sensitive spectroscopic probes are required in the gas phase. In matrix isolation, the carbonyl species can be produced and accumulated over a long period of time, so detection sensitivity can be enhanced and a broad spectral range can be easily explored in a short time. Of more importance, the absorptions of matrix-isolated unsaturated transition-metal carbonyl species are often sharp with many structure-specific features. Most of the early matrix-isolation literature on transition-metal (TM) carbonyls has been reviewed.[9−11]

With advances in light sources and detectors, time-resolved absorption spectroscopy has become a possible probe for coordinatively unsaturated metal carbonyls in the gas phase. Although solution- phase studies have been very important in the development of transient spectroscopy, unsaturated transition-metal carbonyls coordinate with solvent on a very short time scale and thus affect the structure of these species.[12] Compared with matrix-isolation spectroscopic studies, gas-phase studies provide not only spectroscopic information but also some reaction kinetics and photophysical properties of many unsaturated transition-metal carbonyl species. The photolysis of metal carbonyls in the gas phase is typically wavelength dependent, and different coordinated unsaturated carbonyls can be produced with different wavelength light sources. Despite this feature, there are disadvantages involved in absorption spectroscopic study of unsaturated TM carbonyls in the gas phase. The gas-phase absorptions are typically broad and featureless and do not provide much structural information. Spectroscopic and kinetic studies of unsaturated TM carbonyls in the gas phase have been reviewed,[13,14] and some of the spectroscopic results will be compared in this article. With the development of supersonic jet techniques, rotationally resolved diode laser spectroscopic investigation of unsaturated TM carbonyls has become possible, and recent developments in this area will also be compared.

During the past two decades, computational chemistry has made significant advances. There are a large number of theoretical papers concerning the electronic and bonding properties of saturated TM complexes[15,16] and considerable work on unsaturated TM carbonyl complexes, particularly focused on the monocarbonyls, and the latter will be reviewed here. Due to the complexity of these systems, the evaluation of accurate molecular properties needs sophisticated treatments. Unfortunately it is usually difficult to compute vibrational frequencies at the highest levels of theory for large molecules. However, density functional theory (DFT) yields a good description of the bonding in these systems and, more specifically, gives harmonic frequencies that are in good agreement with the experimental fundamentals. One significant advantage of the DFT approaches is the availability of analytic second derivatives, which makes the evaluation of the vibrational frequencies of sizable molecules quite tractable. Since the present article is focused on vibrational frequencies in un-

saturated binary transition-metal mononuclear carbonyl complexes, theoretical studies of saturated carbonyls, multinuclear TM carbonyls, and carbonyls that involve other ligands are beyond the scope of this article. We will concentrate on some of the more recent theoretical calculations of vibrational frequencies and compare these with experimental results for unsaturated binary carbonyls.

The previous reviews of experimental work on unsaturated TM carbonyl complexes focused on neutral species.[9−11,13,14] This article will describe advances in the spectroscopic and theoretical studies of unsaturated binary transition-metal carbonyl neutral complexes and the more challenging cation and anion complexes. We will emphasize infrared (IR) matrix-isolation and density functional theoretical investigations of vibrational frequencies. Recent gas-phase work such as time-resolved transient infrared absorption, diode laser, and photoelectron spectroscopic studies will be included for comparison. Meanwhile, mononuclear homoleptic carbonyl anions in solution and cations in superacid media have been characterized, as outlined in recent reviews.[17] Such carbonyl complexes exhibit quite different properties from typical carbonyls and provide good examples for comparison with isolated carbonyl complexes. Although ion cyclotron resonance and mass spectrometric investigations have provided considerable thermochemical and photochemical properties of carbonyl anions, these methods do not give vibrational and structural information and will be not discussed in detail here.

## *II. Spectroscopic and Theoretical Methods*

### A. Sample Preparation

Synthesis of unsaturated transition-metal carbonyl species is the prerequisite for spectroscopic study. In general, there are two main routes for the production of binary unsaturated transition-metal carbonyls: the first begins with metal atoms and CO molecules (eq 1), and the second starts from saturated transition-metal carbonyls (eq 2)

$$M + CO \rightarrow MCO \rightarrow M(CO)_x \ (x = 2, 3, 4,...) \quad (1)$$

$$M(CO)_n \rightarrow M(CO)_{n-1} \rightarrow M(CO)_{n-2} \rightarrow ... \quad (2)$$

The earlier matrix-isolation spectroscopic studies employed thermal techniques to produce transition-metal atoms.[9−11] This method is very useful for synthesis of small unsaturated carbonyls, especially for the systems where no stable saturated carbonyl precursor is available such as the Sc, Ti, and Cu group carbonyls. Thermally evaporated metal atoms were co-deposited with CO and rare-gas mixtures, and binary transition-metal carbonyls with different coordination numbers were thus prepared in subsequent annealing and photolysis experiments. Infrared absorption and electron spin resonance (ESR) spectroscopic studies of unsaturated transition-metal carbonyls using this technique have been summarized.[9−11] Similar experimental approaches have been used by the Weltner[10,18] and Kasai groups[19,20] in a series of ESR studies of neutral carbonyls isolated in rare-gas matrices.

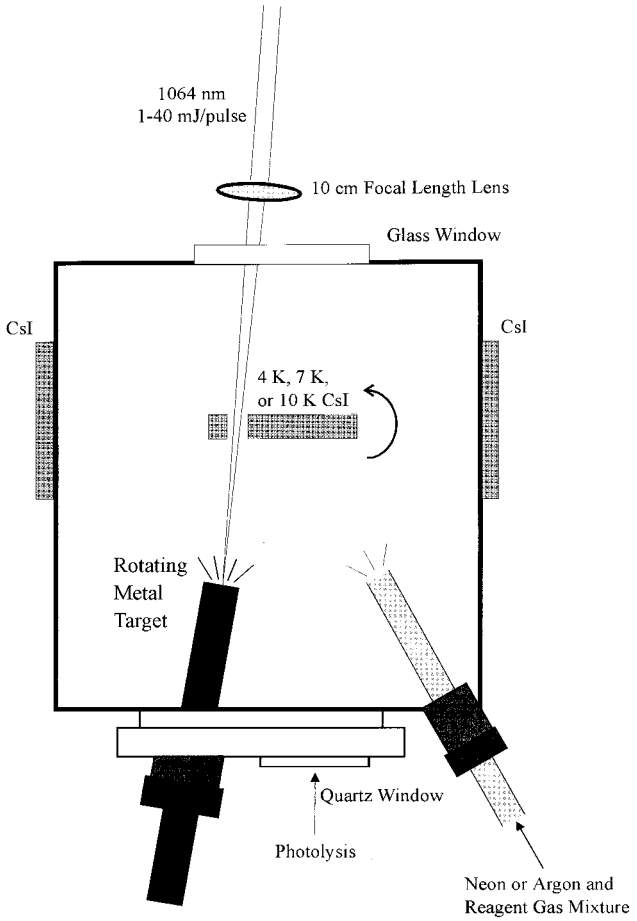


**Figure 1.** Schematic diagram of apparatus for laser-ablation matrix-isolation infrared spectroscopic investigation of unsaturated transition-metal carbonyls.

Another technique to produce metal atoms is laser ablation. This method has been recently employed in our laboratory to synthesize unsaturated transition-metal carbonyls in rare-gas matrices. Laser ablation has proven to be a powerful method to produce reactive intermediates and radicals for gas-phase jet studies as well as lower temperature matrix-isolation investigations.[21] A schematic diagram of our reactive laser-ablation apparatus for matrix-isolation infrared spectroscopic investigation of unsaturated transition-metal carbonyl species is shown in Figure 1, and the experiment has been described earlier.[22,23] The cold window is maintained at 10 K (Model 22 cryocooler, CTI Cryogenics, Waltham, MA) or 7K (Displex, APD Cryogenics, Allentown, PA) for argon matrix studies or at 4 K (Heliplex, APD Cryogenics, Allentown, PA) for neon matrix investigations. Laser ablation has a number of advantages, in contrast to conventional high-temperature oven techniques. With the laser-ablation technique only a small amount of the material is directly heated, thus minimizing the introduction of impurities into the samples and the heat load on the matrix. Of more importance, laser ablation produces electrons and cations as well as neutral atoms, and as a result, anions can be formed by electron capture of the neutral molecules and cations can be produced

by cation−molecule reactions or via photoionization by radiation in the ablation plume. The most obvious disadvantage of laser ablation is the plume of radiation produced by the laser on the target surface; thus, the samples are deposited with concurrent irradiation. Recently, a large number of new unsaturated transition-metal carbonyl neutrals, cations, and anions have been produced in our laboratory upon reactive co-condensation of laser-ablated transition-metal atoms, cations, and electrons with CO in excess argon or neon rare gases.

Quartz crystal microbalances are often used to measure the amount of metal deposited in matrix-isolation experiments.[9,24−26] The present experiments employed 1−40 mJ per 10 ns pulse of 1064 nm radiation focused (10 cm f.l.) on the rotating metal target. Although there is some variation from experiment-to-experiment, quartz crystal microbalance measurements with freshly filed metal targets and the sample geometry and laser energies employed for argon matrix experiments discussed here provide a basis to estimate the metal mole concentration to be 0.1% of the argon matrix (this can range from 0.2% to 0.02% in different experiments, but the metal concentration is always less than the CO concentration). Typically our laser-ablation experiments employ lower metal concentrations than thermal evaporation experiments (also compare product yield).[25,26] The neon matrix experiments included a 10% neutral density filter in the laser beam with the same laser focus, and microbalance measurements typically gave 15% as much metal ablated. The metal mole concentrations in the neon matrix experiments discussed here are therefore approximately 0.02% of the neon matrix (range from 0.03% to 0.01%).

One of the problems of spectroscopic studies of transition-metal carbonyls lies in the unambiguous identification of the observed spectral features. With isotopic substitution and isotopic mixtures, the composition can be established but the real difficulty usually lies in the correct identification of the charge state. Some information about charge state can be obtained from photolysis behavior. Unsaturated transition-metal carbonyl anions have small electron affinities (usually less than 3 eV), and visible or ultraviolet photolysis can easily detach the electron. The cations are usually more strongly bound, and UV irradiation is usually required to destroy them. However, electrons detached from anions may then react with cations and neutralize them. Of more importance, many neutral unsaturated transition-metal carbonyl species are very photosensitive and the charge state identification via photolysis behavior is not reliable. When cations and electrons are present, more information about charge state can be obtained from electron trap molecule (such as $CCl_4$) doping experiments. The role of $CCl_4$ as an electron trap in laser-ablation experiments has been discussed by Zhou and Andrews in a series of cation and anion studies.[27−29] A typical example of the effect of $CCl_4$ doping is shown in Figures 2 and 3. Laser ablation of the metal target produces metal atoms, metal cations, and electrons, and the added $CCl_4$ captures most of the ablated electrons that reach the sample,

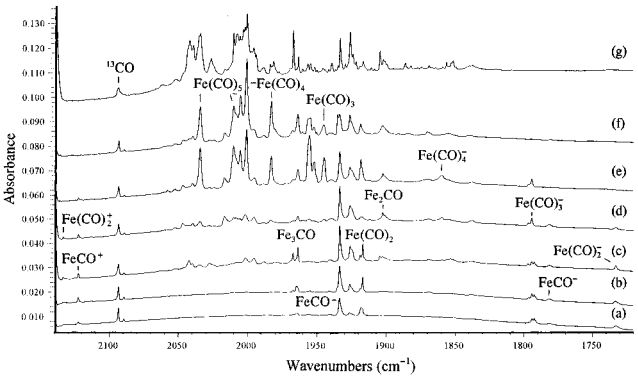


**Figure 2.** Infrared spectra in the 2140−1720 cm$^{-1}$ region for laser-ablated iron atoms co-deposited with 0.1% CO in neon using medium laser power: (a) after 30 min sample deposition at 4 K, (b) after annealing to 6 K, (c) after annealing to 8 K, (d) after 15 min 380−580 nm photolysis, (e) after 15 min 290−580 nm photolysis, (f) after 15 min full-arc photolysis, and (g) after annealing to 11 K. (Reprinted with permission from ref 43. Copyright 1999 American Physical Society).

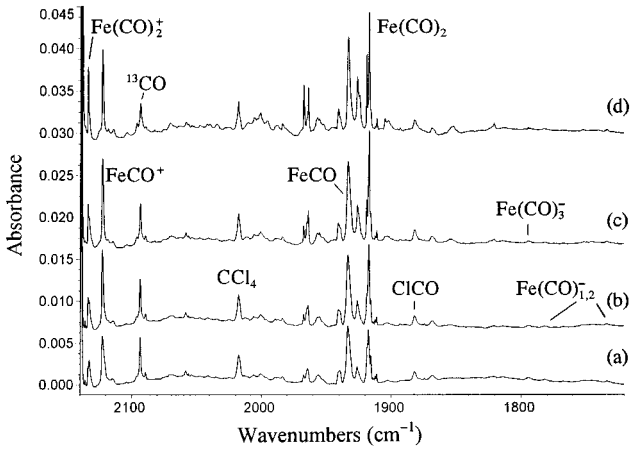


**Figure 3.** Infrared spectra in the 2140−1720 cm$^{-1}$ region for laser-ablated iron atoms co-deposited with 0.1% CO in neon with 0.02% $CCl_4$ added using medium laser power: (a) after 30 min sample deposition at 4 K, (b) after annealing to 6 K, (c) after annealing to 8 K, and (d) after annealing to 10 K. (Reprinted with permission from ref 43. Copyright 1999 American Physical Society).

thus reducing the yield of molecular anions and facilitating the survival of more laser-ablated metal cations and their reaction products.

When stable saturated transition-metal carbonyls are available, dissociation of saturated carbonyls is a powerful method for generating unsaturated carbonyls for spectroscopic investigation. This method is widely used in gas-phase, solution, and rare-gas matrix studies. A variety of techniques have been employed to induce the dissociation, such as photolysis with gamma, ultraviolet, and laser radiation, microwave discharge, and electron or ion beam bombardment. For example, Turner, Poliakoff, and co-workers produced $Fe(CO)_{3,4}$ and $Cr(CO)_{3-5}$ by the photolysis of $Fe(CO)_5$ and $Cr(CO)_6$ in rare-gas matrices for infrared study.[30−35] Lineberger, Leopold, and co-workers formed the unsaturated $Fe(CO)_x^-$, $Ni(CO)_x^-$, and $Cr(CO)_3^-$ anions by microwave discharge for photoelectron spectroscopic study in the gas phase.[36−38] Vibrational fine structure can be

difficult to observe accurately in photoelectron spectra and is generally limited to symmetric vibrational modes. Weitz et al. employed excimer laser photolysis to produce unsaturated transition-metal carbonyls in the gas phase for time-resolved infrared absorption spectroscopic studies,[13,14] and Kompa et al. studied the femtosecond dynamics of $Cr(CO)_6$ and $Fe(CO)_5$ photodissociation.[39,40]

## B. Spectroscopic Methods

### 1. Infrared Absorption

Infrared absorption is the main spectroscopic method in characterization of coordinatively unsaturated transition-metal carbonyls both in gas-phase and rare-gas matrices. As many of the unsaturated transition-metal carbonyls are extremely photolabile and their UV−vis spectra are usually not very structurally sensitive, most optical absorption studies employed infrared absorption spectroscopy. Fortunately, unsaturated transition-metal carbonyls exhibit strong absorptions in the C−O stretching vibrational region, which are often structurally sensitive.

Laser ablation has been successfully employed for generation of unsaturated transition-metal carbonyl species for matrix-isolation infrared absorption studies in our laboratory. As mentioned, laser ablation of transition-metal targets produces not only neutral metal atoms, but also metal cations and electrons, and hence, ionic metal carbonyl species can also be formed. One difficulty of infrared studies of metal carbonyl species lies in the unambiguous identification of carbonyls with different coordination number. By carefully controlling the ablation laser power and reagent concentration, different coordinated mononuclear metal carbonyls can be identified by stepwise annealing to allow diffusion and further reaction, by mixed isotopic substitution experiments, as well as by comparison with theoretical predictions of vibrational frequencies, isotopic shifts, and relative band intensities. These experiments can also produce binuclear and trinuclear metal complexes on annealing, and such complexes can often be identified.[41−43] The use of isotopic mixtures and isotopic band multiplet structure for determining the number of carbonyls will be described with examples in section IV.

Unsaturated transition-metal carbonyl species are extremely reactive; thus, fast and sensitive spectroscopic probes are required in gas and solution phases, and time-resolved transient absorption is particularly suitable for unsaturated transition-metal carbonyl studies. Such investigations can provide spectroscopic data on unsaturated transition-metal carbonyls and can also give rate constants for ligand−metal carbonyl association reactions and bond dissociation energies. In this method, a UV light source is used to photolytically produce the coordinatively unsaturated carbonyls, and a probe light source monitors the spectrum of parent and photoproducts. In early experiments, UV lamps were typically used as the photolysis light sources, and some results have been obtained with UV light probes.[44] More recent experiments have typically employed an excimer laser as the photolysis light source, and a series of interesting results has been obtained with an IR light source as the probe.[13,14,45,46] Recent progress on the photophysics of metal carbonyls and the spectroscopy and reaction kinetics of the resulting coordinatively unsaturated transition-metal carbonyls has been reviewed by Weitz.[13,14] One major disadvantage of gas-phase studies of transition-metal carbonyls is that the IR absorptions are usually broad, and structural information cannot be obtained. However, Davies et al. demonstrated with $Ni(CO)_4$ that it is possible to obtain rotationally resolved IR spectra of jet-cooled metal carbonyls using a diode laser.[47] Such spectra can give high-quality spectroscopic data and structural information. Recently, the Tanaka group successfully extended this technique to unsaturated transition-metal carbonyl systems, including FeCO and $Fe(CO)_2$.[48−50]

### 2. ESR

Electron spin resonance has been extensively employed to study both the neutral and ionic unsaturated transition-metal carbonyls. This approach is usually used in conjunction with the matrix-isolation technique. It is sensitive to open-shell species with unpaired electrons and can provide information about the ground electronic state. This method can also offer good characterization of the density distribution of the unpaired electrons and of the electronic wave function. The disadvantage of this technique is that it is of no use for closed-shell species and open-shell species with degenerate ground states and unquenched orbital angular momentum. The ESR spectra provide valuable information about molecular structure and symmetry but no vibrational frequencies and bond lengths. Many groups have reported the ESR spectra of transition-metal carbonyl neutrals, such as CuCO, $Cu(CO)_3$ , AgCO, $Ag(CO)_3$, AuCO,[19,20] $Co(CO)_3$, $Co(CO)_4$,[51,52] $Mn(CO)_5$,[53] $V(CO)_x$ ($x = 1-5$),[54,55] ScCO, and NbCO.[18] The ESR spectra of $Cr(CO)_4^+$ and $Fe(CO)_5^+$ carbonyl cations have also been obtained.[56,57]

### 3. PES

Negative-ion photoelectron spectroscopy has been used by several groups for studying coordinatively unsaturated transition-metal carbonyls. This technique can provide spectroscopic information about both neutral and anionic carbonyls in the gas phase. The ions are usually produced in a flowing afterglow reactor equipped with a microwave discharge ion source. The ions were mass selected and then interrogated with an electron detachment laser beam and the detached photoelectron kinetic energy analyzed. Negative-ion photoelectron spectroscopy has several unique advantages. Since the selection rules for vibrational transitions are determined by the Franck−Condon factors, it is often possible to observe vibrational states that are forbidden or weak in infrared spectroscopy. In particular, it is possible to observe the bending and metal−CO stretching vibrational modes of the binary neutral transition-metal carbonyls that are usually out of the normal spectral

detection range for other techniques. Negative-ion photoelectron spectroscopy can also provide the electron affinity of the neutral carbonyls. In addition, the intensity ratios observed in the photoelectron spectra yield quantitative information concerning the change in molecular structure induced by addition of the extra electron. To date, the binary unsaturated transition-metal carbonyls studied by negative ion photoelectron spectroscopy include $Fe(CO)_n$ ($n$ = 1−4),[37,38] $Ni(CO)_n$ ($n$ = 1−3),[36] $M(CO)_3$ (M = Cr, Mo and W),[58] MnCO,[59] and PdCO.[60]

#### 4. NMR

The above-mentioned spectroscopic techniques are usually suitable for gas-phase and matrix-isolation studies. For carbonyls in acid media, nuclear magnetic resonance, NMR, has also been used for spectroscopic studies. Carbon-13 shifts and $^1J_{M,C}$ coupling constants are helpful for characterizing the M−CO bonds.[17]

### C. Theoretical Methods

Experience has shown that the Hartree−Fock (HF) (or self-consistent-field (SCF)) approach does not describe the metal−CO systems very accurately. One of the biggest drawbacks of the HF approach is the underestimation of the metal to CO donation; therefore, methods used to study these molecules must include electron correlation. The complete-active-space SCF (CASSCF) approach can be used to obtain some insight into the bonding, but even higher levels of theory must be used to obtain accurate results. While the modified coupled pair functional (MCPF) approach yields a reasonable description of these systems, one must go all the way to the coupled cluster singles and doubles approach, including a perturbational estimate of the triples (CCSD(T)), to obtain a highly accurate description. It must be remembered that even the CCSD(T) approach yields accurate bond energies only when a large basis set is used.[61] While the MCPF and CCSD(T) approaches have been used to compute some bond energies and a few vibrational frequencies, their computational cost means that they are not practical methods for studying large numbers of metal carbonyl species, especially those with several CO groups.

Density functional theory (DFT) is an attractive alternative to the more traditional computational approaches. The computational cost of DFT is much lower than that of CCSD(T), and equally importantly, analytic second derivatives make it possible to compute the harmonic frequencies of even quite large molecules at the DFT level. Experience has shown that the B3LYP[62,63] and BP86[64,65] density functionals, with moderate basis sets, can provide reasonable predictions for transition-metal-containing compounds.[66−68] In addition, isotopic frequencies can be calculated for comparison with the observed values to determine isotopic frequency ratios as a characteristic of the normal mode and another diagnostic for identifying new species. Theoretical and experimental results will be compared for specific TM carbonyl systems in section IV.

## III. Overview of the Bonding

There have been many detailed studies of the bonding in the metal carbonyls using many different approaches,[15,16,69−73] and it is far beyond the scope of this review to discuss them in detail. We point the interested reader to the very recent review by Frenking and Fröhlich.[16] While our main goal is an understanding of the trends in the vibrational frequencies, it is necessary to understand the important components of the bonding in order to understand the observed trends in the TM carbonyl vibrational frequencies. In this regard, we note that the changes in vibrational spectra with the metal atom, with the charge, and with the number of CO molecules can be quite large. In fact, the variation might seem so large that the bonding in these systems does not appear to be systematic. This is not the case, however, as the same bonding mechanisms exist for all of the species, and the changing importance of different components of the bonding can be used to explain the changes in ground state, geometry, and vibrational frequencies. Therefore, we give a short overview of the bonding in this section.

Before discussion the bonding, we need to consider the electronic structure of the metal atoms and ions. We first note that the separation between the electronic states arising from the $d^ns^2$ and $d^{n+1}s^1$ occupations varies greatly. Starting at the left-hand side of the row and moving to the middle, the d orbitals become increasingly stable with respect to the s orbitals; thus, while the ground state of Sc is $^2D(3d^14s^2)$, the ground state of Cr is $^7S(3d^54s^1)$. At the middle of the row (Mn, Tc, and Re), the next electron must either doubly occupy a d or an s orbital. Since the d orbital pairing energy is very large, the $d^5s^2$ state is much below the $d^6s^1$ state; for Mn, the $^6S(3d^54s^2)$ state is 2.14 eV below the $^6D(3d^64s^1)$.[74] In the second half of a given row, as one moves to the right, again the d orbital becomes increasingly stable with respect to the s orbital, and eventually the ground state is derived from the $d^{n+1}s^1$ occupation. Similar changes occur for the cations, but the two states of interest are derived from the $d^ns^1$ and $d^{n+1}$ occupations. Relative to the first transition row, the d orbitals are stabilized with respect to the s orbitals in the second transition row; thus, the separation between the states derived from different occupations changes between the first and second transition rows. In the third transition row, relativisitic effects stabilize the s orbitals with respect to the d orbitals; thus, for a given column, the separation between the atomic states shows considerable variation. For the third transition row, spin−orbit effects add some additional complications, but we do not address this in detail.

In addition to change in the separation between the low-lying states of the metal atoms, the relative size of the d and s orbitals changes across the row.[70] The d orbital contracts with respect to the s orbital as one goes to the right in a given row. The ratio of the s/d radial expectation values are smaller for the second transition row than the first, as the d orbital is less compact for the second transition row. Excluding Sc, ionization reduces the ratio of the size of the d orbital with respect to the s orbital. Since sd

hybridization is easier when the size of the orbitals is more similar, the changing ratio of the d to s orbital size means that hybridization is easier as one goes down a column, easier on the left side of a row than on the right, and easier for a cation than for a neutral.

The discussion of the bonding must begin with the metal d$\pi$ to CO $\pi$* donation. This movement of charge can be observed in the electron density difference between the MCO and M + CO charge density plots.[75] This moves metal charge to the CO $\pi$* antibonding orbital, which results in a weakening of the CO bond and hence a decrease in the CO vibrational frequency. The importance of this effect is expected to depend on the metal ionization potential (IP). The lower the metal IP, the stronger the donation and hence the lower the CO stretching frequency. Clearly an anion would donate more electrons than a neutral, which in turn would donate more electrons than a cation. The donation will also depend on the d population; a metal atom with four $\pi$ electrons is expected to donate more charge than one with fewer electrons.

The second component of the bonding is commonly described as CO $\sigma$ donation, where the CO 5$\sigma$ orbital donates charge to the metal. Analysis of this component of the bonding suggests[76,77] that it ranges from a true CO-to-metal donation to a case where the CO 5$\sigma$ orbital polarizes toward the metal and is stabilized by the positive charge on the metal; that is, a case of CO polarization more than true CO donation to the metal. Goldman and Krogh-Jespersen[73] pointed out that this is best described as electrostatic bonding since there is essentially no CO donation to the metal. Such electrostatic bonding increases the C−O stretching frequency. For $CuCO^+$, the C−O frequency was computed to shift up by 96 $cm^{-1}$ from CO at the CCSD(T) level.[78] More recent calculations at the MP2 level[79] report an increase of 63 $cm^{-1}$, but subsequent B3LYP calculations find a 101 $cm^{-1}$ increase for the $CuCO^+$ cation.[80] The neon matrix experimental observation to be described below reveals a 93.6 $cm^{-1}$ increase. The importance of this bonding component will increase with the positive charge on the metal atom and decrease with the number of metal electrons in $\sigma$ orbitals, especially metal valence s orbitals, which will have a large overlap with the CO molecular orbitals and hence result in a large electrostatic repulsion.

It should be noted that the $\sigma$ and $\pi$ bonding are not completely separate. Davidson et al.[69] concluded that the 5$\sigma$ orbital is stabilized by penetration into the metal valence shell. This penetration gives an increased shielding of the 3d orbitals, which leads to an increased diffuseness of the 3d orbital and hence more metal−CO $\pi$ bonding.

FeCO illustrates several of these points; this important complex has a $^3\Sigma^-$ ground state derived from the $3d^74s^1$ occupation of Fe. It is therefore favorable for the Fe atom to promote an electron from the s to the d orbital, even though this occupation is about 0.9 eV above the Fe $^5D(3d^64s^2)$ ground state. The removal of one 4s electron reduces the Fe−CO repulsion in the $\sigma$ space, and the higher number of 3d electrons enhances the Fe to CO $\pi$* donation. The Fe valence occupation is $3d\sigma^13d\pi^43d\delta^24s^1$, which maximizes the number of d$\pi$ electrons and hence maximizes the $\pi$ donation to the CO. In the free Fe atom, the $3d\sigma^13d\pi^43d\delta^24s^1$ occupation is not the lowest in energy, both the $3d\sigma^13d\pi^33d\delta^34s^1$ and $3d\sigma^23d\pi^23d\delta^34s^1$ occupations are lower, but these do not minimize Fe−CO $\sigma$ repulsion and maximize the CO $\sigma$ donation and the Fe to CO $\pi$ donation. If the 3d$\sigma$ and 4s orbitals are high-spin coupled, only sp hybridization is available to reduce the Fe−CO $\sigma$ repulsion; however, if the 3d$\sigma$ and 4s orbitals are low-spin coupled, sd$\sigma$ hybridization can occur and some $d^8$ can mix into the wave function,[76] and these help to reduce the Fe−CO repulsion. Since the $d^8$ occupation is very high in energy, only a small amount mixes in, but sd$\sigma$ hybridization is very efficient at reducing the Fe−CO repulsion. (We should note that even though the hybridization is dominated by sd$\sigma$, some sp hybridization can still contribute to a reduction of the metal−CO repulsion.) Thus, the cost of low-spin coupling the s and d orbitals is easily paid by the reduction in the $\sigma$ repulsion and the increase in the CO $\sigma$ donation.

For the case of two CO molecules, the bonding components are similar to those for the monocarbonyl. However, since there are two CO molecules to share the cost of s to d promotion, the s population is even lower. Most $M(CO)_2$ species are linear or nearly linear, because the sd$\sigma$ hybridization reduces the electron density on both sides of the metal atom (and increases it in a torus arround the metal atom) and hence it is favorable for the second CO to be on the opposite side from the first. Thus, sp hybridization, which occurs for the monocarbonyl, is not important for $M(CO)_2$ except when the metal s to d promotion energy is very large. If sp polarization (hybridization) occurs, the CMC angle becomes much smaller to allow the valence electron density to polarize away from both CO subunits.

As the number of carbonyls increases further, it becomes easier to promote to higher atomic states; this usually involves lower spin states as these maximize the bonding. For example, in $Fe(CO)_5$, the bonding is derived from $3d^8$, where the d$\sigma$ orbital is empty to accept strong $\sigma$ donation from the axial CO molecules.[81] Thus, this occupation has four doubly occupied d orbitals to maximize metal to CO $\pi$ donation and one empty d orbital to minimize $\sigma$ repulsion and maximize CO $\sigma$ donation. We should also note that as the number of CO molecules increases, the CO−CO repulsion becomes more important and hence the optimal geometries are a compromise between maximizing the metal−CO bonding and minimizing the CO−CO repulsion.

In the following sections we will focus on the vibrational frequencies. In many cases the bonding is straightforward and we do not discuss it in detail but point out interesting examples of the bonding concepts discussed in this section.

## *IV. Binary Transition-Metal Carbonyl Neutrals*

Binary unsaturated mononuclear transition-metal carbonyl neutrals have been intensively studied for several decades both in the gas phase[13,14] and rare-gas matrices.[9−11] Table 1 lists the observed C−O stretching vibrational frequencies of binary unsatur-

**Table 1. C−O Stretching Vibrational Frequencies ($cm^{-1}$) for Neutral Binary Unsaturated Transition-Metal Carbonyls $M(CO)_n$ in the Gas Phase, Solid Neon, and Solid Argon**

| | Sc | Ti | V | Cr | Mn | Fe | Co | Ni | Cu |
|---|---|---|---|---|---|---|---|---|---|
| ref | 87 | 92 | 92, 97, 99 | 33−35, 109−111, 115, 313 | 41, 121 | 42,43, 48−50, 314 | 155, 159, 160 | 25,26, 104, 172, 175 | 80, 191, 196 |
| $n = 1^a$ | | | | | 1955 | 1946.5 | | | |
| | 1851.4 | 1920.0 | 1930.6 | 2018.4 | 1950.7 | 1933.7 | 1973.9 | 2006.6 | 2029.7 |
| | 1834.2 | 1887.8 | 1904 | 1975.3 | 1933.6 | 1922.0 | 1960.7 | 1994.4 | 2010.3 |
| $n = 2$ | | | | | | 1928.2 | | | |
| | | 1893.1<br>1799.3 | 1944.0<br>1844.2 | 1982.1<br>1832.9 | 1972.8<br>1851.5 | 1917.1 | 1945.6 | 2089.7<br>1978.9 | 1904.4 |
| | 1775.5<br>1716.3 | | 1820 | 1970.8<br>1821.5 | 1832.5 | 1984.8<br>1879.2 | 1920.8 | 2071.5<br>1965.5 | 1890.9 |
| $n = 3$ | | | 1859 ? | 1880 | | 1950 | | | |
| | | 1975.1<br>1840.3 | 1911 ? | 1873.8 | 1909.5<br>1891.1 | 1945.0 | 1991.5 | 2025.0 | 1994.3 |
| | 1968.0<br>1822.2 | | 1920 ? | 1867 | 1891.1<br>1865.7 | 2042.0<br>1935.3 | 1983.2 | 2017.2 | 1975.6 |
| $n = 4$ | | | 1920 ? | 1957<br>1920 | | 2000<br>1984 | | 2061.3 | |
| | | 1871.0<br>1853.5 | 1949 ? | 1952.2<br>1911.4 | 1973.9 | 2001.2<br>1983.2 | 2029.6<br>2022.2 | 2056.3 | |
| | 1865.4 | | 1893 ? | 1940<br>1896 | 1957.6 | 1995.8<br>1972.7 | 2023.5<br>2016.6 | 2051.2 | |
| $n = 5$ | | | 1965 | 1980<br>1948 | 2000 | 2038.11<br>2015.55 | | | |
| | | 1912.5<br>1885.6 | 1963.4<br>1958.5 | 1976.2 | 1998 | 2034.5<br>2010.5 | | | |
| | | 1897.7 | 1952<br>1943 | 1965.4<br>1936.0 | 1992 | 2025.2<br>2005.9 | | | |
| $n = 6$ | | | 1986 | 2002.96 | | | | | |
| | | 1945.7 | 1984.3 | 1998 | | | | | |
| | | 1933.5 | 1976 | 1990 | | | | | |

| | Y | Zr | Nb | Mo | Tc | Ru | Rh | Pd | Ag |
|---|---|---|---|---|---|---|---|---|---|
| ref | 87 | 93 | 105 | 34, 111−115, 313 | | 148, 150 | 160,161,163 | 25, 173, 175 | 192, 197 |
| $n = 1$ | | | | | | | | | |
| | | 1899.5 | 1932.0 | 1881.2 | | 1935.6 | 2022.5 | 2056.4 | |
| | 1869.0 | | | 1862.6 | | 1917.7 | 2007.6 | 2050 | |
| $n = 2$ | | | | | | | | | |
| | | 1855.5<br>1785.1 | 1847.2 | 1938.2<br>1895.2 | | 1955.3 | 2031.0 | 2065.8 | 1858.7 |
| | | | | 1891.9 | | 1915.3 | 2014.6 | 2044 | 1842 |
| $n = 3$ | | | | 1885 | | ~ 1987 | | | |
| | | 1960.3<br>1838.2 | | 1886.1 | | 1975.4<br>1970.6 | 2029.2<br>2020.3 | 2062.7 | 1970.4 |
| | | | | 1869 | | | 2011 | 2058 | 1955 |
| $n = 4$ | | | | 1972<br>1911 | | ~ 2005 | | | |
| | | 1916.6 | 1868.3 | 1965.5<br>1908.9 | | 1983.0 | 2021.5 | 2074.6 | |
| | | | | 1951<br>1895 | | | 2010 | 2070 | |
| $n = 5$ | | | | 1985<br>1942 | | 2045<br>2015 | | | |
| | | 1978.1<br>1945.1 | 1963.5 | 1944.6 | | 2049.8<br>2012.3 | | | |
| | | | | 2098<br>1973<br>1933 | | 2039.1<br>2003.8 | | | |
| $n = 6$ | | | | 2005.49 | | | | | |
| | | 1993.1 | 1984.1 | 2000.6 | | | | | |
| | | | | 1992.2 | | | | | |

**Table 1 (Continued)**

| | Hf | Ta | W | Re | Os | Ir | Pt | Au |
|---|---|---|---|---|---|---|---|---|
| ref | 93 | 104,105 | 34, 113, 313 | 41, 127 | 149, 150 | 160−162 | 25, 174, 175 | 193, 197 |
| $n = 1$ | | | | | | | | |
| | 1868.6 | 1865.2 | 1859.9 | | 1972.6 | 2024.5 | 2065.5 | 2053.2 |
| | | | 1848.8 | | | | 2056.8 | 2039.4 |
| $n = 2$ | | | | | | | | |
| | 1850.9<br>1806.7 | 1918.3<br>1838.6 | 1884.5 | 1905.4 | 1975.2 | 2014.5 | 2053.2 | 1943.7 |
| | | | | | | | ? | 1926.6 |
| $n = 3$ | | | | | 1980 | | | |
| | 1951.2<br>1835.5 | | | | 1973.8<br>1966.2 | 2021.3<br>2012.0 | 2044.0 | |
| | | | 1865 | | | | ? | |
| $n = 4$ | | | 1957, 1909 | | 2000 | | | |
| | 1902.6 | 1915.2<br>1900.1 | 1954.0<br>1909.0 | | 1983.1 | 2010.5 | 2058.1 | |
| | | | 1939 | | | 2002.6 | 2053.5 | |
| $n = 5$ | | | 1980 | | 2046<br>2008 | | | |
| | 1969.5<br>1937.1 | 1954.7 | 1975.9 | 2004 | 2048.7<br>2003.4 | | | |
| | | | 1963.0 | 1995 | | | | |
| $n = 6$ | | | 2000.36 | | | | | |
| | 1986.7 | 1976.0 | 1995.3 | | | | | |
| | | | | 1986.6 | | | | |

[a] For each metal carbonyl coordination number, *n*, the first row contains the gas-phase observation, the second row the neon matrix value (s), and the third row the argon matrix value (s).

ated transition-metal carbonyls in the gas phase and rare-gas matrices. As heavier rare-gas solids interact more strongly with host molecules and usually exhibit larger shifts from gas-phase values,[82] only neon and argon matrix values are listed. Since neon matrix observations are usually closer to gas-phase measurements,[42,43,48−50] this review will emphasize the recent neon matrix results, which generally confirm previous argon matrix assignments. Furthermore, solid neon is more effective for trapping cations, and more information on all of the trapped species—cations, neutrals, and anions—can be obtained from the neon matrix spectra recently obtained in our laboratory. Assignments from earlier reports now known to be incorrect are not listed here, but these are discussed in the recent literature where the new assignments are given.

Unsaturated transition-metal carbonyls have also been the subject of a surprisingly large number of theoretical studies, most of which are focused on monocarbonyls, and a variety of computational methods have been used. These calculations have provided accurate predictions of the equilibrium geometries, harmonic frequencies, and bonding energies. There are several systematic studies on monocarbonyls and dicarbonyls of first-row transition-metals.[83−85] While these studies provide great insight into the nature of the bonding, only the more recent DFT calculations give a consistent set of vibrational frequencies for systems containing from one to six CO molecules for virtually all transition-metal atoms, and therefore, we focus on these calculations in the following sections.

Mixed isotopic spectra are extremely important for sorting out the coordination number, i.e., the number of CO subunits in a metal carbonyl. In the mixed 50% $^{12}C^{16}O$ + 50% $^{13}C^{16}O$ isotopic experiment, the monocarbonyl absorption will consist of a 1/1 doublet containing only the pure isotopic molecules but the dicarbonyl will exhibit one new mixed isotopic band for the $M(^{12}C^{16}O)(^{13}C^{16}O)$ isotopic molecule (Figure 4). For the strong antisymmetric C−O vibration not interacting with the usually weaker symmetric vibration, $M(^{12}CO)_2$, $M(^{12}CO)(^{13}CO)$, $M(^{13}CO)_2$, the band intensities will follow the statistical weights of 1/2/1. The tricarbonyl will form four isotopic molecules, and the 1/3/3/1 statistical weights for $M(^{12}CO)_3$, $M(^{12}CO)_2(^{13}CO)$, $M(^{12}CO)(^{13}CO)_2$, and $M(^{13}CO)_3$ apply to the symmetric nondegenerate mode. However, for the doubly degenerate mode, the mixed isotopic molecules have lower symmetry, degeneracy is lifted, and coincident band intensity addition results in a 3/1/1/3 quartet in most cases,[86,87] see, for example, pyramidal $Sc(CO)_3$ in Figure 4. The triply degenerate mode of a tetrahedral $M(CO)_4$ complex will exhibit three new mixed isotopic bands often with 1/2/1 relative intensities in the center of a pentet structure. Darling and Ogden have described these mixed isotopic multiplet structures with varying degrees of vibrational interaction.[86]

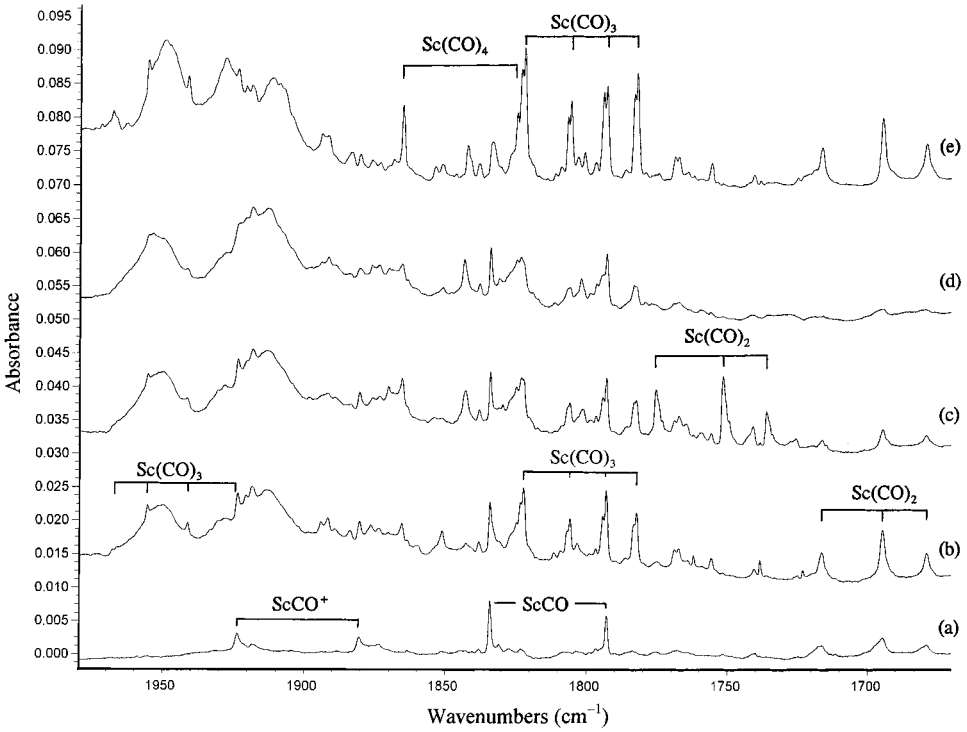


**Figure 4.** Infrared spectra in the 1980−1670 $cm^{-1}$ region for laser-ablated Sc atoms co-deposited with 0.25% $^{12}C^{16}O$ + 0.25% $^{13}C^{16}O$ in excess argon: (a) after 1 h sample deposition at 10 K, (b) after annealing to 25 K, (c) after 20 min $\lambda > 470$ nm photolysis, (d) after 20 min full-arc photolysis, and (e) after annealing to 35 K.

## A. Sc Group

Compared to other transition metals, there is relatively little experimental work on group 3 carbonyls. After co-deposition of thermally evaporated scandium atoms with CO diluted in argon, ESR spectra suggested that the ScCO molecule is linear with a $^4\Sigma^-$ ground state.[18] More recently, we repeated the Sc + CO reaction using the laser-ablation method, and the C−O stretching vibration of ScCO was observed at 1834.2 $cm^{-1}$ in an argon matrix and at 1851.4 $cm^{-1}$ in a neon matrix.[87] Figure 4 clearly shows the mixed isotopic doublet structure for the monocarbonyl. Both traditional ab initio and DFT calculations predicted the ScCO molecule to have a $^4\Sigma^-$ ground state derived from $^1\Sigma^+$ CO and atomic Sc with the first excited $3d\pi^2 4s^1$ occupation.[83−85,87−90] That is, the Sc atom is promoted to the excited state to minimize Sc−CO $\sigma$ repulsion and to maximize the Sc to CO $\pi$ donation. The doublet state of ScCO correlates to $^1\Sigma^+$ CO and the $^2$D ground state of scandium atom, which has a $3d^14s^2$ occupation, and is predicted to be weakly bound, in part because of the large repulsion arising from the doubly occupied Sc 4s orbital. Ab initio calculations predicted that the $Sc(CO)_2$ molecule has a linear $^2\Pi_g$ ground state with the $^4\Sigma_g^-$ state derived directly from $^4\Sigma^-$ ground state ScCO very close in energy.[83] Recent DFT calculations found the bent doublet $Sc(CO)_2$ to be slightly more stable than the linear geometry, and evidence was presented for both structures in solid argon.[87] The $Sc(CO)_3$ molecule was calculated to have a $^4A_1$ ground state with $C_{3v}$ symmetry, and the trigonal pyramidal structure was confirmed by infrared spectra in a solid argon matrix containing both stretching modes (Figure 4).[87]

## B. Ti Group

For Ti group 4 metal carbonyls, the experimental data are also sparse. The titanium hexacarbonyl, $Ti(CO)_6$, was first synthesized in CO, Ar, Kr, and Xe matrices by the Ozin group using titanium atoms and characterized by infrared and ultraviolet−visible absorption spectroscopy.[91] The unsaturated $M(CO)_x$ (M = Ti, Zr, Hf, $x = 1-5$) molecules were synthesized recently in our laboratory by co-deposition of laser-ablated metal atoms and CO molecules in neon.[92,93] The TiCO molecule is predicted to have a $^5\Delta$ ground state,[83,85,94] which correlates with a $^5$F excited-state Ti lying 0.78 eV higher than the $^3$F ground-state atom,[74] and the C−O stretching vibrational frequency is observed at 1920.0 $cm^{-1}$ in a neon matrix.[92] The ZrCO and HfCO molecules are found to have $^3\Sigma^-$ ground states by CASSCF and density functional methods.[93,95] The smaller d−d exchange terms associated with the second and third transition rows leads to the lower spin ground state. The C−O stretching vibrations for TiCO, ZrCO, and HfCO decrease from 1920 to 1900 to 1869 $cm^{-1}$ in solid neon, showing an increase in metal d to CO $\pi$ donation.[93]

The $M(CO)_2$ dicarbonyls are bent molecules with $C_{2v}$ symmetry, as both symmetric and antisymmetric C−O stretching vibrations are observed. The dicarbonyls are identified from 1/2/1 relative intensity triplets in mixed $^{12}C^{16}O$ + $^{13}C^{16}O$ spectra, as shown in Figure 5 for zirconium. Since zirconium and hafnium are refractory metals, the laser-ablation method is particularly appropriate for investigations of these systems.[93,96] All three tricarbonyls in this group have nonplanar geometry with $C_{3v}$ symmetry; the doubly degenerate antisymmetric C−O stretching

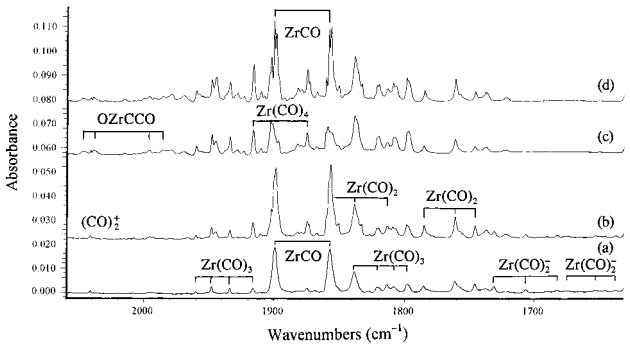


**Figure 5.** Infrared spectra in the 2060−1630 $cm^{-1}$ region from co-deposition of laser-ablated zirconium with 0.1% ($^{12}C^{16}O$ + $^{13}C^{16}O$) in neon: (a) after 45 min sample deposition at 4 K, (b) after annealing to 8 K, (c) after 15 min full-arc photolysis, and (d) after annealing to 10 K.

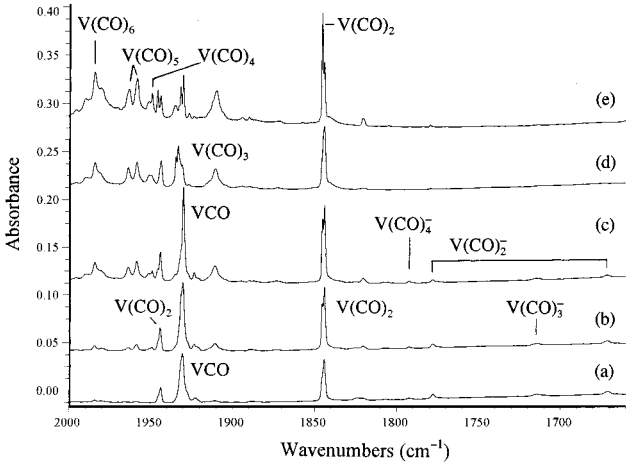


**Figure 6.** Infrared spectra in the 2000−1660 $cm^{-1}$ region from laser-ablated V atoms co-deposited with 0.1% CO in neon: (a) 30 min sample deposition at 4 K, (b) after annealing to 8 K, (c) after annealing to 10 K, (d) after 15 min full-arc photolysis, and (e) after annealing to 10 K.

vibration is characterized by approximately 3:1:1:3 relative intensities of mixed isotopic structure.[86,92,93] The nondegenerate symmetric C−O stretching vibration is characterized by approximately 1:3:3:1 relative intensities of mixed isotopic structure. The tetracarbonyls were predicted to be tetrahedral molecules as only one IR absorption is observed in the C−O stretching region.

## C. V Group

Spectroscopic studies of group 5 metal carbonyls are mainly focused on vanadium carbonyls. The VCO molecule was first synthesized by Hanlan et al.[97] via thermal vanadium atom reactions with CO molecules in rare-gas solids. The C−O stretching vibration was observed at 1904 $cm^{-1}$ in argon, which is in accord with our recent 1930.6 $cm^{-1}$ neon matrix value[92] (Figure 6). In the Weltner ESR study, two forms, one with a bent structure and the other with a linear structure, were observed for sextet VCO in rare-gas matrices.[54] Theoretical calculations predicted a $^6\Sigma^+$ ground-state VCO molecule with linear geometry, which correlates with the metastable $3d^44s^1$ ($^6$D) V atom and ground-state CO. The low-spin quartet VCO, which correlates with the ground-state metal atom, is slightly higher in energy.[83−85,94,98]

Although earlier infrared work reported three isomers of $V(CO)_2$ in solid Ar, Kr, and Xe hosts,[97] ESR results indicated that only one $V(CO)_2$ structure was observed in a neon matrix with a quartet ground state.[54] Our infrared spectra also clearly showed that $V(CO)_2$ has only one bent structure in neon matrix.[92] Earlier ab initio calculations considered a linear geometry, which predicted a $^6\Sigma_g^+$ ground state with a $^4\Pi_g$ state very close in energy,[83] but recent DFT calculations favor the bent structure with a $^4B_2$ ground state derived from a $^4\Pi_g$ state.[92] As mentioned,[83] the bending potential of $V(CO)_2$ is very flat, and this molecule can easily be linear in the gas phase.

There is disagreement on $V(CO)_3$: an argon matrix 1920 $cm^{-1}$ band was assigned to the trigonal species,[97] whereas a gas-phase time-resolved infrared study reported a 1859 $cm^{-1}$ absorption.[99] The ESR spectrum in a neon matrix revealed a doublet ground state.[54] Our DFT calculation predicted a $^2A_1$ ground state with $C_{3v}$ symmetry and a strong $\nu_3$ fundamental at 1799 $cm^{-1}$; however, no absorption in this region can be assigned to this molecule in a neon matrix,[92] but a 1910.8 $cm^{-1}$ band follows the annealing profile for $V(CO)_3$.

The structures of $V(CO)_4$ and $V(CO)_5$ remain undetermined; infrared spectra in rare-gas matrices suggest a $T_d$ or $D_{4h}$ geometry for the $V(CO)_4$ molecule and a $D_{3h}$ geometry for $V(CO)_5$.[97] Morton and Preston reported an electron spin resonance study of $V(CO)_4$ and $V(CO)_5$ in a krypton matrix produced by $\gamma$ irradiation of $V(CO)_6$; their results indicated a $^2B_2$ ground state with distorted trigonal bipyramid ($C_{2v}$) symmetry for $V(CO)_5$ and a high-spin $^6A_1$ ground state with tetrahedral symmetry for $V(CO)_4$.[55]

$V(CO)_6$ was first synthesized in 1959 via high-pressure reductive carbonylation of $VCl_3$ at 120 °C[100] and spectroscopically studied by infrared absorption,[101] electron spin resonance,[102] and nuclear magnetic resonance.[103] In the gas phase, $V(CO)_6$ is subject to a dynamic Jahn−Teller effect and appears to be approximately octahedral; the C−O stretching vibration is observed at 1986 $cm^{-1}$ in the gas phase[99] and at 1984.3 $cm^{-1}$ in solid neon.[92]

Binary tantalum carbonyls have been prepared by reactions of tantalum atoms with CO in an argon matrix and tentatively identified by infrared spectroscopy.[104] The $Nb(CO)_x$ and $Ta(CO)_x$ ($x$ = 1−6) carbonyls were recently synthesized by co-deposition of laser-ablated metal atoms and CO molecules in excess neon.[105] CASSCF[106,107] and DFT calculations[105] predicted a $^6\Sigma^+$ ground state for NbCO, which is in agreement with argon matrix ESR study.[18] The ground state of TaCO was predicted to be $^4\Delta$, with a $^6\Sigma^+$ state very close in energy.[105,107] The ground states of NbCO and TaCO correlate with ground-state Nb($^6$D) and Ta($^4$F) atoms[74] and CO($^1\Sigma^+$) and are observed at 1932.0 and 1865.2 $cm^{-1}$, respectively, in solid neon.[105]

## D. Cr Group

Unsaturated group 6 carbonyls have been extensively studied in rare-gas matrices,[10,33−35] solution,[108] and the gas phase.[109−112] The Turner group produced

the penta-, tetra-, and tricarbonyls in rare-gas matrices for characterization by infrared spectroscopy.[33−35] The pentacarbonyls were found to have the $C_{4v}$ structure, while $C_{2v}$ and $C_{3v}$ structures were determined for the tetra- and tricarbonyls. Gas-phase time-resolved infrared absorption studies by the Weitz,[109] Rosenfeld,[110,111] and Rayner[112,113] groups provided evidence that these unsaturated molecules adopt the same structures. The latter investigations also found that bimolecular rate constants for CO addition to $Cr(CO)_n$ ($n = 2-5$) and $Mo(CO)_n$ ($n = 3-5$) were within an order of magnitude of the gas kinetic collision rate, indicating that the ground states of the tri-, tetra-, and pentacarbonyls all have the same spin, which is singlet for these species.

The CrCO molecule was characterized by Weltner and co-workers, who reported a 1977 $cm^{-1}$ absorption from the co-deposition of thermal Cr atoms and CO diluted in argon.[10] Laser-ablated Cr gave a 1975.6 $cm^{-1}$ argon matrix absorption,[114] which shifted to 2018.4 $cm^{-1}$ in solid neon,[115] a relatively large argon-to-neon matrix shift.[82] The CrCO molecule was predicted to have a $^7A'$ ground state which correlates with ground-state Cr atom and CO ($^1\Sigma^+$).[83−85] The ground-state CrCO molecule adopts a bent geometry.[116] The 5$\sigma$ orbital of CO does not point directly toward the metal in bent CrCO, and the $\sigma$ repulsion can be reduced; this repulsion, coupled with the fact that sd$\sigma$ hybridization is not possible for the $^7S$ state of Cr due to the spin coupling of the s and d$\sigma$ orbitals, acts as a driving force for bending. The MoCO and WCO complexes exhibit low-spin ground states,[117] which arise from the smaller Mo and W s to d promotion energy than that found for Cr. Because the low-spin state has lower repulsion due to s to d promotion and more metal to CO $\pi$ donation, the C−O stretching frequencies significantly decreased to 1881.2 and 1859.2 $cm^{-1}$, respectively, for MoCO and WCO in solid neon.[115]

The group 6 $M(CO)_x$ carbonyls have also been investigated in solid neon in our laboratory.[115] The neon matrix studies give a strong 1832.9 $cm^{-1}$ band, which exhibits a 1/2/1 triplet with $^{12}CO + {}^{13}CO$ and an associated weaker 1982.1 $cm^{-1}$ band for $Cr(CO)_2$; our BP86 calculations provide 1882.3 ($b_2$) and 1963.8 $cm^{-1}$ ($a_1$) modes for $^5A_1$ ground-state $Cr(CO)_2$. Chromium dicarbonyl appears at 1821.5 $cm^{-1}$ in solid argon.[115] The bands considered earlier for $Cr(CO)_2$ in solid methane at 1903 $cm^{-1}$ and in the gas phase at 1914 $cm^{-1}$ must be due to another species.[33,109] The gas-phase, neon matrix, and argon matrix results appear to be compatible for $Cr(CO)_{3,4,5,6}$ (Table 1).

Although binuclear complexes are only peripheral to this review, the strongest product band in Cr experiments, even stronger than CO precursor at 0.1% in neon,[115] is at 1735.4 $cm^{-1}$; so brief mention will be made of $(Cr_2)(CO)_2$. This band becomes a sharp triplet at 1735.4, 1715.6, 1698.9 $cm^{-1}$ with a weak 1799.0 $cm^{-1}$ band for the mixed isotopic molecule of lower symmetry using $^{12}CO + {}^{13}CO$. Our DFT calculations find a low-energy $^3A_u$ rhombus structure $OC(Cr_2)CO$ with two bridging carbonyls; the geometrical parameters are 1.761 Å Cr−Cr bond, 2.070 Å Cr−C bond, and 1.183 Å C−O bond. This rhombus has calculated carbonyl frequencies of 1795.6 $cm^{-1}$ ($b_{1u}$, 2271 km/mol) and 1862.3 $cm^{-1}$ ($a_g$, 0 km/mol) that are in excellent agreement with the observed bands. This rhombus structure is the dimer of CrCO and exhibits substantial Cr−Cr bonding.

## E. Mn Group

Mn has a $^6S$ ($3d^54s^2$) ground-state configuration, and the two lowest excited states are $^6D(3d^64s^1)$ and $^8P$ ($3d^54s^14p^1$). Because both of these atomic excited states are very high in energy, a weakly bound $^6\Sigma^+$ van der Waals complex, derived from ground-state Mn ($^6S$), might be expected for the ground state of MnCO. Although Huber et al. tentatively assigned an 1850 $cm^{-1}$ band in argon to MnCO,[118] similar studies in the Weltner group[10] and our group failed to produce this absorption.[41] Instead, we assign a weak new 1933.6 $cm^{-1}$ band in solid argon and 1950.7 $cm^{-1}$ in solid neon to MnCO, in agreement with a 1955 $cm^{-1}$ prediction by DFT/BP86 for MnCO.[41] Fenn and Leopold[59] measured the photoelectron spectra of $MnCO^-$, and two states of the neutral MnCO were observed. The lower state of neutral MnCO is 1.115 ± 0.006 eV above the ground state of the $MnCO^-$ anion. The Mn−CO and C−O stretching vibrational frequencies for this state of MnCO are 370 ± 20 and 1955 ± 15 $cm^{-1}$, respectively. The upper state of the MnCO neutral is 2610 ± 20 $cm^{-1}$ above the lower state; the Mn−CO and C−O stretching frequencies are 430 ± 10 and 1925 ± 15 $cm^{-1}$. On the basis of ACPF calculations,[119] these two MnCO states are assigned as $^6\Pi$ and $^4\Pi$; hence, the MnCO ground state is $^6\Pi$ and not $^6\Sigma^+$. Both TcCO and ReCO were found to be very weakly bonded in $^4\Sigma^-$ ground states with respect to the ground state $^6S$ metal atoms and CO.[120]

The strongest features in reactions of laser-ablated Mn and Re with CO in excess neon are at 1865.7 and 1905.4 $cm^{-1}$. These strong bands give the 1/2/1 triplets with $^{12}CO + {}^{13}CO$, which is characteristic of a dicarbonyl absorption. DFT calculations support these $Mn(CO)_2$ and $Re(CO)_2$ assignments. $Mn(CO)_3$ and $Mn(CO)_4$ are also formed by diffusion and further reaction of CO in these experiments.[41]

Among this group carbonyls, $Mn(CO)_5$ and $Re(CO)_5$ have received the most study and are now well characterized. Turner and co-workers produced the $Mn(CO)_5$ radical via UV photolysis of $HMn(CO)_5$ in a CO matrix at 10 K; the IR absorption spectrum at 1988, 1978 $cm^{-1}$ suggested that $Mn(CO)_5$ has a square pyramidal $C_{4v}$ structure with an axial−equatorial bond angle of (96 ± 3)°.[121] This reassignment of $Mn(CO)_5$ from the earlier thermal Mn atom work[118] is in agreement with our laser-ablation experiments in solid argon and neon[41] and the gas-phase assignment.[122] By reacting $Mn(CO)_5Cl$ or $Mn(CO)_5Br$ with Na or Ag atoms using a rotating cryostat, Howard and co-workers generated $Mn(CO)_5$ in a $C_6D_6$ matrix at 77 K for examination by ESR spectroscopy.[53] The ESR spectrum is characteristic of anisotropic interactions between one unpaired electron, one Mn nucleus, and the magnetic field; the unpaired electron occupies an $a_1$ orbital. This characterization has been confirmed for $Mn(CO)_5$ from the photolysis or radiolysis of $HMn(CO)_5$ in solid argon[123] or krypton[124] in a sealed tube at 77 K.

The $Re(CO)_5$ radical was first detected in a mass spectroscopic study of $Re_2(CO)_{10}$ vapor.[125] Wrighton

and Bredesen investigated the photoreaction of $Re_2(CO)_{10}$ with $CCl_4$ and provided evidence for a $Re(CO)_5$ radical.[126] However, photolysis of $Re_2(CO)_{10}$ apparently does not give $Re(CO)_5$. By reaction of Re atoms with CO, Huber et al. produced $Re(CO)_5$ in argon matrix for IR study and suggested that $Re(CO)_5$ also has a square pyramidal $C_{4v}$ structure.[127] These argon matrix observations are in accord with our neon matrix experiments.[41]

## F. Fe Group

A considerable amount of experimental and theoretical work has been done to elucidate the fundamental physical properties of binary unsaturated iron carbonyls. Poliakoff and Turner were the first to obtain direct spectroscopic evidence for unsaturated $Fe(CO)_4$ and $Fe(CO)_3$ in rare-gas matrices from photodissociation of the saturated $Fe(CO)_5$ precursor;[30−32] $Fe(CO)_4$ is an important intermediate. The $Fe(CO)_4$ molecule has $C_{2v}$ symmetry with three IR-active absorptions, and $Fe(CO)_3$ is trigonal with $C_{3v}$ symmetry and two IR absorption bands in the C−O stretching region. The $Fe(CO)_2$ and FeCO molecules were reported from early reactions of thermal iron atoms with CO in solid argon; a 1898 $cm^{-1}$ absorption was first assigned to the C−O stretching vibration of FeCO and an 1860 $cm^{-1}$ absorption to the $Fe(CO)_2$ molecule.[9,128] However, in the diode laser spectroscopic studies of iron carbonyl radicals generated by ultraviolet laser photolysis of $Fe(CO)_5$ in a supersonic jet, the C−O stretching vibration of FeCO was determined to be 1946.5 $cm^{-1}$ and the antisymmetric stretching vibration of linear $Fe(CO)_2$ was measured at 1928.2 $cm^{-1}$.[48−50] The latter studies with rotational resolution provide definitive identifications and suggest that the original matrix infrared spectra are in fact due to another species.

Reactions of iron atoms with CO were reinvestigated in our laboratory using the laser-ablation technique, which showed that the earlier matrix assignments to FeCO and $Fe(CO)_2$ are incorrect.[42,43] On the basis of concentration studies, isotopic shifts, and DFT calculations, the FeCO molecule is observed at 1922.0 $cm^{-1}$ in argon and at 1933.7 $cm^{-1}$ in neon and the antisymmetric C−O stretching vibration for $Fe(CO)_2$ is observed at 1879.2 $cm^{-1}$ in solid argon and 1917.1 $cm^{-1}$ in neon, which are compatible with the gas-phase high-resolution results[48−50] considering the expected matrix shifts. The neon matrix spectrum[43] for iron and $^{12}C^{16}O + {}^{13}C^{16}O$ gives a mixed isotopic 1/1 doublet for FeCO and 1/2/1 triplet for $Fe(CO)_2$. The $Fe(CO)_3$, $Fe(CO)_4$, and $Fe(CO)_5$ absorptions appeared on annealing to allow diffusion and further reaction of CO and on irradiation. Sweany also produced the same $Fe(CO)_4$ bands upon photolysis of $H_2Fe(CO)_4$ in solid argon.[129] Although our laser-ablation studies provide new assignments for FeCO and $Fe(CO)_2$, the same infrared absorptions were observed for $Fe(CO)_{3,4,5}$ as first reported from the photodissociation experiments with $Fe(CO)_5$.[30−32] The 1898 $cm^{-1}$ band first assigned[9,128] to FeCO has been reassigned to $Fe_2CO$, a species of considerable interest in its own right.[42]

On the theoretical side, there has been long discussion on the ground state of FeCO.[76,83−85,130−147] Berthier and co-workers found $^3\Sigma^-$ to be the ground state, with a $^5\Sigma^-$ state lying 12 kcal/mol higher in energy using the CIPSI method.[134] At the MCPF level, the quintet state was predicted to be 1.6 kcal/mol more stable than the triplet state.[137] Even the CCSD(T) level of theory in a quintuple basis set predicts the $^5\Sigma^-$ state to be lower.[145] Very recent MRCI calculations, including the Davidson correction, yield the $^3\Sigma^-$ state slightly below the $^5\Sigma^-$ state.[146] Earlier DFT-based calculations indicated that the $^3\Sigma^-$ state is more stable than the quintet state.[136,147] Clearly it is very difficult to accurately compute this small energy separation. The Villalta and Leopold[38] photodetachment studies of $FeCO^-$ showed vibrationally resolved transitions to two electronic states of neutral FeCO, and the $^3\Sigma^-$ state was assigned as the ground electronic state, with the quintet state about 1135 $cm^{-1}$ higher in energy. DFT calculations predicted that $Fe(CO)_2$, $Fe(CO)_3$, and $Fe(CO)_4$ all have triplet ground states with linear, trigonal planar, and distorted tetrahedral $C_{2v}$ structures, in agreement with experimental observations.[42,43]

There are interesting matrix effects on the FeCO and $Fe(CO)_2$ molecules. Our experimental and calculational results strongly suggest that FeCO in argon has a $^3\Delta$ ground state, while in neon, the ground state is a $^3\Sigma^-$ state as is in the gas phase.[42,43] We note that FeCO increases on annealing in neon but not in argon. Apparently $^5D$ iron atoms react readily with CO to form $^3\Sigma^-$ FeCO in neon but not to form $^3\Delta$ FeCO in argon on annealing. However, RuCO ($^3\Delta$) increases on annealing in both matrices. The $Fe(CO)_2$ molecule is demonstrated to be linear in the gas phase from the observation of alternately missing spin components in the antisymmetric vibration band spectrum.[50] The $Fe(CO)_2$ molecule is probably linear in solid neon as no symmetric C−O stretching vibration is observed; however, it is bent in solid argon based on the observation of the symmetric C−O stretching mode at 1984.8 $cm^{-1}$. As the bent molecule has a large dipole moment, the bent state is stabilized due to stronger argon matrix solvent interaction. The 1876 $cm^{-1}$ band in solid methane presumed due to a lower carbonyl[30] is probably due to bent $Fe(CO)_2$. Our DFT calculations suggest that the bent and linear states are within a few kcal/mol of each other,[42] so such a matrix effect on structure is reasonable.

Compared to iron carbonyls, ruthenium and osmium carbonyls have received far less attention, in part because the ruthenium and osmium pentacarbonyl precursor molecules are unstable. The infrared spectrum of $Os(CO)_4$ has been observed at 1972 and 1955 $cm^{-1}$ from photolysis of $Os(CO)_5$ in a methane matrix.[32] Broad absorptions have been reported for the tetracarbonyls and tricarbonyls in gas-phase time-resolved infrared spectroscopic studies.[148,149] Recently, the $Ru(CO)_x$ and $Os(CO)_x$ ($x = 1-4$) molecules were produced by co-deposition of laser-ablated Ru and Os with CO in neon, and infrared spectra and DFT calculations were reported.[150] The tetracarbonyls were computed to have $D_{2d}$ symmetry. Both experimental spectra and DFT calculations showed that the tricarbonyls have T-shaped structures with $C_{2v}$ symmetry and the dicarbonyls have linear structures. According to DFT calculations RuCO has a $^3\Delta$ ground state, as shown by high-level calculations,[151]

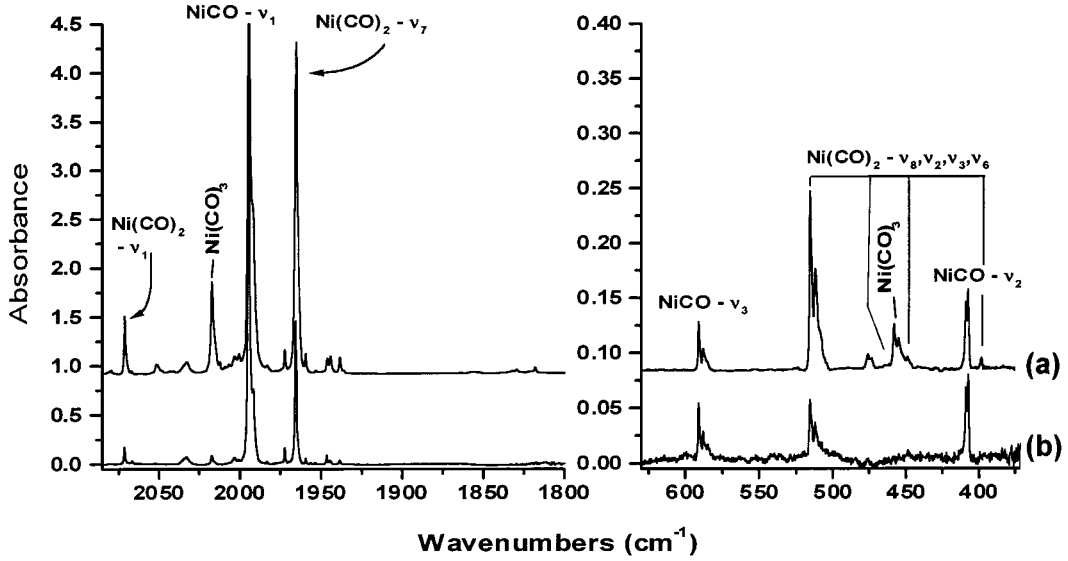


**Figure 7.** Concentration study for NiCO and $Ni(CO)_2$ produced by reaction of thermally evaporated Ni atoms and CO in excess argon during co-deposition at 9 K. Infrared spectra in the 2100−1800 and 650−370 $cm^{-1}$ regions. (a) Ni/CO/Ar = 0.4/2/100, and (b) Ni/CO/Ar = 0.1/0.5/100, with the absorbance scale multiplied by 6 to scale approximately the NiCO absorptions. (Figure courtesy of L. Manceron).

but OsCO has the $^3\Sigma^-$ ground state as does the FeCO molecule.[150] Within the iron group, we see a reversal in the trend going down the transition series rows from 1933.7 to 1925.6 to 1973.8 $cm^{-1}$ for the monocarbonyl complex.

## G. Co Group

$Co(CO)_4$ was first observed by Keller and Wawersik from the sublimation of $Co_2(CO)_8$ at 77 K.[152] Subsequently, the existence of $Co(CO)_4$ has been confirmed by several studies.[153−155] In 1975, Hanlan et al. isolated $Co(CO)_{1-4}$ in solid Ar, Kr, and Xe and characterized the complexes by infrared and electron spin resonance spectroscopy[155] and others investigated $Co(CO)_4$ by ESR.[156,157] Theoretical calculations[158] predicted that ground-state $Co(CO)_4$ has a pyramidal structure with $C_{3v}$ symmetry and three IR-active C−O stretching modes, which is consistent with the observed spectrum. Our subsequent laser-ablation experiments are in agreement with the early thermal work on $Co(CO)_{1-4}$.[155,159] The tricarbonyl $Co(CO)_3$ is a planar trigonal species with $D_{3h}$ symmetry, and the doubly degenerate C−O streching vibration was observed at 1983.2 $cm^{-1}$ in solid argon.[159] Our DFT calculations predicted that the $Co(CO)_2$ molecule has a bent $^2A_1$ ground state with a quite open C−Co−C angle and two IR-active C−O stretching vibrations; however, the symmetric mode is much weaker than the antisymmetric mode, so only one C−O stretching vibration was observed in solid argon.[159] The CoCO complex was recorded at 1960.7 $cm^{-1}$ in solid argon and at 1973.9 $cm^{-1}$ in solid neon.[159,160] All calculations performed on CoCO have predicted a $^2\Delta$ ground state with a linear geometry, which correlates with ground-state Co atom.[84,85,159,160]

The neutral $Rh(CO)_{1-4}$ and $Ir(CO)_{1-4}$ species were identified in solid argon in earlier thermal atom experiments;[161,162] however, recent investigations of laser-ablated Rh and Ir reactions in excess neon produce better resolved spectra for these neutral species.[160,163] The RhCO and IrCO molecules also have the $^2\Delta$ ground state[164−168] and show an increase down the row to 2022.5 and 2024.5 $cm^{-1}$ in solid neon.[160] The isolated $Rh(CO)_2$ and $Ir(CO)_2$ dicarbonyls are linear as evidenced by one IR-active C−O stretching vibration and DFT predictions. The $Rh(CO)_3$ and $Ir(CO)_3$ molecules have T-shaped structures with $C_{2v}$ symmetry, as do the isoelectronic $Ru(CO)_3^-$ and $Os(CO)_3^-$ anions. One strong C−O stretching vibration was observed for the $Rh(CO)_4$ and $Ir(CO)_4$ molecules, and DFT calculations suggest that $Rh(CO)_4$ and $Ir(CO)_4$ molecules have $D_{2d}$ structure with the $C_{3v}$ structure slightly higher in energy.[160] This $D_{2d}$ structure has been determined by ESR, which shows that $Co(CO)_4$ has a different structure, namely $C_{3v}$.[169]

## H. Ni Group

Nickel tetracarbonyl was the first metal carbonyl to be prepared,[8] and nickel group carbonyls are among the most studied metal carbonyls both experimentally[25,26,104,170−175] and theoretically.[78,84,85,141,143,176−189] The neutral $M(CO)_x$ ($x = 1-4$) carbonyls have been synthesized using the matrix-isolation technique, and their infrared spectra have been reported.[25,26,104,170−175] Very recently the complete vibrational spectrum has been recorded for the important NiCO intermediate by Joly and Manceron using thermal evaporation of nickel atoms for reaction with CO in excess argon.[26] These workers measured the intense carbonyl fundamental at 1994.5 $cm^{-1}$ and the much weaker Ni−C stretch at 591.1 $cm^{-1}$ and the bending mode at 409.1 $cm^{-1}$ (Figure 7). It is significant to note that the latter two bands are 0.5% and 1% of the carbonyl mode intensity. The assignments are confirmed by isotopic substitution at all atomic positions and through observation of the overtone and combination bands of the carbonyl fundamental. Most of what we know about binary transition-metal carbonyl intermediates is based on the strong carbonyl mode, but in the case of NiCO very careful measurements in the mid-IR and far-IR *on the same sample* have provided a more complete picture of the bonding in NiCO.

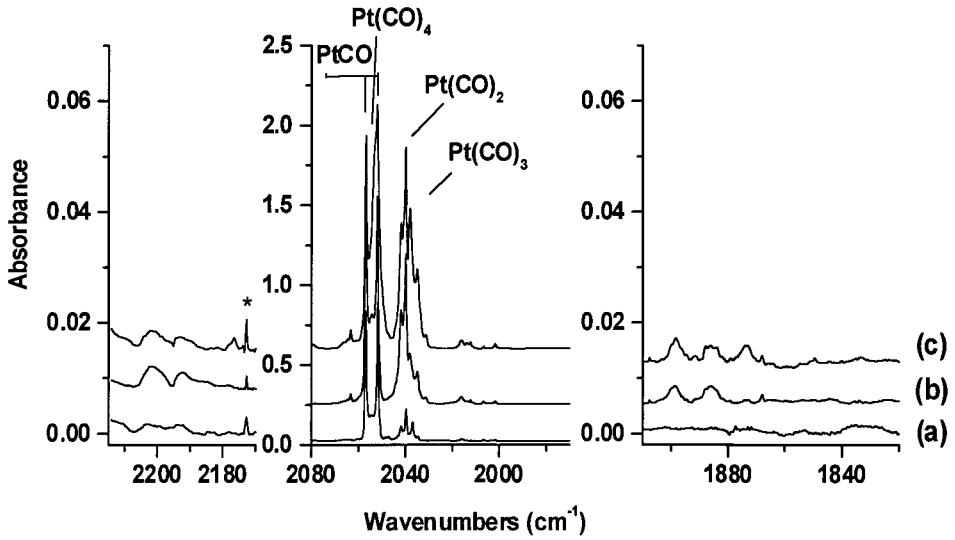


**Figure 8.** Infrared spectra in the 2215−2170, 2080−1970, and 1910−1820 $cm^{-1}$ regions for thermally evaporated Pt atoms co-deposited with CO in excess argon at 9 K. (a) Pt/CO/Ar = 0.03/0.5/100, absorbance scale ×4, (b) Pt/CO/Ar = 0.07/2/100 deposition, and (c) same as (b) after annealing. (Figure courtesy of L. Manceron).

The $Ni(CO)_{1-4}$ carbonyls blue shift on going from argon to neon matrices by 12.1, 13.4, 7.8, and 5.1 $cm^{-1}$, respectively, which indicates relatively little matrix interaction and demonstrates consistency in the assignments.[26,175] The Ni group monocarbonyls have $^1\Sigma^+$ electronic ground states and show an increase in C−O frequency going down the Ni, Pd, Pt group from 2006.6 to 2056.4 to 2065.5 $cm^{-1}$ in solid neon and from 1994.5 to 2044.2 to 2054.3 $cm^{-1}$ in solid argon.[26,173−175] The 2140 ± 60 $cm^{-1}$ fundamental for PdCO deduced from the photoelectron spectrum[60] of $PdCO^-$ is too high and probably suffers from inaccuracy in the weak fine structure band measurement. A fine structure measurement[37] in the $NiCO^-$ PES at 1940 ± 80 $cm^{-1}$, however, is within the matrix NiCO fundamental values. Ab initio calculations show that peaks in the $NiCO^-$ photodetachment spectra are consistent with a bound $^3\Pi$ state and possibly a $^3\Sigma^+$ state of NiCO, in addition to the ground $^1\Sigma^+$ state.[37,182]

Manceron and co-workers investigated PdCO and PtCO in detail and found an interesting increase in the Pt−C stretching and Pt−C−O bending modes from the PdCO values.[173] These results show that perturbation of the CO ligand is an unreliable indicator of the evolution of metal−ligand interaction energies in contrast to the metal−carbon force constant. Comparisons with theoretical predictions, including relativistic effects,[189] of the fundamental frequencies indicate a systematic underestimation of the bending frequencies, which is especially sensitive for heavy metal monocarbonyls, although the carbonyl frequencies are more reliably predicted.[174] Clearly an accurate description of the TM−carbon bond is a more difficult theoretical challenge than the CO bond, and more far-IR studies are needed to measure the TM−carbon frequencies and to test theoretical calculations.

The dicarbonyl molecules were first claimed to be linear based on the absence of the symmetric C−O stretching mode in the infrared spectrum;[25,104,170] however, recent IR studies have shown that the $Ni(CO)_2$ molecule is bent as the symmetric vibration is observed in argon (Figure 7) and neon matrices.[171−175] The bent $Ni(CO)_2$ structural characterization is further supported by DFT calculations.[136,172,175] Again, the far-IR spectrum reveals crucial Ni−C stretching and Ni−C−O bending modes.[172]

The recent thermal Pd investigation found two sharp absorptions at 2050.3 and 2044.2 $cm^{-1}$ for PdCO and a weaker 2051.6 $cm^{-1}$ absorption for $Pd(CO)_2$, which requires a revision of several earlier assignments.[25,173] The new argon matrix and neon matrix assignments are in accord.[173,175] The mid-IR region of the spectrum from a very recent thermal Pt study in solid argon is illustrated in Figure 8. Two sharp absorptions at 2056.8 and 2051.9 $cm^{-1}$ are identified as PtCO. Increasing CO concentration produced new bands near 2040 $cm^{-1}$, which give a 1/2/1 triplet with mixed $^{12}CO/^{13}CO$, identify $Pt(CO)_2$, and revise the older assignment.[25] The lower frequency region (not shown) also reveals important Pt−C stretching and Pt−C−O bending modes for PtCO and $Pt(CO)_2$. The combination of symmetric and antisymmetric C−O modes was observed for $Pt(CO)_2$, but the symmetric C−O fundamental was absent from the spectrum. The $Pd(CO)_2$ and $Pt(CO)_2$ molecules might be linear as the symmetric C−O stretching vibrational modes were not observed in solid argon and neon; however, the possibility of nonlinear dicarbonyl complexes has been considered, and recent DFT calculations suggest bent forms.[175]

It is generally accepted that the nickel group tricarbonyls are trigonal planar molecules with $D_{3h}$ symmetry and the tetracarbonyls are tetrahedral molecules with $T_d$ symmetry. Infrared spectra for the platinum species are shown in Figures 9 and 10 using laser ablation and solid neon; note the different intensity scales and the 2 orders of magnitude greater intensities for the neutral over the charged species. Clearly, laser ablation produces mostly neutral atoms under the conditions of these experiments. Note the absence of charged species in the appropri-

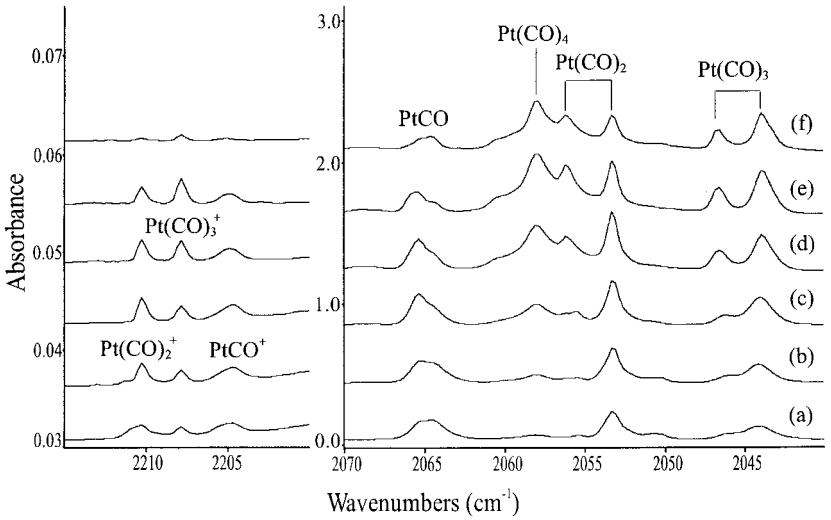


**Figure 9.** Infrared spectra in the 2215−2200 and 2070−2040 $cm^{-1}$ regions for laser-ablated Pt co-deposited with 0.2% CO in neon at 4 K: (a) sample deposited for 40 min, (b) after 6 K annealing, (c) after 10 K annealing, (d) after 11 K annealing, (e) after 12 K annealing, and (f) after 240−580 nm photolysis.

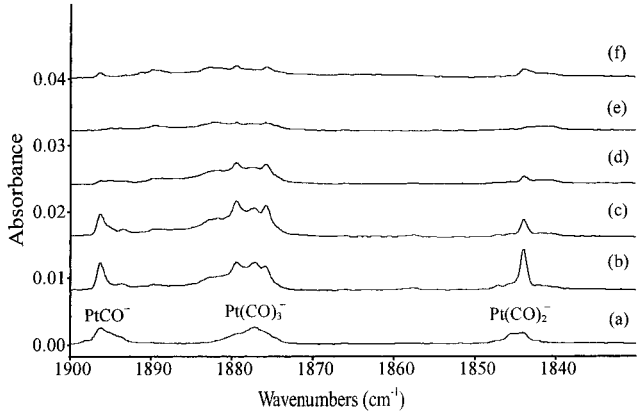


**Figure 10.** Infrared spectra in the 1900−1830 $cm^{-1}$ region for laser-ablated Pt co-deposited with 0.2% CO in neon at 4 K: (a) sample deposited for 35 min, (b) after 8 K annealing, (c) after >470 nm photolysis, (d) after >380 nm photolysis, (e) after 240−580 nm photolysis, and (f) after 12 K annealing.

ate regions of the thermal platinum experiments using solid argon (Figure 8) and the fortunately better resolution of different $Pt(CO)_{1-4}$ species in solid neon.

## I. Cu Group

There have been a large number of spectroscopic studies of the interaction of Cu group metal atoms with CO in rare-gas solids.[19,20,80,190−197] In very early work, Odgen found that reaction of copper and CO at 12 K gave an IR spectrum with two bands in the C−O stretching region attributable to copper carbonyls.[190] In similar studies, Ozin and co-workers synthesized $Cu(CO)_x$ ($x = 1-3$), $Ag(CO)_x$ ($x = 1-3$), and $Au(CO)_x$ ($x = 1, 2$) and characterized them by infrared spectroscopy.[191−193] Although the AgCO assignment has been challenged and AgCO explained as a silver atom perturbed by CO,[20,198] the $Cu(CO)_{1-3}$ assignments have been confirmed by very recent thermal work[196] and the $Ag(CO)_{2,3}$ and $Au(CO)_{1,2}$ identifications supported by recent neon matrix investigations.[197] For comparison, infrared spectra of copper carbonyls in solid neon are illustrated in Figure 11. Again, the stoichiometric identification is based on mixed isotopic multiplet absorptions and the $Cu(CO)_{1-3}$ species are blue shifted 19.4, 13.5, and 18.7 $cm^{-1}$ from solid argon to neon.[80,196] The formation of CuCO, $Cu(CO)_3$, $Ag(CO)_3$, and AuCO has also been confirmed by ESR spectroscopy.[19,20,194,195] These studies suggested that CuCO and AuCO are linear with the $^2\Sigma^+$ ground state and that $Cu(CO)_3$ and $Ag(CO)_3$ are trigonal planar with the $^2A_2''$ electronic ground state in $D_{3h}$ symmetry. It is interesting to note that $Au(CO)_3$ is not a stable species, in contrast to $Cu(CO)_3$ and $Ag(CO)_3$. Even with 10% CO in neon[193] (where no AuCO is trapped and the $Au(CO)_2$ bands are broadened and red shifted 8 $cm^{-1}$ from the isolated $Au(CO)_2$ position of 1943.7 $cm^{-1}$ observed for 0.1% CO in neon,[197] due to apparent perturbation by the gross excess of CO present) $Au(CO)_3$ still does not form. This has been rationalized by the higher $n$s → $n$p promotion energy of gold.[19]

Due to the extra stability of the filled $nd^{10}$ shell of the metal, the bonding in the copper group carbonyls is quite different from the other transition-metal carbonyls. In the case of copper monocarbonyl, most earlier calculations yield a weak van der Waals type interaction with a linear arrangement.[199−214] However, using DFT, Fournier found that CuCO is nonlinear and predicted a binding energy of 80 kJ/mol.[84,116] The bent structure was confirmed by MCPF and CCSD(T) calculations, which gave a much lower binding energy (about 20 kJ/mol) and a quite low barrier to linearity (about 2 kJ/mol).[213] This later binding energy is in good agreement with the experimental value of 25 ± 5 kJ/mol reported by Blitz et al.[215] The structure and binding energy of CuCO have been further studied using extended basis sets with a number of different density functional approaches, and all methods agree in forecasting a bent equilibrium structure with a significant barrier to linearity (about 15 kJ/mol).[214] Finally, on the basis of isotopic shifts in the $\nu_2$ and $\nu_3$ fundamentals of CuCO recently observed in the far-infrared spectrum, Tremblay and

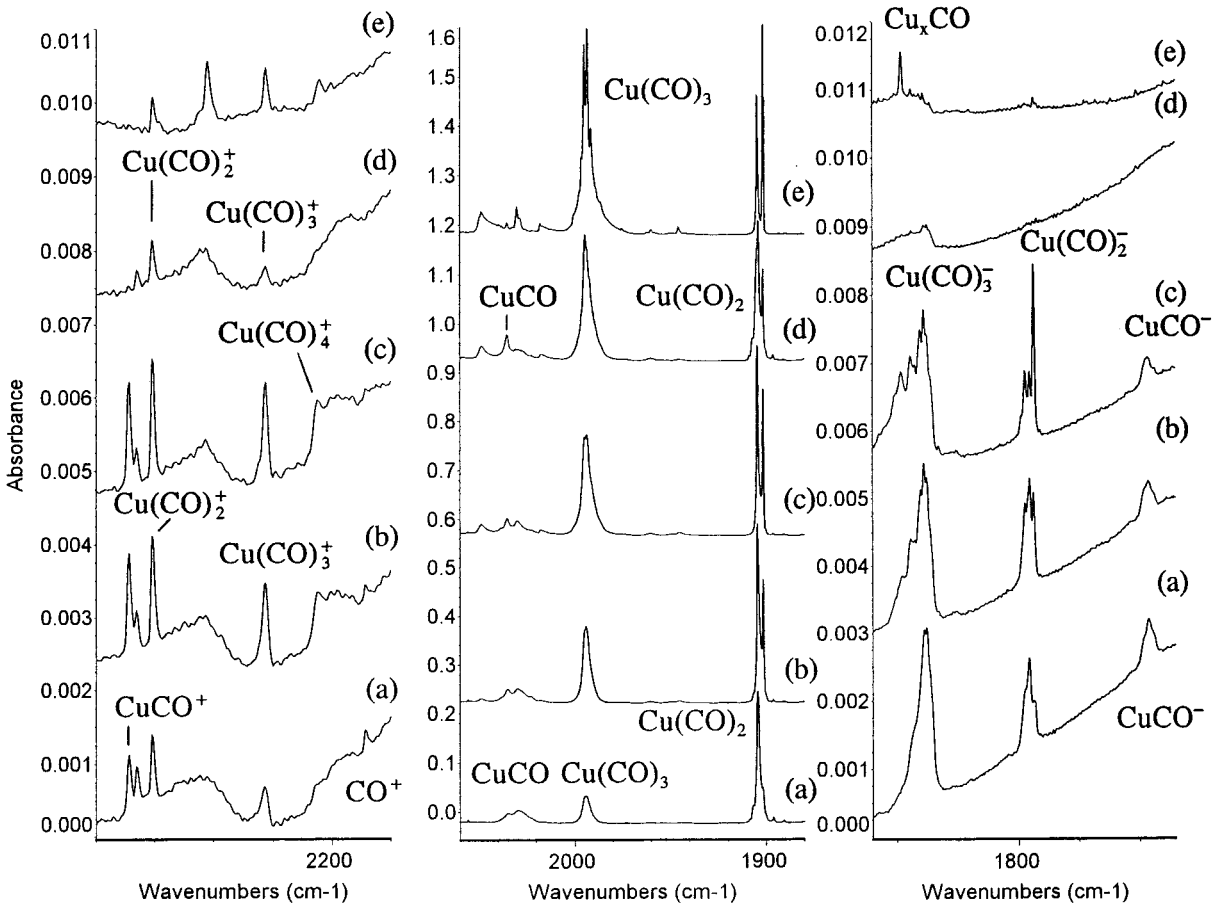


**Figure 11.** Infrared spectra in the 2240−2190, 2040−1880, and 1860−1735 cm$^{-1}$ regions for laser-ablated copper atoms co-deposited with 0.2% CO in neon: (a) 30 min sample deposition at 4 K, (b) after annealing to 6 K, (c) after annealing to 8 K, (d) after 15 min full mercury arc photolysis, and (e) after annealing to 10 K. (Reprinted with permission from ref 80. Copyright 1999 American Physical Society).

Manceron[196] conclude that CuCO is bent with an angle near 160°.

Upon addition of another CO molecule to CuCO, the unpaired electron on Cu is promoted into the $\pi_u$ orbital, which significantly changes the situation. The $Cu(CO)_2$ molecule has a $^2\Pi_u$ ground state with linear equilibrium geometry and is more strongly bound due to the reduction of two-orbital three-electron repulsion interactions and the increase in the metal p$\pi$ to CO $\pi^*$ donation. The bonding remains essentially the same in $Cu(CO)_3$.[80,214]

ESR results showed that the bonding schemes of AuCO and CuCO are very similar,[19,20] while AgCO can only be regarded as an Ag atom perturbed by a CO molecule in the nearest neighbor sphere of the host lattice.[198] The weak Ag−CO interaction is evidenced in the nearly one unpaired electron density in the Ag 5s orbital, negligible density in the 5p orbital, and small $^{13}C$ hyperfine coupling tensor. Kasai and Jones discussed in detail why CuCO and AuCO are stable complexes while AgCO is not, based on energy levels of the valence ($n$ − 1)d, $n$s, and $n$p orbitals of the Cu, Ag, and Au atoms and those of the lone-pair $\sigma$ electrons of CO and its vacant $\pi^*$ orbitals.[19,20] For the CuCO complex, the metal d$\pi$ and CO $\pi^*$ levels are close but the Cu metal s and CO 5$\sigma$ orbitals are far apart, so in CuCO, the $\sigma$ donation is small and the d$\pi \rightarrow$ p* donation is primarily responsible for the formation of CuCO. The valence s and p orbitals of Ag are at the same levels as those of Cu, so the $\sigma$ donation is small, as found for CuCO. However, the increased stability of the valence d orbital level for the second transition row dramatically increases the separation between the Ag d$\pi$ and CO $\pi^*$ levels and therefore reduces the Ag 4d to CO $\pi^*$ donation relative to CuCO. With neither CO $\sigma$ donation to the metal nor metal $\pi$ donation to the CO, it is not surprising that AgCO is not formed. In the case of AuCO, the metal d$\pi$ is between Cu and Ag, so there is more metal $\pi$ donation than for Ag but less than for Cu. The larger CO frequency in AuCO than CuCO is consistent with a smaller $\pi$ donation in AuCO. However, the Au metal s orbital is much closer to the CO 5$\sigma$ than for Cu or Ag; therefore, AuCO has significantly more $\sigma$ donation than either CuCO or AgCO. Thus, Kasai and Jones concluded that both $\sigma$ and $\pi$ donation are operative in AuCO and hence AuCO is a stable complex.[19,20]

## J. Actinide-Metal Carbonyls

The coordination chemistry of CO with actinide elements is a relatively new area of research, in part because of the experimental challenges faced in handling and characterizing actinide complexes. Early matrix infrared experiments with thermal U atoms and CO gave evidence for a number of $U(CO)_x$ species.[216] Recently, we have investigated reactions of laser-ablated Th and U metal atoms with CO

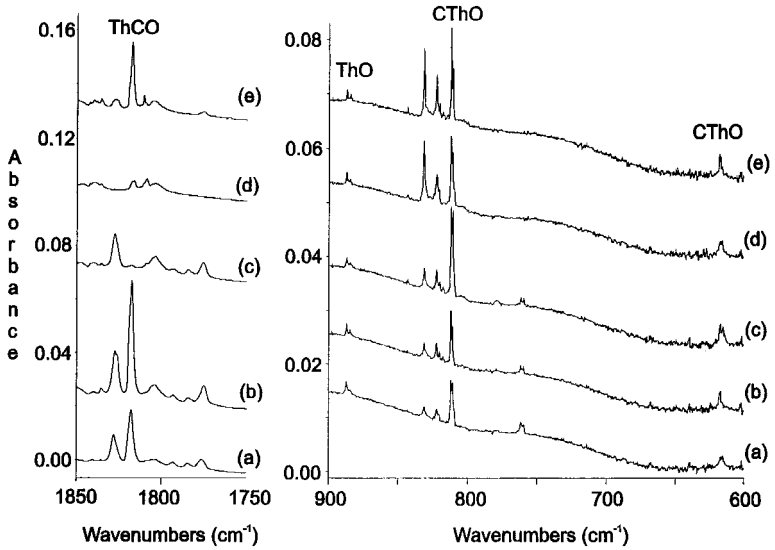


**Figure 12.** Infrared spectra in the 1850−1750 and 900−600 $cm^{-1}$ regions for laser-ablated thorium co-deposited with 0.1% CO in neon at 4 K: Spectrum after (a) 30 min sample deposition, (b) annealing to 8 K, (c) 15 min $\lambda > 470$ nm photolysis, (d) 15 min full-arc photolysis, and (e) annealing to 10 K.

molecules in a neon matrix, and new thorium and uranium carbonyls have been characterized.[217−219] The experimental C−O stretching frequency in ThCO, 1817.5 $cm^{-1}$, is the lowest of any neutral binary terminal metal carbonyl complex, Figure 12, which implies a very large metal to CO $\pi$ donation in this molecule. Scalar relativistic DFT calculations predict ThCO to have a $^3\Sigma^-$ ground state that reflects the Th $7s^26d^2$ ground electron configuration. The UCO molecule has a C−O stretching frequency 100 $cm^{-1}$ higher than ThCO despite the fact that U has a greater number of valence electrons for donation to the CO $\pi^*$ orbital than does Th. The differences between ThCO and UCO are mainly reflective of the much more electropositive nature of thorium.

For Th and U, the dicarbonyls are bent molecules with $C_{2v}$ symmetry while the tricarbonyls are nonplanar trigonal molecules with $C_{3v}$ symmetry and the tetracarbonyls are tetrahedral molecules with $T_d$ symmetry. The bent dicarbonyls are evidenced by strong symmetric C−O stretching vibrations and by relativistic DFT calculations.[217−219]

## K. Photon-Induced Isomerization Reactions

Several unprecedented photon-induced isomerization reactions were observed for several early transition-metal carbonyls and actinide metal carbonyls in our laboratory. Figure 12 shows the spectra of ThCO and CThO and their photolysis behavior. The monocarbonyls of Nb,[105] Th,[218] and U[217] can be isomerized to the inserted carbide−oxide molecules on visible light photolysis, eq 3.

$$MCO + h\nu \rightarrow CMO\ (M = Nb, Th, U) \quad (3)$$

According to relativistic DFT calculations, the uranium insertion product CUO is linear with a singlet ground state and the shortest U−C bond yet characterized; it has a U−C triple bond with substantial U 5f character. The CThO molecule appears to be bent with a triplet ground state, and it is an unsaturated metallocarbene complex analogous to ketenylidene, which has a triplet ground state.[217−220]

The dicarbonyls of the Ti group,[92,93] the V group,[105] and the actinide metals Th and U[217−219] undergo photoinduced isomerization to OMCCO molecules with visible or UV photons, eq 4. The OMCCO molecules can undergo further photochemical rearrangment to the OM−($\eta^3$-CCO) or $(C_2)MO_2$ molecules with UV photons, eqs 5 and 6. The strong metal−oxygen bond provides part of the thermodynamic driving force for these isomerizations.

$$M(CO)_2 + h\nu \rightarrow OMCCO\ (M = Ti, Zr, Hf, Nb, Ta, Th, U) \quad (4)$$

$$OThCCO + h\nu \rightarrow OTh\text{-}(\eta^3\text{-}CCO) \quad (5)$$

$$OMCCO + h\nu \rightarrow (C_2)MO_2 (M = Nb, Ta, U) \quad (6)$$

## L. Addition Reactions in Rare-Gas Matrices and the Gas Phase

The photochemistry of metal carbonyls such as $V(CO)_6$, chromium group hexacarbonyls, $Mn_2(CO)_{10}$, iron group pentacarbonyls, and nickel group tetracarbonyls and the spectroscopy and kinetics of the resultant coordinatively unsaturated carbonyls have been the subject of many studies.[39,40,108,109,221,222] In the gas phase, the rates of reaction of coordinatively unsaturated metal carbonyls with CO are typically very fast but there is a wide range in the magnitudes of rate constants for association reactions. Taking the iron carbonyl system for example, which is the best studied, the association reactions of $Fe(CO)_2$, $Fe(CO)_3$, and $Fe(CO)_4$ with CO have been extensively discussed by Weitz.[13,14] It is well-known that $Fe(CO)_5$ has the singlet ground state, and calculations predicted that $Fe(CO)_4$, $Fe(CO)_3$ and $Fe(CO)_2$ all have triplet ground states.[42,43] The rate constants for CO association with $Fe(CO)_2$ and $Fe(CO)_3$ are larger, consistent with spin conservation. However, the rate constant for CO association with $Fe(CO)_4$ to form $Fe(CO)_5$ is more than 2 orders of magnitude smaller,

as this addition reaction is spin forbidden. The ramifications of spin conservation on the kinetics of association reactions of unsaturated transition-metal carbonyls have been widely studied; although other factors can affect the rate constant, apparently spin conservation is the major effect on the rate constant of ligand addition reactions in the gas phase.

Addition reactions of unsaturated transition-metal carbonyls with CO are quite different in matrix environments. Although kinetic information cannot be obtained in matrix-isolation experiments, some qualitative information can be drawn from annealing and photolysis behavior. In the iron carbonyl systems $Fe(CO)_2$ and $Fe(CO)_3$ are both triplet states. Linear $Fe(CO)_2$ in neon reacting with CO to form $Fe(CO)_3$, which has $C_{3v}$ symmetry, requires a large tricarbonyl geometry change and some activation energy is required; as a result there is no growth on annealing. In solid argon, the $Fe(CO)_2$ molecule is bent, so there is less geometry change and the absorption of $Fe(CO)_3$ increased slightly on annealing. In solid neon, $Fe(CO)_3$ increased greatly on photolysis, and the same applies to the formation of $Fe(CO)_4$ and $Fe(CO)_5$ in both matrices. Apparently, the spin restriction on reaction in the matrix environment is less rigorous than in the gas phase, and geometry change plays an important role in controlling the addition reactions in rare-gas matrices.[42,43] Annealing is an important part of the matrix synthesis as diffusion in the cryogenic solid allows the controlled growth of higher carbonyl complexes, as shown in Figures 5−14.

We noted earlier that FeCO increased on annealing in solid neon but not argon. However, NO is more reactive and FeNO, $Fe(NO)_2$, and $Fe(NO)_3$ all increase on annealing in solid argon.[223] When mixtures of NO and CO are investigated the mixed ligand species Fe(CO)(NO), $Fe(CO)_2(NO)$, $Fe(CO)(NO)_2$, and $Fe(CO)_2(NO)_2$ are observed with the latter dominating on annealing.[224]

## V. Binary Unsaturated Transition-Metal Carbonyl Anions

Carbonyl anions are more difficult to study than the neutral species because anions are more reactive and photosensitive. In general, near-infrared or visible radiation can detach electrons from anionic carbonyls. As early as three decades ago, several reports appeared on the synthesis and spectroscopic characterization of mono- or multinegative charged carbonyl species in solution.[225,226] Since then, many metal carbonyl anions have been prepared through chemical reduction in basic solvents, and recent progress in this field has been reviewed by Ellis.[17a] These anions are of the general type $M(CO)_n^{m-}$, where M is an element from groups 4−9, the ionic charges $m$, falls between −2 and −4, and the coordination numbers $n$ are between 3 and 6. The molecular geometries are comparable to those of typical carbonyls. Multicharged anions are beyond the scope of this review, and only monocharged anions will be discussed. In solution, counterion perturbation is very significant in vibrational spectroscopic studies. Even in the absence of counterion perturbation, the vibrational spectrum is still very sensitive to solvent.[226] Metal carbonyl bond strengths in $M(CO)_n^-$ anions have been determined by energy-resolved collision-induced dissociation investigations,[227,228] and many of these anions are observed in the infrared spectra of laser-ablated metal reaction products to be reviewed here.

Matrix isolation has a number of advantages for studying infrared spectra of transition-metal carbonyl anions. By choosing a suitable noble-gas host, minimal spectral and structural perturbation can be expected. Of more importance, preparation of matrix-isolated carbonyl anions can be done over long periods of time, and the detection sensitivity can thus be enhanced. Again, $CCl_4$ doping can be employed to capture laser-ablated electrons and to identify anion absorptions by their marked reduction in the sample spectrum.[159,171] Various techniques have been used to prepare saturated carbonyl anions, including vacuum-UV irradiation and electron bombardment of saturated neutral carbonyls,[229,230] and these observations will be compared with the present laser-ablation results.

Table 2 lists the experimentally observed C−O stretching frequencies of TM carbonyl anions in rare-gas matrices and in solution. Electron capture by MCO results in the $MCO^-$ anion. The bonding of CO to transition-metal anions is very similar to bonding in neutral MCO, which involves the mechanism of CO $\sigma$ donation to the metal and metal to CO $\pi^*$ donation. In general, addition of an electron to the metal atom results in a significantly larger metal to CO $\pi^*$ donation, and as a result, the C−O stretching vibrational frequency is lowered with respect to the neutral molecules. As can be seen from Tables 1 and 2, the C−O stretching vibrational frequencies of anions are 100−200 $cm^{-1}$ lower than those of the corresponding neutral complexes, which is confirmed by DFT frequency calculations.

### A. Early Transition-Metal Carbonyl Anions

The $ScCO^-$ anion has a $^3\Sigma^-$ ground state, where, relative to the neutral system, the extra electron is added to the open-shell $\sigma$ orbital. The C−O stretching vibration is observed at 1732.0 $cm^{-1}$ in solid neon, which is red shifted by 119.4 $cm^{-1}$ relative to that of the neutral ScCO complex.[87] Clearly the effect of the extra metal $\pi$ donation in the anion is more important than the increase in the $\sigma$ repulsion and the CO vibrational frequency is lower for the anion than the neutral. Our DFT calculation also predicted a triplet ground state for $Sc(CO)_2^-$ with bent structure, where the bending helps to reduce the $\sigma$ repulsion. Unfortunately, no experimental evidence was found for this anion.[87]

The $TiCO^-$ anion was predicted to have a $^4\Delta$ ground state which correlates mainly with the $^4F$ ground state of $Ti^-$ and the $^1\Sigma^+$ state of CO, and the C−O stretching vibration was observed at 1789.9 $cm^{-1}$ in solid neon.[92] The $Ti(CO)_2^-$ anion was computed to have a $^4B_2$ ground state as the isoelectronic $V(CO)_2$ molecule, and the symmetric and antisymmetric C−O stretching vibrations were observed at 1742.1 and 1677.5 $cm^{-1}$ in solid neon. $Ti(CO)_3^-$ is

**Table 2. C−O Stretching Vibrational Frequencies ($cm^{-1}$) for Binary Unsaturated Transition-Metal Carbonyl Anions**

| | Ne | Ar | solution | ref | | Ne | Ar | solution | ref |
|---|---|---|---|---|---|---|---|---|---|
| $ScCO^-$ | 1732.0 | | | 87 | $Ru(CO)_2^-$ | 1830.6 | 1834.2 | | 150 |
| $TiCO^-$ | 1789.9 | | | 92 | | 1766.5 | 1756.9 | | |
| $Ti(CO)_2^-$ | 1742.1 | | | 92 | $Ru(CO)_3^-$ | 1823.6 | 1810.3 | | 150 |
| | 1677.5 | | | | $Ru(CO)_4^-$ | 1864.8 | 1857 | | 150 |
| $Ti(CO)_3^-$ | 1730.9 | | | 92 | ($D_{2d}$) | 1860.1 | | | |
| $Ti(CO)_4^-$ | 1760.6 | | | 92 | $Ru(CO)_4^-$ | 1881.0 | 1882.0 | | 150 |
| $Ti(CO)_5^-$ | 1824.5 | | | 92 | ($C_{3v}$) | 1868.6 | 1862.4 | | |
| $Ti(CO)_6^-$ | 1861.0 | | | 92 | $OsCO^-$ | 1785.5 | | | 150 |
| $Zr(CO)_2^-$ | 1745.9 | | | 93 | $Os(CO)_2^-$ | 1898.8 | | | 150 |
| | 1682.2 | | | | | 1783.5 | | | |
| $Hf(CO)_2^-$ | 1747.4 | | | 93 | $Os(CO)_3^-$ | 1843.1 | | | 150 |
| | 1681.0 | | | | | 1826.9 | | | |
| $VCO^-$ | 1806.7 | | | 92 | $Os(CO)_4^-$ | 1866.3 | | | 150 |
| $V(CO)_2^-$ | 1777.9 | | | 92 | ($D_{2d}$) | 1858.3 | | | |
| | 1670.6 | | | | $Os(CO)_4^-$ | 1882.6 | | | 150 |
| $V(CO)_3^-$ | 1714.3 | | | 92 | ($C_{3v}$) | 1862 | | | |
| $V(CO)_4^-$ | 1792.6 | | | 92 | $CoCO^-$ | 1820.2 | 1804.0 | | 159, 160 |
| | 1775.3 | | | | $Co(CO)_2^-$ | 1847.1 | 1860.2 | | 159, 160 |
| $V(CO)_5^-$ | 1835.1 | | | 92 | | 1789.2 | 1768.9 | | |
| $V(CO)_6^-$ | | 1864 | 1843 | 230 | $Co(CO)_3^-$ | 1829.1 | 1826.9 | | 159, 160 |
| $Nb(CO)_2^-$ | 1768.6 | | | 105 | $Co(CO)_4^-$ | 1894.8 | 1890.0 | 1887 | 159, 160, 225 |
| | 1656.7 | | | | $RhCO^-$ | 1828.6 | 1813.7 | | 160, 163 |
| $Nb(CO)_3^-$ | 1793.7 | | | 105 | $Rh(CO)_2^-$ | 1900.4 | | | 160, 163 |
| | 1713.7 | | | | | 1816.7 | 1799.4 | | |
| $CrCO^-$ | 1678.0 | | | 115 | $Rh(CO)_3^-$ | 1864.8 | 1851.9 | | 160, 163 |
| $Cr(CO)_2^-$ | 1705.0 | | | 115 | $Rh(CO)_4^-$ | 1906.4 | 1901.5 | 1900 | 160, 163, 241 |
| $Cr(CO)_5^-$ | | 1855 | | 230 | $IrCO^-$ | 1842.6 | | | 160 |
| | | 1838 | | | $Ir(CO)_2^-$ | 1818.1 | | | 160 |
| $Mo(CO)_2^-$ | 1718.7 | | | 115 | $Ir(CO)_3^-$ | 1860.4 | | | 160 |
| $WCO^-$ | 1640.8 | | | 115 | $Ir(CO)_4^-$ | 1901.8 | | 1898 | 160, 242 |
| $W(CO)_2^-$ | 1751.5 | | | 115 | $NiCO^-$ | 1860.6 | 1847.0 | | 171, 175 |
| $MnCO^-$ | 1807.5 | 1789.4 | | 41 | $Ni(CO)_2^-$ | 1813.8 | 1801.7 | | 171, 175 |
| $Mn(CO)_2^-$ | 1756.2 | 1754.9 | | 41 | $Ni(CO)_3^-$ | 1864.7 | 1858.8 | | 171, 175, 230 |
| $Mn(CO)_3^-$ | 1781.8 | | | 41 | $PdCO^-$ | 1909.0 | | | 175 |
| $ReCO^-$ | 1728.0 | 1713.7 | | 41 | $Pd(CO)_2^-$ | 1832.3 | | | 175 |
| $Re(CO)_2^-$ | 1788.7 | | | 41 | $Pd(CO)_3^-$ | 1872.2 | | | 175 |
| $FeCO^-$ | 1782.0 | 1770.3 | | 42,43 | $PtCO^-$ | 1896.3 | | | 175 |
| $Fe(CO)_2^-$ | 1732.9 | 1815.0 | | 42,43 | $Pt(CO)_2^-$ | 1844.0 | | | 175 |
| | | 1721.9 | | | $Pt(CO)_3^-$ | 1875.8 | | | 175 |
| $Fe(CO)_3^-$ | 1794.5 | 1786.5 | | 42,43 | $CuCO^-$ | 1746.2 | 1733.4 | | 80 |
| $Fe(CO)_4^-$ | 1859.7 | 1853.5 | | 42,43, 230 | $Cu(CO)_2^-$ | 1793.9 | 1780.8 | | 80 |
| $RuCO^-$ | 1792.8 | 1782.5 | | 150 | $Cu(CO)_3^-$ | 1838.9 | 1829.7 | | 80 |

expected to have a $^2A_1$ ground state with $C_{3v}$ symmetry like the isoelectronic $V(CO)_3$ complex.

The $VCO^-$ anion in the $^5\Sigma^+$ ground state has a C−O stretching vibration at 1806.7 $cm^{-1}$ in solid neon.[92] $V(CO)_2^-$ is predicted to have a $^5A_1$ ground state with bent geometry, and the symmetric and antisymmetric C−O stretching vibrations are observed at 1777.9 and 1670.6 $cm^{-1}$ in neon. $V(CO)_3^-$ anion has a $^1A_1$ ground state with $C_{3v}$ symmetry as does the isoelectronic $Cr(CO)_3$ molecule. The doubly degenerate C−O stretching vibration is observed at 1714.3 $cm^{-1}$ in neon.[92] Two bands at 1792.6 and 1775.3 $cm^{-1}$ in neon were tentatively assigned to the $V(CO)_4^-$ anion with $C_{2v}$ symmetry as is the isoelectronic $Cr(CO)_4$ molecule. It is not clear whether the $V(CO)_5^-$ is a singlet or triplet. Molecular orbital calculations suggest that the ground-state $V(CO)_5^-$ should be a $d^6$ singlet with $C_{4v}$ symmetry as is the isoelectronic $Cr(CO)_5$ molecule;[231,232] however, experimental observation of low reactivity with two electron donor ligands suggests that $V(CO)_5^-$ is a 16 electron triplet.[233] The saturated $V(CO)_6^-$ anion is an octahedral singlet, which has been observed in solution and solid argon.[230]

The $Cr(CO)_5^-$ anion has been identified by 1855, 1838 $cm^{-1}$ frequencies in solid argon[230] and characterized as a doublet ground state with a square pyramidal $C_{4v}$ structure like the isoelectronic $Mn(CO)_5$ molecule. Molecular orbital calculations suggest that the $Cr(CO)_4^-$ anion has a doublet ground state with either the $C_{2v}$ or $D_{4h}$ structure.[231,232] Photoelectron spectra of $Cr(CO)_3^-$ indicated a $C_{3v}$ equilibrium geometry like the neutral molecule.[58] McDonald et al. observed that CO adds rapidly to $Cr(CO)_3^-$ and $Cr(CO)_4^-$ in the gas phase, suggesting that both $Cr(CO)_3^-$ and $Cr(CO)_4^-$ have doublet ground states.[234]

The ground state of $MnCO^-$, predicted to be a $^5\Pi$ state derived from a mixture of the $3d^64s^2$ and $3d^54s^24p^1$ occupations of $Mn^-$,[119] is observed at 1807.5 $cm^{-1}$ in solid neon and at 1789.4 $cm^{-1}$ in solid argon.[41] $Mn(CO)_2^-$ is found to have a triplet ground state like the isoelectronic $Fe(CO)_2$ molecule, and $Mn(CO)_3^-$ is also calculated to be a $C_{3v}$ triplet like $Fe(CO)_3$. Slow rates for addition of ligands to $Mn(CO)_4^-$ suggest that it has a triplet ground state like the $Fe(CO)_4$ molecule.[235,236] Following this rationale, $Mn(CO)_5^-$, like $Fe(CO)_5$, has the singlet ground state and trigonal bipyramidal structure.[41,225] Infrared spectroscopic evidence for the $Mn(CO)^-_{1,2,3}$ anions has been found in our laser-ablation matrix-isolation experiments.[41]

## B. Fe Group Carbonyl Anions

The $Fe(CO)_x^-$ ($x = 1-4$) anions have been studied by photoelectron spectroscopy in the gas phase.[37,38] In addition, $Fe(CO)_4^-$ was formed by vacuum-UV irradiation of $Fe(CO)_5$ in solid argon and characterized by infrared absorptions at 1864.2 and 1854.1 $cm^{-1}$.[230] All four binary carbonyl anions $Fe(CO)_x^-$ were prepared in solid argon and neon from co-deposition of laser-ablated iron, electrons, and CO in our laboratory, and the later 1853.5 $cm^{-1}$ argon matrix band for $Fe(CO)_4^-$ is in excellent agreement with the earlier work.[42,43,230] Figure 3 shows the typical spectra of $Fe(CO)_x^-$ in solid neon; the anion yield was relatively higher in solid argon. Earlier photoelectron spectroscopic data suggested that the $FeCO^-$ anion is a doublet. Later higher resolution photoelectron spectroscopic data indicated that $FeCO^-$ has a quartet ground state, in agreement with recent theoretical calculations,[237] which predicted a $^4\Sigma^-$ ground state. Rapid addition of CO to $Fe(CO)_2^-$ and $Fe(CO)_3^-$ in gas-phase investigations suggested that $Fe(CO)_x^-$ ($x = 2-4$) all have doublet ground states.[238] DFT calculations predicted that the $Fe(CO)_2^-$ anion has a linear $^2\Pi_u$ ground state with a bent $^2A_1$ state slightly higher in energy. Analogous to the $Fe(CO)_2$ neutral, the $Fe(CO)_2^-$ anion in neon has a linear geometry, but in argon $Fe(CO)_2^-$ adopts a bent geometry, since both symmetric and antisymmetric C−O stretching vibrations were observed. The $Fe(CO)_3^-$ anion was predicted to have a $^2A_1'$ ground state with $D_{3h}$ symmetry, which was confirmed from the infrared spectrum of the mixed isotopically substituted molecule. Recent B3LYP calculations predicted a $^2A_1$ ground state for $Fe(CO)_4^-$ with $C_{3v}$ symmetry, as is the isoelectronic $Co(CO)_4$ molecule, in agreement with earlier infrared structural characterization in a solid argon matrix.[230]

The matrix photochemistry of $Fe(CO)_{1-4}^-$ is different from the gas-phase ion cyclotron mass spectroscopy result in that electron detachment dominates in the matrix[42,43,230] whereas CO dissociation is favored in the gas phase.[239,240] This may be governed by the relative ease of diffusion of an electron compared to a CO ligand away from the anion site in the matrix cage.

The Ru and Os carbonyl anions exhibit different properties from Fe carbonyl anions. Both $RuCO^-$ and $OsCO^-$ have $^2\Delta$ ground states, and $Ru(CO)_2^-$ and $Os(CO)_2^-$ appear to have bent $^2B_2$ ground states. The $Ru(CO)_3^-$ and $Os(CO)_3^-$ anions have T-shaped $C_{2v}$ geometries, like the isoelectronic $Rh(CO)_3$ and $Ir(CO)_3$ molecules. For $Ru(CO)_4^-$ and $Os(CO)_4^-$, two structural isomers coexist in the neon matrix; one form exhibits the $C_{3v}$ geometry like $Fe(CO)_4^-$, and the other form has the $D_{2d}$ structure.[150]

## C. Co Group Carbonyl Anions

The properties of group 9 carbonyl anions are very similar, except for the monocarbonyl anions. The $CoCO^-$ anion was predicted to have a $^3\Delta$ ground state, arising from adding an extra electron to an empty $\sigma$ orbital, relative to the $^2\Delta$ ground state of CoCO. For $RhCO^-$ and $IrCO^-$, the $^1\Sigma^+$ configuration is the ground state.[159,160] The singlet state can utilize sd$\sigma$ hybridization to remove s electron density from the metal−C region and reduce repulsion. This occurs for the second and third transition rows because the s and d orbitals are more similar in size and the increased stability of the metal d orbitals relative to the first transition row. The dicarbonyl anions have $^1A_1$ ground states with bent structures. Infrared spectra and DFT calculations both indicate that the tricarbonyl anions have $^1A_1'$ ground states with $D_{3h}$ symmetry. The tetracarbonyl anions exhibit $^1A_1$ ground states with $T_d$ symmetry, as do the isoelectronic molecules of the Ni group tetracarbonyls. All 12 of these anions have been observed in our laser-ablation experiments, and the frequencies are listed in Table 2.

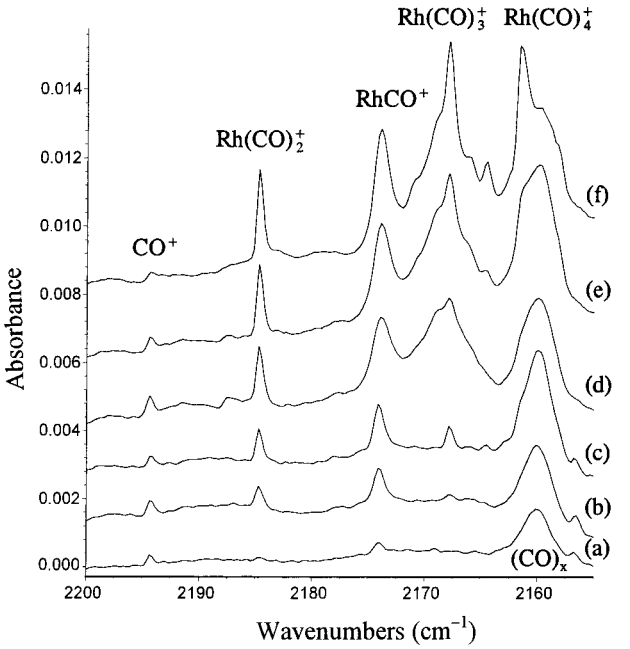


**Figure 13.** Infrared spectra in the 2200−2155 $cm^{-1}$ region for laser-ablated Rh co-deposited with CO in neon at 4 K after (a) 0.1% CO sample co-deposited for 60 min, (b) 0.2% CO sample deposited for 60 min, (c) annealing to 8 K, (d) 0.2% CO sample with 0.1% $CCl_4$ co-deposited for 60 min, (e) annealing to 8 K, and (f) annealing to 11 K.

Figures 13 and 14 illustrate the rhodium carbonyl cation and anion regions and show the effect of concentration, annealing, photolysis, and $CCl_4$ doping. Note the growth of higher carbonyl species on annealing, the *enhancement* of cation bands in the upper region, and the *reduction* of anion absorptions in the lower region with added $CCl_4$ electron trap. Also note that $Rh(CO)_4^-$ is the most photostable as it increases on 290−580 nm irradiation before decreasing with 240−580 nm photolysis. In the saturated $M(CO)_4^-$ cases, these anions are known in solution and the strongest infrared absorption is within 10 $cm^{-1}$ of our matrix bands.[225,241,242] Finally, $Co(CO)_4^-$ has been observed by ICR and determined to have a large (≥2.35 eV) electron affinity.[243]

## D. Ni Group Carbonyl Anions

Figure 15 shows IR spectra in the C−O stretching region for nickel carbonyl anions in solid argon, which

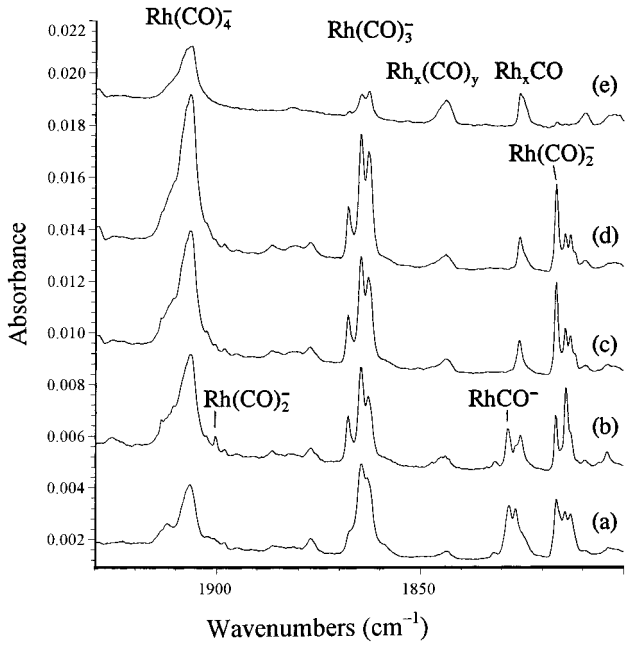


**Figure 14.** Infrared spectra in the 1930−1800 $cm^{-1}$ region for laser-ablated Rh co-deposited with CO in neon at 4 K after (a) 0.1% CO sample co-deposited for 60 min, (b) 0.2% CO sample deposited for 60 min, (c) $\lambda > 380$ nm photolysis, (d) $\lambda > 290$ nm photolysis, and (e) full-arc photolysis.

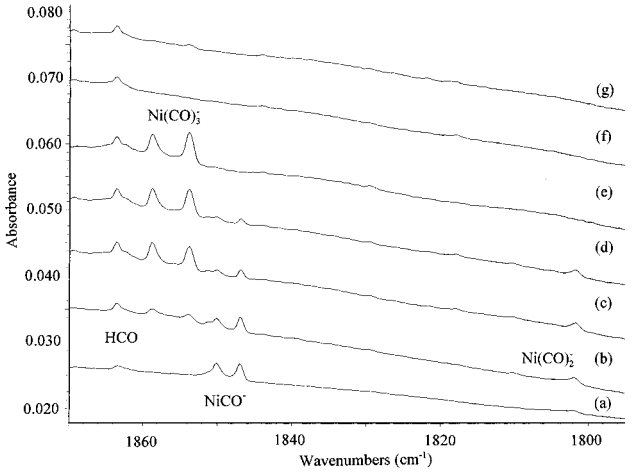


**Figure 15.** Infrared spectra in the 1870−1795 $cm^{-1}$ region for laser-ablated Ni co-deposited with 0.4% CO in argon at 10 ± 1 K: (a) sample co-deposited for 1.5 h, (b) after 20 K annealing, (c) after 25 K annealing, (d) after 850−1000 nm photolysis, (e) after 630−1000 nm photolysis, (f) after 470−1000 nm photolysis, and (g) after 30 K annealing.

may be compared with neon matrix bands 13.6, 12.1, and 5.9 $cm^{-1}$ higher.[171,175] It is important to note that the $Ni(CO)_{1,2,3}^-$ anions were not observed in the thermal Ni experiments (Figure 7).[26,172] $Ni(CO)_3^-$ was first observed at 1857.9 $cm^{-1}$ in solid argon[230] from the vacuum-UV photolysis of $Ni(CO)_4$, which is in excellent agreement with the 1858.8 $cm^{-1}$ assignment from our laser-ablation experiments.[171] The tricarbonyl anions of this group have trigonal planar $D_{3h}$ structures, which is confirmed by DFT calculations and isotopically substituted IR spectra.[171] The ground state of $Ni(CO)_3^-$ is predicted to be a $^2A_2''$ state. Photoelectron spectroscopic measurements suggest that both $NiCO^-$ and $Ni(CO)_2^-$ have doublet ground states.[38] Density functional theoretical calculations predicted that the dicarbonyl anions of this group adopt linear $^2\Pi_u$ ground states in agreement with vibrational spectroscopic results. All three monocarbonyl anions have doublet ground states: the $NiCO^-$ anion forms a $^2\Sigma^+$ state with linear geometry, while $PdCO^-$ and $PtCO^-$ are predicted to be bent.[171,175]

Figure 15 also contrasts the photochemistry of $NiCO^-$, $Ni(CO)_2^-$, and $Ni(CO)_3^-$. The monocarbonyl anion is the most photosensitive: 850−1000 nm photolysis reduced the 1850.1, 1847.0 $cm^{-1}$ absorptions about 40% with no effect on the $Ni(CO)_2^-$ and $Ni(CO)_3^-$ bands, but radiation in the 630−1000 nm region totally destroyed the $NiCO^-$ and $Ni(CO)_2^-$ absorptions, while the 1853.8 $cm^{-1}$ site band of $Ni(CO)_3^-$ increased about 20% with no change for the 1858.8 $cm^{-1}$ site band. Continued photolysis in the 470−1000 nm region destroyed the $Ni(CO)_3^-$ absorptions, which is in agreement with the photodisappearance of $Ni(CO)_3^-$ when irradiated at 2.0−2.5 eV using the techniques of ion cyclotron resonance.[244] The matrix photolysis behavior is in accord with the low electron affinities for the neutral species derived from photoelectron spectra in the gas phase[38] and provides further evidence to support the matrix identification of the $Ni(CO)_x^-$ anions.

## E. Cu Group Carbonyl Anions

The $Cu(CO)_x^-$ anions have been produced in argon and neon matrices and characterized by vibrational spectroscopy and DFT calculations.[80] The CuCO complex adds an electron to form $CuCO^-$ with a $^1A'$ ground state, correlates with ground-state $Cu^-$, and has an usually low carbonyl frequency. As the $Cu(CO)_2$ neutral is a $^2\Pi_u$ ground state with linear geometry, addition of another electron gives two unpaired electrons in the $\pi_u$ orbitals, and results in a $^3\Sigma_g^-$ ground state for the $Cu(CO)_2^-$ anion. The $Cu(CO)_3^-$ anion has $^1A_1$ ground state with trigonal planar geometry. Figure 11 shows copper carbonyl anion spectra in solid neon; again, it is important to note that these features are absent from the thermal copper experiments.[196]

## F. Electron Affinities

The DFT calculations and selected wavelength range photolysis provide some rough measure of the electron affinities of the neutral carbonyl molecules. Before considering the carbonyl species, we first compare $CrO_2$, where the electron affinity has been precisely measured as 2.413 ± 0.008 eV (55.6 kcal/mol) in the gas phase.[245] For this calibration system, our DFT calculations[246] give 53.9 (BP86) and 58.1 kcal/mol (B3LYP) for the adiabatic electron affinity (computed as the energy difference between anion and the neutral, each at its equilibrium geometry), which are very close (±3%) to the experimental electron affinity. The $CrO_2^-$ anion absorption remained unchanged on $\lambda > 380$ nm photolysis and disappeared on $\lambda > 290$ nm photolysis; it appears that approximately 1.0 eV in excess of the gas-phase detachment energy is required for photodetachment in the matrix environment.

The matrix photochemistry of $CuCO^-$ is of interest, in part because no gas-phase data are available. We

**Table 3. DFT Calculated and Experimental Electron Affinities for Neutral Late Transition-Metal $M(CO)_x$ Complexes (kcal/mol)**

| *x* | Mn | Fe | Co | Ni | Cu |
|---|---|---|---|---|---|
| 1 | 25.7[a]<br>25.0[b]<br>24.0[c] | 26.7[a]<br>25.7[b]<br>21.8[c] | 22.3[b] | 18.5[a]<br>19.1[b]<br>13.8[c] | 26.6[b]<br>23.0[c] |
| 2 | 38.2[b] | 28.1<br>32.6[b] | 41.8 | 14.8<br>19.9<br>16.0 | 29.2<br>22.2 |
| 3 | 53.1[b] | 41<br>52[b] | 59.8 | 24.8<br>35.3<br>27.9 | 32.5 |
| 4 | 61.9[d] | 55<br>67 | >54[a]<br>77 | | |

[a] Underlined values are gas-phase experimental, refs 36−38, 59, and 243. [b] BP86/6-311+G*calculated energy difference is second value. [c] B3LYP/6-311+G* calculated energy difference is third value. [d] BP86 $Mn(CO)_4^-$ ($^3B_1$) and $Mn(CO)_4$ ($^2B_2$) energy difference; BP86 difference for $Mn(CO)_5$ is 70.8 kcal/mol.

note that the matrix photolysis of $CuCO^-$ is almost exactly like that observed for $FeCO^-$ in solid argon, which suggests that the electron affinity for CuCO may be near the 26.7 kcal/mol value observed for FeCO.[38] Although DFT energies for anions are subject to error, we also note that our calculated energy for $FeCO^-$ is below FeCO by an amount (25.7 kcal/mol)[42] near the experimental electron affinity[38] and our BP86 calculation finds $CuCO^-$ below CuCO by a similar 26.6 kcal/mol amount. Since DFT/B3LYP energies are commonly more accurate than BP86 energies, we have repeated the calculations for $FeCO(^3\Sigma^-)$, $FeCO^-(^4\Sigma^-)$, $CuCO(^2A')$, and $CuCO^-(^1A')$ with the B3LYP functional. The iron carbonyl anion is 21.0 kcal/mol below the neutral and the copper carbonyl anion is 23.0 kcal/mol below at the B3LYP level, which are in reasonable agreement with the BP86 energy differences.

We list in Table 3 a comparison of experimental (underlined) and DFT electron affinities. The results for both the BP86 and B3LYP functionals are presented. For the two most thoroughly studied metal carbonyl species, Fe and Ni, the electron affinity as a function of number of CO molecules has been measured. Despite the approximation involved, the calculated values are in reasonable agreement with experimental measurements. Note that $Mn(CO)_x^-$, $Co(CO)_x^-$, and $Cu(CO)_x^-$ values increase with *x* just as do the known iron and nickel carbonyl anion measurements. Our DFT calculations suggest that $Ru(CO)_x$ and $Os(CO)_x$ have comparable electron affinities to the iron analogues but $Rh(CO)_x$ and $Ir(CO)_x$ have higher electron affinities than the cobalt and the iron analogues.[150,160] These DFT energy differences provide reliable electron affinity estimates until gas-phase measurements can be made.

## *VI. Binary Unsaturated Transition-Metal Carbonyl Cations*

Binary unsaturated transition-metal carbonyl cations are important as intermediates in the reactions of metal ions with organic systems containing CO, such as aldehydes and ketones.[247,248] The mechanisms of reactions involving these ions are often discussed in terms of the metal ion−ligand bond energies, some of which have been measured in extensive guided ion beam mass spectrometry investigations.[249−253] Due to the high energies needed for their production and to their high reactivity, spectroscopic studies of carbonyl cations are quite difficult.[254−257]

The first method to gain significant use for vibrational spectroscopic study of mononuclear transition-metal carbonyl cations employed strongly oxidizing superacid media.[14b,258,259] Under these conditions, counterions coordinate to the carbonyl cation and influence the CO bonding. For example, the C−O fundamental in $CuCO^+$ ranges from 2127 to 2180 $cm^{-1}$, depending on the counterion,[258,259] but absorbs at 2234 $cm^{-1}$ isolated in solid neon.[80]

After some early reports for synthesis of the $CuCO^+$ and $Cu(CO)_3^+$ cations in salts and acid media,[258,260,261] the Strauss group succeeded in the synthesis and characterization of the carbonyl cation complexes $Cu(CO)_{1-4}^+$, $Ag(CO)_{1-3}^+$, and $Au(CO)_{1-2}^+$ by using weakly coordinating counterions[262−266] including $Sb_2F_{11}^-$, $OTeF_5^-$, and $B(OTeF_5)_4^-$. These compounds are stable enough to be isolated as crystalline solids under CO atmosphere or at low temperature. New homoleptic carbonyl cations of the type $M(CO)_n^{m+}$ (with M = group 8−11, $n = 6, 4, 2$ and $m = 1, 2, 3$) have been synthesized by Aubke and co-workers via carbonylation of metal salts in such superacids as fluorosulfuric acid and "magic acid" $(HSO_3F)$-$(SbF_5)$.[267−274] Thermally stable salts with $Sb_2F_{11}^-$ as counterion are obtained with antimony pentafluoride as the reaction medium. As noted above, these cationic species exhibit higher C−O stretching vibrational frequencies due to the very small metal $\pi$ donation to the CO ligands. However, vibrational perturbations from the medium must be recognized.

Matrix isolation is perhaps the most efficient technique for studying infrared spectroscopy of isolated carbonyl cations. Although cations interact more with the matrix than neutrals, recent studies have shown that with a suitable choice of host matrix, well resolved and relatively unperturbed spectra of cations can be obtained.[254−257] Cations are unique to laser-ablation experiments as thermal evaporation produces only neutral species. Recently, Van Zee and Weltner observed ESR spectra of $Ni^+$, $Pd^+$, and $Pt^+$ cations in solid argon and krypton, and Knight and

**Table 4. C−O Stretching Vibrational Frequencies ($cm^{-1}$) for Binary Unsaturated Transition-Metal Carbonyl Cations**

| | Ne | media | ref | | Ne | media | ref |
|---|---|---|---|---|---|---|---|
| $ScCO^+$ | 1962.4 | | 87 | $Ni(CO)_2^+$ | 2205.3 | | 175 |
| $Sc(CO)_2^+$ | 1926.0 | | 87 | $Ni(CO)_3^+$ | 2192.4 | | 175 |
| $TiCO^+$ | 2041.3 | | 92 | | 2186.2 | | |
| $VCO^+$ | (2116.3)[a] | | 92 | $Ni(CO)_4^+$ | 2176.2 | | 175 |
| $CrCO^+$ | 2200.8 | | 115 | $PdCO^+$ | 2206.4 | | 175 |
| $MoCO^+$ | 2189.1 | | 115 | $Pd(CO)_2^+$ | 2210.5 | | 175 |
| $MnCO^+$ | 2089.5 | | 41 | $PtCO^+$ | 2204.7 | | 175 |
| $FeCO^+$ | 2123.0 | | 42,43 | $Pt(CO)_2^+$ | 2210.3 | | 175 |
| $Fe(CO)_2^+$ | 2134.0 | | 42,43 | $Pt(CO)_3^+$ | 2207.9 | | 175 |
| $RuCO^+$ | 2134.9 | | 150 | $CuCO^+$ | 2234.4 | 2178, 2127 | 17b, 80, 258 |
| $OsCO^+$ | 2106.0 | | 150 | $Cu(CO)_2^+$ | 2230.4 | 2164 | 80, 259, 262 |
| $CoCO^+$ | 2165.5 | | 160 | $Cu(CO)_3^+$ | 2211.3 | 2179 | 80, 259, 262 |
| $Co(CO)_2^+$ | 2168.9 | | 160 | $Cu(CO)_4^+$ | 2202.1 | 2183 | 80, 259, 262 |
| $RhCO^+$ | 2174.1 | | 160, 163 | $AgCO^+$ | 2233.1 | 2204, 2197 | 197, 263, 265 |
| $Rh(CO)_2^+$ | 2184.7 | 2115 | 160, 163, 283 | $Ag(CO)_2^+$ | 2234.6 | 2209 | 197, 265 |
| $Rh(CO)_3^+$ | 2167.8 | | 160, 163 | $Ag(CO)_3^+$ | 2216.0 | 2192 | 197, 266 |
| $Rh(CO)_4^+$ | 2161.5 | 2138 | 160, 283 | $Ag(CO)_4^+$ | 2205.7 | | 197 |
| $IrCO^+$ | 2156.5 | | 160 | $AuCO^+$ | 2236.8 | 2195 | 197, 268 |
| $Ir(CO)_2^+$ | 2153.8 | | 160 | $Au(CO)_2^+$ | 2233.4 | 2211, 2217 | 197, 267, 268 |
| $NiCO^+$ | 2206.5 | | 175 | $Au(CO)_3^+$ | 2203.5 | | 197 |
| | | | | $Au(CO)_4^+$ | 2193.4 | | 197 |

[a] In an argon matrix.

co-workers also reported reactions of $Pd^+$ using laser ablation.[275] Due to its higher ionization energy and lower polarizability, neon is the most suitable matrix host for cation investigations.

Recent evolution of the laser-ablation technique in our laboratory has extended neon matrix infrared spectroscopy to the study of unsaturated transition-metal carbonyl cations. As mentioned, laser ablation of metal targets also produces metal cations and photons ranging from vacuum ultraviolet to visible, and hence, metal carbonyl cations can be formed via metal cation and CO reactions or by photoionization of neutral metal carbonyls. The presence of an electron trap also greatly facilitates the survival and identification of cations in the matrix. By adding a small amount of the electron trap molecule $CCl_4$ (<10% of CO) to the matrix gas/CO mixture, the yield of cations is enhanced (usually two to four times) while the yield of anions is reduced (usually to less than 10%) with little effect on neutral species. Figures 2, 3, 9, 11, and 13 show typical spectra for carbonyl cations prepared by co-deposition of laser-ablated metals with CO in excess neon.

Numerous theoretical studies of small transition-metal carbonyl cations have been performed,[73,78−80,276−282] and for a systematic study of first- and second-row transition-metal mono- and dicarbonyl cations, see ref 276. As discussed above, the bonding mechanisms for the cations are similar to the neutral carbonyl molecules but the relative importance of the bonding contributions changes. For the cations, the metal d to $\pi^*$ donation is, in general, much smaller than for the neutrals. As the number of CO ligands increases, the increasing CO $\sigma$ repulsion favors the $3d^{n+1}$ states over the $3d^n4s^1$ states and the metal d to $\pi^*$ donation increases. This is similar to the neutrals, but for a given number of CO molecules, the cation donation is naturally smaller than for the analogous neutral. For the cation, $sd\sigma$ hybridization and s to d promotion are important mechanisms for reducing the $\sigma$ repulsion, but in the cations, the p orbital lies too high in energy to permit efficient hybridization, so $sp\sigma$ hybridization effects are small. Electrostatic effects in the cation bonding interaction are found to be important.[73,79]

Table 4 lists the observed C−O stretching vibrational frequencies of transition-metal cations in solid neon and in superacid media. Compared to the neutral molecules, the C−O stretching vibrational frequencies of cations are normally higher by about 100−200 $cm^{-1}$, which is consistent with the reduction in metal to CO $\pi$ donation. For the earlier transition-metal carbonyl cations, the C−O stretching frequency is usually lower, and for later transition-metal carbonyl cations, the C−O stretching vibrational frequency is normally higher than the free CO molecule frequency. This is consistent with the increasing second ionization potential with increasing nuclear charge and therefore a decrease in the metal to CO $\pi^*$ donation with heavier metals.

## A. Early Transition-Metal Carbonyl Cations

The C−O stretching vibration of $ScCO^+$, 1962.4 $cm^{-1}$ in neon and 1923.5 $cm^{-1}$ in argon, is the lowest frequency binary terminal transition-metal carbonyl cation yet known.[87] The $ScCO^+$ cation has a $^3\Sigma^-$ ground state derived from the $3d^2(^3F)$ $Sc^+$ excited-state lying 13.8 kcal/mol above the ground state.[74,276] It is interesting to note that $ScCO^+$ has very large $\pi^*$ donation for a cation, which increases the CO bond length and decreases the C−O stretching vibrational frequency.

The C−O stretching vibrational frequency of $TiCO^+$, 2041.3 $cm^{-1}$ in neon, is also lower than that of the free CO molecule. The ground state of $TiCO^+$ is predicted to be $^4\Delta$, which correlates with the $3d^3$ ($^4F$) state $Ti^+$ lying 2.3 kcal/mol above the $3d^24s^1(^4F)$ ground state.[74,276] No band could be assigned to $VCO^+$ in solid neon. The $^5\Sigma^+$ ground state was predicted at 2098.5 $cm^{-1}$ by DFT, and the strong 2140 ± 10 $cm^{-1}$ CO precursor absorption probably masks $VCO^+$.

However, a 2116.3 $cm^{-1}$ argon matrix band behaves appropriately for $VCO^+$, and this observation may have been made possible by the larger argon matrix shift for the cation species.

The $CrCO^+$ cation has a $^6\Sigma^+$ ground state, derived from the $3d^5$ ($^6S$) $Cr^+$ state. Due to the stability of the half-filled $d^5$ configuration, the $CrCO^+$ cation is weakly bonded[276] and the C−O stretching vibrational frequency is observed at 2200.8 $cm^{-1}$ in neon,[115] above CO and even the $CO^+$ value of 2194.3 $cm^{-1}$ in solid neon.[160] The $Cr(CO)_2^+$ cation is predicted to have a $^6\Sigma_g^+$ ground state.[276] Preston and co-workers prepared the $Cr(CO)_4^+$ cation in a krypton matrix via $\gamma$-irradiation of $Cr(CO)_6$, and ESR spectra showed that the chromium atom is tetrahedrally bound to four CO submolecules in a $^6A_1$ ground state.[56]

## B. Fe Group Carbonyl Cations

The three monocarbonyl cations of this group adopt $^4\Sigma^-$ ground states derived from the $d^7$($^4F$) metal cation states, although the $^4F$ state of $Fe^+$ is 5.8 kcal/mol higher in energy than the $3d^64s^1$ ($^6D$) ground state, while for $Ru^+$ and $Os^+$, the $^4F$ state is the ground state. The C−O stretching frequencies are very close for these three metal carbonyl cations (Table 4).[42,43,150] The dicarbonyl cations of this group have $^4\Sigma_g^-$ ground states, which correlate with ground-state monocarbonyl cations.[43,150,276] ESR study of $Fe(CO)_5^+$ in chromium hexacarbonyl crystal indicated that $Fe(CO)_5^+$ has a $^2A_1$ ground state with $C_{4v}$ symmetry.[57] Our laser-ablation experiments characterized $FeCO^+$, $RuCO^+$, and $OsCO^+$ at 2123.0, 2134.9, and 2106.0 $cm^{-1}$ in solid neon and $Fe(CO)_2^+$ at 2134.0 $cm^{-1}$ in solid neon.[43,150]

## C. Co Group Carbonyl Cations

The monocarbonyl cations of this group all have $^3\Delta$ ground states derived from $3d^8$ ($^3F$) ground-state metal cations. The C−O stretching frequencies were observed at 2165.5, 2174.1, and 2156.5 $cm^{-1}$ in solid neon, respectively.[159,160] The dicarbonyl cations form $^3\Delta_g$ ground states that correlate with adding CO to the ground-state monocarbonyl cations.[160,276] The antisymmetric C−O stretching frequencies were observed for Co, Rh, and Ir dicarbonyl cations at 2168.9, 2184.7, and 2153.8 $cm^{-1}$ in solid neon, respectively.[159,160] Figure 13 shows the $Rh(CO)_{1-4}^+$ cation region. Note the CO concentration dependence on the relative populations of the 1, 2, 3 carbonyl cations and the increase in cation yield on doping with $CCl_4$ to capture ablated electrons. Note also the strong growth of $Rh(CO)_4^+$ on the last annealing cycle. Finally, the $Rh(CO)_4^+$ cation with carborane anions gives a strong IR absorption at 2138 $cm^{-1}$, some 24 $cm^{-1}$ lower than our neon matrix value of 2162 $cm^{-1}$ for the isolated $Ru(CO)_4^+$ cation.[160,283] Clearly counterion interaction perturbs the carbonyl vibrations.

## D. Ni Group Carbonyl Cations

The monocarbonyl cations of the nickel group have $^2\Sigma^+$ ground states, which correlate with ground-state metal cations and almost the same frequencies in solid neon (Table 4),[175] again suggesting the importance of electrostatic effects.[73] The dicarbonyl cations form linear $^2\Sigma_g^+$ ground states.[175,276] The tricarbonyl cations have T-shaped structures with $C_{2v}$ symmetry and the tetracarbonyl cations the $D_{2d}$ structure instead of $T_d$.[175] Figure 9 shows growth of the $Pt(CO)_{1-3}^+$ cations on annealing and reaction of $Pt^+$ and CO in solid neon. In our laser-ablation experiments, the $MCO^{+,0,-}$ species have been observed for the Ni, Pd, and Pt metals in solid neon,[175] and from the infrared absorptions for the trapped $MCO^{+,0,-}$ species and the calculated infrared intensities, we estimate that cation and electron ablation is 2−3% of neutral atom ablation, assuming that different charged species are equally reactive.

## E. Cu Group Carbonyl Cations

All of the $M(CO)_x^+$ ($x = 1-4$) cations of this group exhibit singlet ground states which are derived from ground-state metal cations. The monocarbonyl and dicarbonyl cations are linear, while the tricarbonyl cations are trigonal planar, and the tetracarbonyls have the tetrahedral structure.[80,164,280] Several groups have reported the synthesis of copper group carbonyl cations using weakly coordinating counteranions.[260−268] A striking feature of these carbonyl cations is that the C−O stretching frequencies are higher than that of free CO, which is supported by theory.[73,78−80] More recently, we produced the isolated copper carbonyl cations in solid neon from the reaction of laser-ablated $Cu^+$ and CO,[80] as shown in Figure 11. As carbonyl cations in media are usually stabilized by coordination with counteranions, the C−O stretching frequencies depend on the counteranions and exhibit frequencies 19−56 $cm^{-1}$ lower than the neon matrix-isolated cations. The same applies to $Ag(CO)_{1,2,3}^+$ and $Au(CO)_{1,2}^+$ (Table 4). Taking the copper carbonyl cations for example, the C−O stretching frequencies decrease with increasing CO coordination number, as predicted by DFT calculations,[80] but a different situation is observed in superacid media[259,283] owing to structure-dependent media perturbations. In our neon matrix investigations, the same general frequency decrease with increasing CO subunits is observed for the silver and gold carbonyl cations as that found for copper carbonyl cations.[80,197]

# *VII. Carbonyls in Complex Ions and Supported Metal Catalyst Systems*

There is an extensive literature for the use of CO as a probe for the state of transition metals on supported oxide and zeolite catalyst systems. It is relevant to compare late first row and rhodium investigations with the spectra of isolated $MCO^+$ species in solid neon to gain better understanding of the local catalyst sites.

Transition-metal(II) ions supported on amporphous $AlPO_4$ have given the following monocarbonyl frequencies: Mn, 2198 $cm^{-1}$; Fe, 2180 $cm^{-1}$; Co, 2189 $cm^{-1}$; Ni, 2093 $cm^{-1}$; Cu, 2220 $cm^{-1}$.[284] What is the local charge on the metal ions as reflected in the carbonyl frequencies? Comparison with the $MCO^+$ frequencies in Table 4 shows that the supported Mn,

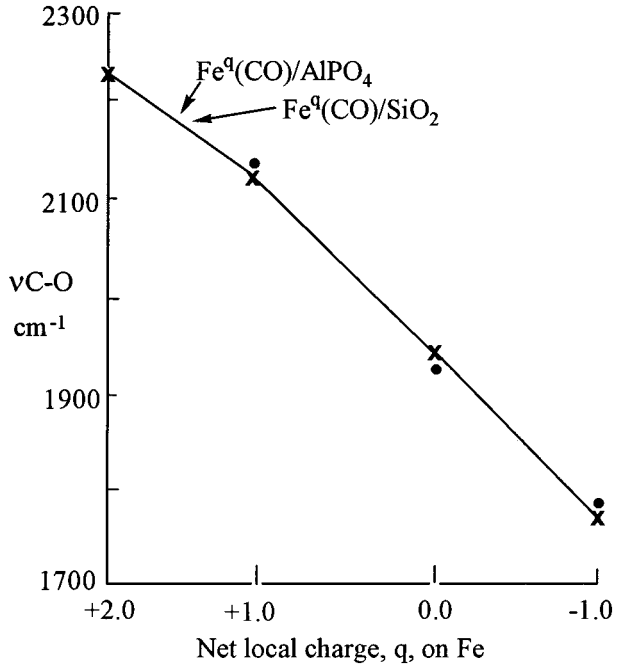


**Figure 16.** Plot of observed and calculated (BP86/6-311+G*) carbonyl frequencies for FeCO species vs net local charge on each FeCO species: (×) calculated frequencies and (• • •) the experimental values.

Fe, Co, Ni, and Cu values are 108, 57, and 23 $cm^{-1}$ higher and 13 and 14 $cm^{-1}$ lower, respectively. This suggests first that the supported Ni and Cu states are just below +1 and that the supported Co, Fe, and Mn states are above +1 but not near as high as +2. Figure 16 shows a plot of carbonyl frequencies vs charge, $q$, for BP86 calculated (×) and neon matrix observed (•) $Fe(CO)^q$ frequencies.[42] This plot suggests, based on the observed carbonyl probe frequency, that $q = +1.4$ for $Fe^q(CO)/AlPO_4$ and $q = +1.3$ for $Fe^q(CO)/SiO_2$. A new calculation for $FeCO^{2+}$ gives a $^3\Sigma^-$ state 405 kcal/mol above $FeCO^+$, with 1.885 and 1.126 Å bond lengths and 2220.4 $cm^{-1}$ carbonyl frequency, which is included in the plot.

In examining responses of the $Fe(CN)_2(CO)$ subunit to electronic charges in [NiFe] hydrogenases, we note that for $Fe^{II}$ complexes the C−O frequency ranges from 1950 to 2000 $cm^{-1}$ and for $Fe^{I}$ species the frequency appears from 1860 to 1900 $cm^{-1}$.[285] This work shows large blue shifts in the coordinated C−O fundamental on electrochemical oxidation of the Fe center. However, it is clear from the neon matrix frequencies reported here for $FeCO^+$, FeCO, and $FeCO^-$ that the above $Fe^{I}$ carbonyl has in fact a slight negative local charge and the above $Fe^{II}$ carbonyl has only a slight positive charge (less than +1 as $FeCO^+$ absorbs at 2123 $cm^{-1}$ in solid neon).

A similar point is made for the $[Ru^{II}(NH_3)_5CO]Cl_2$ complex with a 1925 $cm^{-1}$ C−O frequency.[286] Tables 1 and 4 show that RuCO and $RuCO^+$ absorb at 1936 and 2103 $cm^{-1}$. Clearly the Ru center in this complex is effectively neutral owing to electron donation from the five ammonia ligands, based on the C−O probe frequency.[150]

Rhodium-supported catalyst systems are used for many important reactions including the hydrogenation of carbon monoxide and the hydroformylation of olefins. The chemisorption of CO on supported Rh produces a discrete $Rh(CO)_2$ species, and the oxidation state and charge on the metal center have been considered.[287−293] This rhodium dicarbonyl species is usually designated $Rh^{I}(CO)_2$ because of agreement with the C−O stretching modes of the $(OC)_2Rh(Cl)_2Rh(CO)_2$ molecule, where the oxidation state of rhodium is +1.[269−271] The rhodium dicarbonyl on alumina, silica, and zeolites is widely used as a catalyst system for activation of many molecules including $H_2$, $N_2$, and $CO_2$[294−298] through a coordinatively unsaturated $Rh^{I}(CO)$ center, which absorbs near 2096 $cm^{-1}$ on zeolites,[299] 2070 $cm^{-1}$ on silica,[297,300] and 2060 $cm^{-1}$ on alumina.[289,295] Furthermore, the activation of C−H bonds in alkanes by a transient CpRh(CO) species absorbing near 1985 $cm^{-1}$ in the gas phase readily occurs.[301,302] Finally, the rhodium−phosphine complexes, $Rh(CO)(Cl)(PR_3)_2$, exhibit carbonyl frequencies ranging from 2016 (R = OPh) to 1956 $cm^{-1}$ (R = Et).[303] What is the local charge on the Rh(CO) centers in these active species?

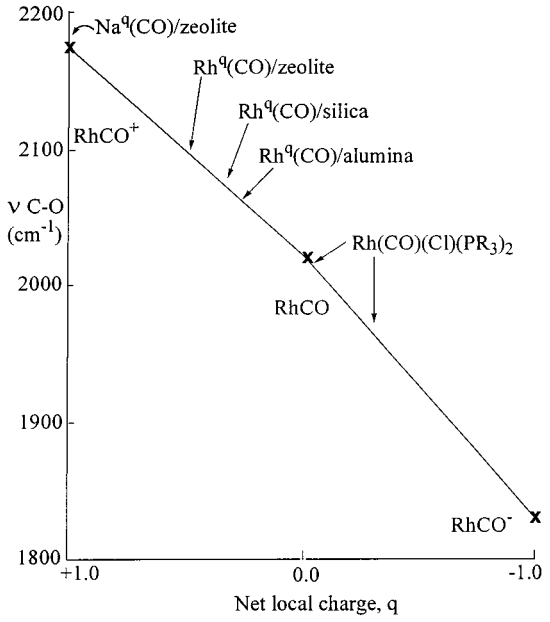


**Figure 17.** Plot of $RhCO^+$, RhCO, and $RhCO^-$ carbonyl stretching frequencies observed in solid neon vs net local charge on each RhCO species.

The carbonyl frequencies of $RhCO^+$ (2174 $cm^{-1}$), RhCO (2022 $cm^{-1}$), and $RhCO^-$ (1828 $cm^{-1}$) show a pronounced dependence on net charge. The calculated Mulliken charges show that most of the net charge resides on the metal. An added electron decreases the Rh−C bond length and increases the C−O bond length, thus decreasing the C−O frequency. Hence, the carbonyl stretching frequency is a measure of charge on the RhCO species, which approximates local charge on the Rh metal center. We offer the $RhCO^+$, RhCO, and $RhCO^-$ frequencies as a scale for estimating charge on Rh in the active catalyst media[163] and plot our observed monocarbonyl frequency vs net charge in Figure 17. The highest frequency for $Na^q(CO)$/zeolite[304] at 2178 $cm^{-1}$ almost matches our isolated $RhCO^+$ at 2174 $cm^{-1}$; so $q = +1.0$ is a reasonable description of local charge. The frequency for $Rh^q(CO)$/zeolite at 2096 $cm^{-1}$ is halfway between $RhCO^+$ and RhCO, and $q$ near +0.5 is

**Table 5. Scale Factors (observed neon matrix/calculated DFT/6-311+G*) for the First-Row Transition-Metal Monocarbonyl Cations, Neutrals, and Anions**

| | cations | | neutrals | | anions | |
|---|---|---|---|---|---|---|
| | B3LYP | BP86 | B3LYP | BP86 | B3LYP | BP86 |
| Sc | | 0.993 | | 1.005 | | 1.001 |
| Ti | 0.947 | 1.003 | 0.973 | 1.017 | 0.975 | 1.006 |
| V | | | 0.963 | 1.003 | 0.974 | 0.993 |
| Cr | 0.971 | 1.025 | 1.002 | 1.046 | 0.946 | 0.977 |
| Mn | | | 0.966 | 0.998 | 0.964 | 0.997 |
| Fe | 0.953 | 1.003 | 0.954 | 0.995 | 0.965 | 0.999 |
| Co | | 1.009 | | 0.997 | | 0.991 |
| Ni | 0.962 | 1.015 | 0.963 | 1.000 | 0.960 | 0.995 |
| Cu | 0.966 | 1.012 | 0.996 | 0.965 | 0.928 | 1.007 |

**Table 6. Observed and Calculated (BP86/6-311+G*) Frequencies ($cm^{-1}$) and Isotopic Frequency Ratios for $RhCO^+$, RhCO, and $RhCO^-$**

| | observed | | | calculated | | |
|---|---|---|---|---|---|---|
| | $^{12}C^{16}O$ | $^{12}C^{16}O/^{13}C^{16}O$ | $^{12}C^{16}O/^{12}C^{18}O$ | $^{12}C^{16}O$ | $^{12}C^{16}O/^{13}C^{16}O$ | $^{12}C^{16}O/^{12}C^{18}O$ |
| $RhCO^+$ | 2174.1 | 1.0231 | 1.0237 | 2129.4 | 1.0238 | 1.0232 |
| RhCO | 2022.5 | 1.0240 | 1.0218 | 2004.7 | 1.0250 | 1.0215 |
| $RhCO^-$ | 1828.6 | 1.0257 | 1.0195 | 1843.6 | 1.0268 | 1.0186 |

proposed. The $Rh^q(CO)$/alumina frequency at 2060 $cm^{-1}$ suggests $q$ near +0.3. The $Rh(CO)(Cl)(PR_3)_2$ complexes range from $q = 0$ to −0.3, and the CpRh-(CO) transient at 1985 $cm^{-1}$ indicates a slightly negative charge near −0.2. An analogous correlation has been made for the important rhodium dicarbonyl $Rh^q(CO)_2$ species.[163]

We conclude that the frequencies for CO attached to metal centers in complexes and supported catalyst systems can be used as a probe for the local charge at the metal center using neon matrix-isolated $MCO^+$, MCO, and $MCO^-$ frequencies as a scale. It appears that the local charge on these metal centers is not nearly as positive as assumed owing to partial neutralization by ligands or the support system.

## *VIII. Summary*

Figure 18 presents the C−O stretching vibrational frequencies of the first-row transition-metal monocarbonyl cations, neutrals, and anions in solid neon; similar diagrams[9a,10] have been reported for neutral MCO species in solid argon, but three of the early assignments have been changed by recent work[41,43,87] and one new assignment added.[92] The laser-ablation method produces mostly neutral atoms with a few percent cations and electrons for capture to make anions; in contrast, thermal evaporation gives only neutral species. Hence, the very recent neon matrix investigations in our laboratory provide carbonyl cations and anions for comparison to neutrals on a level playing field. Several trends are very interesting. First, for all metals, the C−O stretching frequencies follow the order cations > neutrals > anions with large diagnostic 100−200 $cm^{-1}$ separations, which is consistent with the magnitude of the metal d to CO $\pi^*$ donation. Second, for a given charge, there is a general increase in C−O stretching vibrational frequencies with increasing metal atomic number, which demonstrates the expected decrease in the metal to CO $\pi^*$ donation with increasing metal ionization potential. Some of the structure in this plot arises from the extra stability of the filled and half-filled d shell and from the electron pairing that occurs at the middle of the TM row; the plot resembles the "double-humped" graph found for the variation in properties across a row of transition metals.[10] For the anions, the variation with metal atom is the smallest since all of the metals can easily donate charge to the CO ligand. Third, for the early transition-metal Ti, V, and Cr families, the C−O stretching frequencies decrease when going down the family, but the reverse relationship is observed for the late transition-metal Fe, Co, and Ni families.

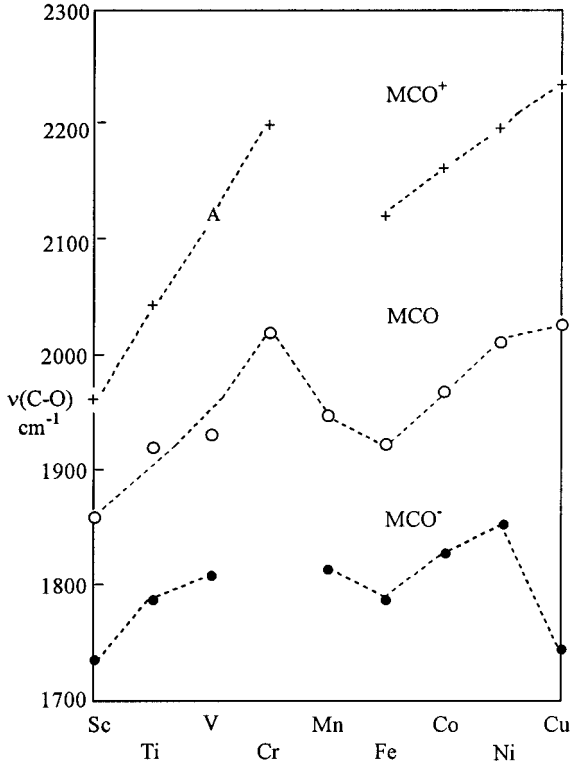


**Figure 18.** Plot of C−O stretching frequencies for first-row transition-metal monocarbonyl cations, neutrals, and anions in solid neon (A denotes argon matrix value).

In most of the present discussion, we have referred to neon matrix frequencies; however, the argon

matrix frequencies are complementary, and useful information can be obtained from comparison of the two matrix hosts.[82] In most cases, the neon-to-argon red shift for neutral carbonyls is from 11 to 26 $cm^{-1}$, but a few (CrCO) lie outside of this range. In the case of FeCO and $Fe(CO)_2$, it appears that neon and argon trap different low-lying electronic states.[42,43] In general, the carbonyl neutrals and anions have similar shifts but carbonyl cations have larger matrix shifts. For example, the $FeCO^+$ fundamental is at 2123.0 $cm^{-1}$ in neon and 2081.5 $cm^{-1}$ in argon, a 42.5 $cm^{-1}$ shift, which is larger than those found for $FeCO^-$ (11.7 $cm^{-1}$) and FeCO (11.7 $cm^{-1}$).[42,43]

It is unusual for different low-lying electronic states to be trapped in different matrices, but CUO provides another example. The linear singlet state (1047.3, 872.2 $cm^{-1}$) is trapped in solid neon,[217] and a calculated 1.2 kcal/mol higher triplet state is trapped in solid argon (852.5, 804.3 $cm^{-1}$) and stabilized by a specific interaction with argon.[305]

The bonding trends are well described by theoretical calculations of vibrational frequencies. Table 5 compares the scale factors (observed neon matrix/calculated) for the C−O stretching modes of the monocarbonyl cations, neutrals, and anions of the first-row transition metals observed in a neon matrix using the B3LYP and BP86 density functionals. Most of the calculated carbonyl harmonic stretching frequencies are within 1% of the experimental fundamentals at the BP86 level of theory, while calculations using the B3LYP functional give frequencies that are 3−4% higher as expected for these density functionals and calculations on saturated TM−carbonyls.[68,306−312] For second- and third-row carbonyls using the BP86 density functional and the LANL effective core potential in conjunction with the DZ basis set, the agreement between theory and experiment is just as good. For example, the 16 $M(CO)_{1-4}$ neutral and anion and 2 $MCO^+$ cation (M = Ru, Os) carbonyl frequencies are fit within 1.5%.[150] The 16 species (M = Rh, Ir) are fit within 1%, but the $Rh(CO)_{1-4}^+$ calculations are 2−3% too low and $Ir(CO)_{1-4}^+$ computations are 1−2% too low.[160]

In addition to predicting the vibrational frequencies, DFT can be used to calculate different isotopic frequencies, and isotopic frequency ratios can be computed as a measure of the normal vibrational mode in the molecule for an additional diagnostic. For diatomic CO, the $^{12}CO/^{13}CO$ ratio 1.0225 and $C^{16}O/C^{18}O$ ratio 1.0244 characterize a pure C−O stretching mode. In a series of molecules such as $RhCO^+$, RhCO, and $RhCO^-$, where the metal−CO bonding varies, the Rh−C, C−O vibrational interaction is different and the unique isotopic ratios for the carbonyl vibration are characteristic of that particular molecule.[160] Table 6 summarizes the isotopic ratios observed and calculated for the $RhCO^{+,0,-}$ species. Note that $RhCO^+$ exhibits slightly more carbon-13 and less oxygen-18 involvement in the C−O vibration than CO itself and that this trend increases to RhCO and to $RhCO^-$ as the Rh−C bond becomes shorter and stronger. Note also how closely the calculated and observed ratios both follow this trend. In a molecule with two C−O stretching modes, for example, bent $Ni(CO)_2$ exhibits a strong $b_2$ mode at 1978.9 $cm^{-1}$ and a weak $a_1$ mode at 2089.7 $cm^{-1}$ in solid neon,[175] and these two modes involve different C and O participations. The symmetric mode shows substantially more C (1.0242) and less O (1.0217) participation than does the antisymmetric mode with C (1.0228) and O (1.0238) involvement, based on the given isotopic frequency ratios, which are nicely matched by DFT calculations ($a_1$ 1.0244, 1.0224 and $b_2$ 1.0232, 1.0241, respectively).

These investigations of vibrational frequencies in unsaturated transition-metal carbonyl cations, neutrals, and anions clearly demonstrate the value of a close working relationship between experiment and theory to identify and characterize new molecular species.

## IX. Acknowledgments

The authors gratefully acknowledge the assistance of B. Liang and G. P. Kushto with microbalance measurements, helpful discussions and two figures from L. Manceron, and financial support from NSF Grant CHE 97-00116 and the NKBRSF of China.

## X. References and Notes

(1) Cotton, F. A.; Wilkinson, G.; Murillo, C. A.; Bochmann, M. *Advanced Inorganic Chemistry*, 6th ed.; Wiley: New York, 1999.
(2) Muetterties, E. L.; Stein, J. *Chem. Rev.* **1979**, *79*, 479.
(3) Tumas, W.; Gitlin, B.; Rosan, A. M.; Yardley, J. T. *J. Am. Chem. Soc.* **1982**, *104*, 55.
(4) Walch, S. P.; Goddard, W. A., III *J. Am. Chem. Soc.* **1976**, *98*, 7908.
(5) (a) Luckhart, C. M. *Fundamental Transition Metal Organometallic Chemistry*; Brooks-Cole: Monterey, CA, 1985. (b) Parshall, G. W.; Ittel, S. D. *Homogeneous Catalysis*; Wiley-Interscience: New York, 1992.
(6) (a) Falbe, J. *Carbon Monoxide in Organic Synthesis*; Springer-Verlag: Berlin, 1980. (b) Weber, L. *Angew. Chem., Int. Ed. Engl.* **1994**, *33*, 1077. (c) van Rooy, A.; de Bruijn, J. N. H.; Roobek, K. F.; Kramer, P. C. J.; Van Leeuwen, P. W. N. M. *J. Organomet. Chem.* **1996**, *507*, 69 and references cited.
(7) Schröder, D.; Bärsch, S.; Schwarz, H. *Chem. Phys. Lett.* **1999**, *309*, 407.
(8) Mond, L.; Langer, C.; Quincke, F. *J. Chem. Soc.* **1890**, 749.
(9) (a) Ozin, G. A.; Vander Voet *Prog. Inorg. Chem.* **1975**, *19*, 137. (b) Moskovits, M.; Ozin, G. A. Matrix Cryochemistry Using Transition Metal Atoms. *Cryochemistry*; Wiley: New York, 1976.
(10) Bach, S. B. H.; Taylor, C. A.; Van Zee, R. J.; Vala, M. T.; Weltner, W., Jr. *J. Am. Chem. Soc.* **1986**, *108*, 7104.
(11) Almond, M. J.; Downs, A. J. Spectroscopy of Matrix Isolated Species. *Advances in Spectroscopy*; Wiley: New York, 1989; Vol. 17.
(12) See, for example: Welch, J. A.; Peters, K. S.; Vaida, V. *J. Phys. Chem.* **1982**, *86*, 1941.
(13) (a) Weitz, W. *J. Phys. Chem.* **1987**, *91*, 3945. (b) Poliakoff, M.; Weitz, E. *Acc. Chem. Res.* **1987**, *20*, 408.
(14) Weitz, E. *J. Phys. Chem.* **1994**, *98*, 11256.
(15) Diefenbach, A.; Bickelhaupt, F. M.; Frenking, G. *J. Am. Chem. Soc.* **2000**, *122*, 6449.
(16) Frenking, G.; Fröhlich, N. *Chem. Rev.* **2000**, *100*, 717 and references therein.
(17) (a) Ellis, J. E. *Adv. Organomet. Chem.* **1990**, *31*, 1. (b) Willner, H.; Aubke, F. *Angew. Chem., Int. Ed. Engl.* **1997**, *36*, 2403.
(18) Van Zee, R. J.; Weltner, W., Jr. *J. Am. Chem. Soc.* **1989**, *111*, 4519.
(19) Kasai, P. H.; Jones, P. M. *J. Am. Chem. Soc.* **1985**, *107*, 6385.
(20) Kasai, P. H.; Jones, P. M. *J. Phys. Chem.* **1985**, *89*, 1147.
(21) Bondybey, V. E.; Smith, A. M.; Agreiter, J. *Chem. Rev.* **1996**, *96*, 2113.
(22) Burkholder, T. R.; Andrews, L. *J. Chem. Phys.* **1991**, *95*, 8697.
(23) Hassanzadeh, P.; Andrews, L. *J. Phys. Chem.* **1992**, *96*, 9177.
(24) Lu, C.; Lewis, O. *J. Appl. Phys.* **1972**, *43*, 4385. Moskovits, M.; Ozin, G. A. *Appl. Spectrosc.* **1972**, *26*, 481.
(25) Kundig, E. P.; McIntosh, D.; Moskovits, M.; Ozin, G. A. *J. Am. Chem. Soc.* **1973**, *95*, 7234 (Ni, Pd, Pt + CO).
(26) Joly, H. A.; Manceron, L. *Chem. Phys.* **1998**, *226*, 61 (Ni + CO).

(27) Zhou, M. F.; Andrews, L. *J. Chem. Phys.* **1999**, *110*, 2414, 6820 (M + $CO_2$).
(28) Zhou, M. F.; Andrews, L. *J. Phys. Chem. A* **1998**, *102*, 8251 (Ta + $O_2$).
(29) Zhou, M. F.; Andrews, L. *J. Am. Chem. Soc.* **1998**, *120*, 13230 (Sc + $CO_2$).
(30) Poliakoff, M.; Turner, J. J. *J. Chem. Soc., Dalton Trans.* **1973**, 1351.
(31) Poliakoff, M. *J. Chem. Soc., Dalton Trans.* **1974**, 210.
(32) Poliakoff, M.; Turner, J. J. *J. Chem. Soc., Dalton Trans.* **1974**, 2276.
(33) Perutz, R. N.; Turner, J. J. *J. Am. Chem. Soc.* **1975**, *97*, 4800.
(34) Burdett, J. K.; Graham, M. A.; Perutz, R. N.; Poliakoff, M.; Rest, A. J.; Turner, J. J.; Turner, R. F. *J. Am. Chem. Soc.* **1975**, *97*, 4085.
(35) Graham, M. A.; Poliakoff, M.; Turner, J. J. *J. Chem. Soc. A* **1971**, 2939.
(36) Engelking, P. C.; Lineberger, W. C. *J. Am. Chem. Soc.* **1979**, *101*, 5569.
(37) Stevens, A. E.; Feigerle, C. S.; Lineberger, W. C. *J. Am. Chem. Soc.* **1982**, *104*, 5026.
(38) Villalta, P. W.; Leopold, D. G. *J. Chem. Phys.* **1993**, *98*, 7730.
(39) Trushin, S. A.; Fuss, W.; Schmid, W. E.; Kompa, K. L. *J. Phys. Chem. A* **1998**, *102*, 4129.
(40) Trushin, S. A.; Fuss, W.; Schmid, W. E.; Kompa, K. L. *J. Phys. Chem. A* **2000**, *104*, 1997.
(41) Andrews, L.; Zhou, M. F.; Wang, X.; Bauschlicher, C. W., Jr. *J. Phys. Chem. A* **2000**, *104*, 8887 (Mn + CO).
(42) Zhou, M. F.; Chertihin, G. V.; Andrews, L. *J. Chem. Phys.* **1998**, *109*, 10893 (Fe + CO in Ar).
(43) Zhou, M. F.; Andrews, L. *J. Chem. Phys.* **1999**, *110*, 10370 (Fe + CO in Ne).
(44) See for example, Kelly, J. M.; Bent, D. V.; Hermann, H.; Schulte-Frohlinde, D.; Koerner Von Gustorf, E. *J. Organomet. Chem.* **1974**, *69*, 259.
(45) Duray, S. J.; Becher, D. M.; Grant, E. R. *Laser Chem.* **1988**, *9*, 63.
(46) Ryther, R. J.; Weitz, E. *J. Phys. Chem.* **1992**, *96*, 2561.
(47) Davies, P. D.; Martin, N. A.; Nunes, M. D.; Pope, D. A.; Russell, D. K. *Chem. Phys. Lett.* **1989**, *156*, 553.
(48) Tanaka, K.; Tachikawa, Y.; Tanaka, T. *Chem. Phys. Lett.* **1997**, *281*, 285.
(49) Tanaka, K.; Sakaguchi, K.; Tanaka, T. *J. Chem. Phys.* **1997**, *106*, 2118.
(50) Tanaka, K.; Sakaguchi, K.; Tanaka, T. *J. Chem. Phys.* **1999**, *111*, 3970.
(51) Hanlan, L. A.; Huber, H.; Ozin, G. A. *J. Am. Chem. Soc.* **1975**, *97*, 7054.
(52) Fairhurst, S. A.; Morton, J. R.; Preston, K. F. *J. Magn. Reson.* **1983**, *55*, 453.
(53) Howard, J. A.; Morton, J. R.; Preston, K. F. *Chem. Phys. Lett.* **1981**, *83*, 226.
(54) Van Zee, R. J.; Bach, S. B. H.; Weltner, W., Jr. *J. Phys. Chem.* **1986**, *90*, 583.
(55) Morton, J. R.; Preston, K. F. *Organometallics* **1984**, *3*, 1386.
(56) Fairhurst, S. A.; Morton, J. R.; Preston, K. F. *Chem. Phys. Lett.* **1984**, *104*, 112.
(57) Lionel, T.; Morton, J. R.; Preston, K. F. *J. Chem. Phys.* **1982**, *76*, 234.
(58) Bengali, A. A.; Casey, S. M.; Cheng, C. L.; Dick, J. P.; Fenn, P. T.; Villalta, P. W.; Leopold, D. G. *J. Am. Chem. Soc.* **1992**, *114*, 5257.
(59) Fenn, P. T.; Leopold, D. G. Unpublished data as quoted in ref 119.
(60) Klopcic, S. A.; Moravec, V. D.; Jarrold, C. C. *J. Chem. Phys.* **1999**, *110*, 8986.
(61) Dargel, T. K.; Hertwig, R. H.; Koch, W. *J. Chem. Phys.* **1998**, *108*, 3876.
(62) Becke, A. D. *J. Chem. Phys.* **1993**, *98*, 5648.
(63) Stephens, P. J.; Devlin, F. J.; Chabalowski, C. F.; Frisch, M. J. *J. Phys. Chem.* **1994**, *98*, 11623.
(64) Becke, A. D. *Phys. Rev. A* **1988**, *38*, 3098.
(65) Perdew, J. P. *Phys. Rev. B* **1986**, *33*, 8822 and erratum Perdew, J. P. *Phys. Rev. B* **1986**, *34*, 7406.
(66) Bauschlicher, C. W., Jr.; Ricca, A.; Partridge, H.; Langhoff, S. R. In *Recent Advances in Density Functional Theory, Part II*; Chong, D. P., Ed.; World Scientific Publishing: Singapore, 1997.
(67) Siegbahn, P. E. M. Electronic Structure Calculations for Molecules Containing Transition Metals. *Adv. Chem. Phys.* **1996**, XCIII.
(68) Bytheway, I.; Wong, M. H. *Chem. Phys. Lett.* **1998**, *282*, 219.
(69) Davidson, E. R.; Kunze, K. L.; Machado, F. B. C.; Chakravorty, S. J. *Acc. Chem. Res.* **1993**, *26*, 628.
(70) Bauschlicher, C. W., Jr.; Langhoff, S. R.; Partridge, H. In *Modern Electronic Structure Theory*; Yarkony, D. R., Ed.; World Scientific Publishing: Singapore, 1995.
(71) Li, J.; Schreckenbach, G.; Ziegler, T. *J. Am. Chem. Soc.* **1995**, *117*, 486.
(72) Büker, H. H.; Maître, P.; Onanessian, G. *J. Phys. Chem. A* **1997**, *101*, 3966.
(73) Goldman, A. S.; Krogh-Jespersen, K. *J. Am. Chem. Soc.* **1996**, *118*, 12159.
(74) Moore, C. E., *Atomic Energy Levels*; Natational Bureau of Standards: Washington, D.C., 1949.
(75) Bauschlicher, C. W., Jr.; Barnes, L. A. *Chem. Phys.* **1988**, *124*, 383.
(76) Bauschlicher, C. W., Jr.; Bagus, P. S.; Nelin, C. J.; Roos, B. O. *J. Chem. Phys.* **1986**, *85*, 354.
(77) Bauschlicher, C. W., Jr. *J. Chem. Phys.* **1986**, *84*, 260.
(78) Sodupe, M.; Bauschlicher, C. W., Jr.; Lee, T. J. *Chem. Phys. Lett.* **1992**, *189*, 266.
(79) Lupinetti, A. J.; Fan, S.; Frenking, G.; Strauss, S. H. *J. Phys. Chem. A* **1997**, *101*, 9551.
(80) Zhou, M. F.; Andrews, L. *J. Chem. Phys.* **1999**, *111*, 4548 (Cu + CO).
(81) Bauschlicher, C. W., Jr.; Bagus, P. S. *J. Chem. Phys.* **1984**, *81*, 5889.
(82) Jacox, M. E. *Chem. Phys.* **1994**, *189*, 149.
(83) Barnes, L. A.; Bauschlicher, C. W., Jr. *J. Chem. Phys.* **1989**, *91*, 314.
(84) Fournier, R. *J. Chem. Phys.* **1993**, *99*, 1801.
(85) Adamo, C.; Lelj, F. *J. Chem. Phys.* **1995**, *103*, 10605. Adamo, C.; Lelj, F. *Chem. Phys. Lett.* **1995**, *246*, 463.
(86) Darling, J. H.; Ogden, J. S. *J. Chem. Soc., Dalton Trans.* **1972**, 2496.
(87) Zhou, M. F.; Andrews, L. *J. Phys. Chem. A* **1999**, *103*, 2964 (Sc+CO).
(88) Frey, R. F.; Davidson, E. R. *J. Chem. Phys.* **1989**, *90*, 5541.
(89) Jeung, G. H. *J. Am. Chem. Soc.* **1992**, *114*, 3211.
(90) Jeung, G. H.; Haettel, S. *Int. J. Quantum Chem.* **1997**, *61*, 547.
(91) Busby, R.; Klotzbucher, W.; Ozin, G. A. *Inorg. Chem.* **1977**, *16*, 822. See also: Chertihin, G. V.; Andrews. L. *J. Am. Chem. Soc.* **1995**, *117*, 1595 (Ti + CO).
(92) Zhou, M. F.; Andrews, L. *J. Phys. Chem. A* **1999**, *103*, 5259 (Ti, V + CO).
(93) Zhou, M. F.; Andrews, L. *J. Am. Chem. Soc.* **2000**, *122*, 1531 (Zr, Hf + CO).
(94) Berthier, G.; Daoudi, A.; Suard, M. *J. Mol. Struct. (THEOCHEM)* **1988**, *179*, 407.
(95) Tan, H.; Liao, M.; Balasubramanian, K. *J. Phys. Chem. A* **1998**, *102*, 1602.
(96) Van Zee, R. J.; Li, S.; Weltner, W., Jr. *Chem. Phys. Lett.* **1994**, *217*, 381.
(97) Hanlan, L.; Huber, H.; Ozin, G. A. *Inorg.Chem.* **1976**, *15*, 2592.
(98) Matter, M.; Hamilton, W. *J. Mol. Struct. (THEOCHEM)* **1991**, *226*, 147.
(99) Ishikawa, Y.; Hackett, P. A.; Rayner, D. M. *J. Am. Chem. Soc.* **1987**, *109*, 6644.
(100) Ercoli, R.; Calderazzo, F.; Alberola, A. *J. Am. Chem. Soc.* **1960**, *82*, 2966.
(101) Haas, H.; Sheline, R. K. *J. Am. Chem. Soc.* **1966**, *88*, 3219.
(102) Pratt, D. W.; Myers, R. J. *J. Am. Chem. Soc.* **1967**, *89*, 6470.
(103) Pruett, R. L.; Wyman, J. E. *Chem. Ind. (London)* **1960**, 119.
(104) DeKock, R. L. *Inorg. Chem.* **1971**, *10*, 1205.
(105) Zhou, M. F.; Andrews, L. *J. Phys. Chem. A* **1999**, *103*, 7775 (Nb, Ta + CO).
(106) Tan, H.; Liao, M.; Dai, D.; Balasubramanian, K. *Chem. Phys. Lett.* **1998**, *297*, 173.
(107) Majumdar, D.; Balasubramanian, K. *Chem. Phys. Lett.* **1996**, *262*, 263.
(108) Church, S. P.; Hermann, H.; Grevels, F. W.; Shaffner, K. *J. Chem. Soc., Chem. Commun.* **1984**, 785.
(109) Seder, T. A.; Church, S. P.; Weitz, E. *J. Am. Chem. Soc.* **1986**, *108*, 4721.
(110) Fletcher, T. R.; Rosenfeld, R. N. *J. Am. Chem. Soc.* **1985**, *107*, 2203.
(111) Ganske, J. A.; Rosenfeld, R. N. *J. Phys. Chem.* **1989**, *93*, 1959.
(112) Ishikawa, Y.; Brown, C. E.; Hackett, P. A.; Rayner, D. M. *J. Phys. Chem.* **1990**, *94*, 2404.
(113) Ishikawa, Y.; Hackett, P. A.; Rayner, D. M. *J. Phys. Chem.* **1988**, *922*, 3863.
(114) Souter, P. F.; Andrews, L. *J. Am. Chem. Soc.* **1997**, *119*, 7350 (Cr + $CO_2$, CO).
(115) Zhou, M. F.; Andrews, L. Manuscript in preparation (Cr, Mo, W + CO).
(116) Fournier, R. *J. Chem. Phys.* **1993**, *98*, 8041.
(117) Tan, H.; Liao, M.; Dai, D.; Balasubramanian, K. *J. Phys. Chem. A* **1998**, *102*, 6801.
(118) Huber, H.; Kundig, E. P.; Ozin, G. A.; Poe, A. J. *J. Am. Chem. Soc.* **1975**, *97*, 308 (Mn+CO).
(119) Bauschlicher, C. W., Jr. *Chem. Phys. Lett.* **1996**, *249*, 244.
(120) Tan, H.; Liao, M.; Dai, D.; Balasubramanian, K. *J. Phys. Chem. A* **1999**, *103*, 3495.
(121) Church, S. P.; Poliakoff, M.; Timney, J. A.; Turner, J. J. *J. Am. Chem. Soc.* **1981**, *103*, 7515. Church, S. P.; Poliakoff, M.; Timney, J. A.; Turner, J. J. *Inorg. Chem.* **1983**, *22*, 3259.

(122) Seder, T. A.; Church, S. P.; Weitz, E. *J. Am. Chem. Soc.* **1986**, *108*, 7518.
(123) Symons, M. C. R.; Sweany, R. L. *Organometallics* **1982**, *1*, 834.
(124) Fairhurst, S. A.; Morton, J. R.; Perutz, R.; Preston, K. F. *Organometallics* **1984**, *3*, 1389.
(125) Junk, G. A.; Svec, H. J. *J. Chem. Soc. A* **1970**, 2102.
(126) Wrighton, M.; Bredesen, D. *J. Organomet. Chem.* **1973**, *50*, C35.
(127) Huber, H.; Kundig, E. P.; Ozin, G. A. *J. Am. Chem. Soc.* **1974**, *96*, 5585.
(128) Peden, C. H. F.; Parker, S. F.; Barrett, P. H.; Pearson, R. G. *J. Phys. Chem.* **1983**, *87*, 2329 (Fe + CO).
(129) Sweany, R. L. *J. Am. Chem. Soc.* **1981**, *103*, 2410.
(130) Bursten, B. E.; Freier, D. G.; Fenske, R. F. *Inorg. Chem.* **1980**, *19*, 1810.
(131) Bagus, P. S.; Nelin, C. J.; Bauschlicher, C. W., Jr. *J. Vac. Sci. Technol. A* **1984**, *2*, 905.
(132) Guenzburger, D.; Saitovitch, E. M. B.; DePaoli, M. A.; Manela, H. *J. Chem. Phys.* **1984**, *80*, 735.
(133) Bauschlicher, C. W., Jr.; Petterson, L. G. M.; Siegbahn, P. E. M. *J. Chem. Phys.* **1987**, *87*, 2129.
(134) Barbier, C.; Berthier, G.; Daoudi, A.; Suard, M. *Theor. Chim. Acta* **1988**, *73*, 419.
(135) Braga, M.; Almeida, A. L.; Taft, C. A.; Hammond, B. L.; Lester, W. A., Jr. *J. Chem. Phys.* **1988**, *89*, 4867.
(136) Daoudi, A.; Suard, M.; Gerthier, G. *J. Mol. Struct. (THEOCHEM)* **1990**, *210*, 139.
(137) Barnes, L. A.; Rosi, M.; Bauschlicher, C. W., Jr. *J. Chem. Phys.* **1991**, *94*, 2031.
(138) Castro, M.; Salahub, D. R.; Fournier, R. *J. Chem. Phys.* **1994**, *100*, 8233.
(139) Ricca, A.; Bauschlicher, C. W., Jr.; Rosi, M. *J. Phys. Chem.* **1994**, *98*, 9498.
(140) Ricca, A.; Bauschlicher, C. W., Jr.; Rosi, M. *J. Phys. Chem.* **1994**, *98*, 12899.
(141) Persson, B. J.; Roos, B. O.; Pierloot, K. *J. Chem. Phys.* **1994**, *101*, 6810.
(142) Bauschlicher, C. W., Jr. *Chem. Phys. Lett.* **1995**, *246*, 40.
(143) Sosa, R. M.; Gardiol, P. *Int. J. Quantum Chem., Quantum Chem. Symp.* **1996**, *30*, 217.
(144) Xu, X.; Lü, X.; Wang, N.; Zhang, Q.; Ehara, M.; Nakatsuji, H. *Int. J. Quantum Chem.* **1999**, *72*, 221.
(145) Ricca, A., Bauschlicher, C. W., Jr. *Theor. Chem. Acc.*, in press.
(146) Noro, T.; Sekiya, M.; Koga, T.; Matsuyama, H. *Theor. Chem. Acc.* **2000**, *104*, 146.
(147) Ricca, A.; Bauschlicher, C. W., Jr. *Theor. Chim. Acta* **1995**, *92*, 123.
(148) Bogdan, P. L.; Weitz, E. *J. Am. Chem. Soc.* **1989**, *111*, 3163.
(149) Bogdan, P. L.; Weitz, E.; *J. Am. Chem. Soc.* **1990**, *112*, 639.
(150) Zhou, M. F.; Andrews, L. *J. Phys. Chem. A* **1999**, *103*, 6956 (Ru, Os + CO).
(151) Tan, H.; Liao, M. Z.; Balasubramanian, K. *Chem. Phys. Lett.* **1998**, *284*, 1.
(152) Keller, H. J.; Wawersik, B. W. *Z. Naturforsch.* **1965**, *206*, 938.
(153) Bidinosti, D. R.; McIntyre, N. S. *Chem. Commun.* **1967**, 1.
(154) Rest, A. J.; Crichton, O.; Poliakoff, M.; Turner, J. J. *J. Chem. Soc., Dalton Trans.* **1973**, 1321.
(155) Hanlan, A. J. L.; Huber, H.; Kundig, E. P.; McGarvey, B. R.; Ozin, G. A. *J. Am. Chem. Soc.* **1975**, *97*, 7054 (Co + CO).
(156) Kasai, P. H.; Jones, P. M. *J. Am. Chem. Soc.* **1985**, *107*, 813.
(157) Chenier, J. H. B.; Hampson, C. A.; Howard, J. A.; Mile, B. *J. Phys. Chem.* **1989**, *93*, 114.
(158) Ryeng, H.; Gropen, O.; Swang, O. *J. Phys. Chem. A* **1997**, *101*, 8956.
(159) Zhou, M. F.; Andrews, L. *J. Phys. Chem. A* **1998**, *102*, 10250 (Co + CO in Ar).
(160) Zhou, M. F.; Andrews, L. *J. Phys. Chem. A* **1999**, *103*, 7763 (Co, Rh, Ir + CO in Ne).
(161) Ozin, G. A.; Hanlan, A. J. L. *Inorg. Chem.* **1979**, *18*, 2091 (Rh, Ir + CO in Ar).
(162) see also Hanlan, A. J. L.; Ozin, G. A. *J. Organomet. Chem.* **1979**, *179*, 57.
(163) Zhou, M. F.; Andrews, L. *J. Am. Chem. Soc.* **1999,** *121*, 9171 (Rh + CO in Ne).
(164) Mains, G. J.; White, J. M.; *J. Phys. Chem.* **1991**, *95*, 112.
(165) Papai, I.; Goursot, A.; St. Amant, A.; Salahub, D. R. *Theor. Chim. Acta* **1992**, *84*, 217.
(166) Dai, D.; Balasubramanian, K. *J. Chem. Phys.* **1994**, *101*, 2148.
(167) McKee, M. L.; Worley, S. D. *J. Phys. Chem.* **1988**, *92*, 3699.
(168) McKee, M. L.; Worley, S. D. *J. Phys. Chem. A* **1997**, *101*, 5600.
(169) Chenier, J. H. B.; Histed, M.; Howard, J. A.; Joly, H. A.; Morris, H.; Mile, B. *Inorg. Chem.* **1989**, *28*, 4114.
(170) Darling, J. H.; Ogden, J. S. *J. Chem. Soc., Dalton Trans.* **1973**, 1079 (Pd + CO).
(171) Zhou, M. F.; Andrews, L. *J. Am. Chem. Soc.* **1998**, *120*, 11499 (Ni + CO in Ar).
(172) Manceron, L.; Alikhani, M. E. *Chem. Phys.* **1999**, *244*, 215 (Ni + CO in Ar).
(173) Tremblay, B.; Manceron, L. *Chem. Phys.* **1999**, *250*, 187 (Pd + CO in Ar).
(174) Manceron, L.; Tremblay, B.; Alikhani, M. E. *J. Phys. Chem. A.* **2000**, *104*, 3750 (Pt + CO in Ar).
(175) Liang, B. Y.; Zhou, M. F.; Andrews, L. *J. Phys. Chem. A* **2000**, *104*, 3905 (Ni, Pd, Pt + CO in Ne).
(176) Rives, A. B.; Weinhold, F. *Int. J. Quantum Chem., Quantum Chem. Symp.* **1980**, *14*, 201.
(177) Rives, A. B.; Fenske, R. F. *J. Chem. Phys.* **1981**, *75*, 1293.
(178) Dunlap, B. I.; Yu, H. L.; Antoniewicz, P. R. *Phys. Rev. A* **1982**, *25*, 7.
(179) Basch, H.; Cohen, D. *J. Am. Chem. Soc.* **1983**, *105*, 3856.
(180) Rohlfing, C. M.; Hay, P. J. *J. Chem. Phys.* **1985**, *83*, 4641
(181) Carsky, P.; Dedieu, A. *Chem. Phys.* **1986**, *103*, 265.
(182) Bauschlicher, C. W., Jr.; Barnes, L. A.; Langhoff, S. R. *Chem. Phys. Lett.* **1988**, *151*, 391.
(183) Blomberg, M.; Brandemark, U.; Johansson, J.; Siegbahn, P.; Wennerberg, J. *J. Chem. Phys.* **1988**, *88*, 4324.
(184) Blomberg, M.; Siegbahn, P.; Lee, T. J.; Rendell, A. P.; Rice, J. E. *J. Chem. Phys.* **1991**, *95*, 5898.
(185) Smith, G. W.; Carter, E. A. *J. Phys. Chem.* **1991**, *95*, 2327.
(186) Roszak, S.; Balasubramanian, K. *J. Phys. Chem.* **1993**, *97*, 11238.
(187) Barone, V. *Chem. Phys. Lett.* **1995**, *233*, 129.
(188) Papai, I.; Goursot, A.; St.-Amant, A.; Salahub, D. R. *Thero. Chim. Acta* **1992**, *84*, 217.
(189) Chung, S.-C.; Krüger, S.; Pacchioni, G.; Rösch, N. *J. Chem. Phys.* **1995**, *102*, 3695.
(190) Ogden, J. S. *J. Chem. Soc., Chem. Commun.* **1971**, 978.
(191) Huber, H.; Kundig, E. P.; Moskovits, M.; Ozin, G. A. *J. Am. Chem. Soc.* **1975**, *97*, 2097 (Cu + CO).
(192) McIntosh, D.; Ozin, G. A. *J. Am. Chem. Soc.* **1976**, *98*, 3167.
(193) McIntosh, D.; Ozin, G. A. *Inorg. Chem.* **1977**, *16*, 51.
(194) Howard, J. A.; Mile, B.; Morton, J. R.; Preston, K. F.; Sutcliffe, R. *Chem. Phys. Lett.* **1985**, *117*, 115.
(195) Howard, J. A.; Mile, B.; Morton, J. R.; Preston, K. F.; Sutcliffe, R. *J. Phys. Chem.* **1986**, *90*, 1033.
(196) Tremblay, B.; Manceron, L. *Chem. Phys.* **1999**, *242*, 235 (Cu + CO).
(197) Liang, B.; Andrews, L. *J. Phys. Chem. A.* **2000**, *104*, 9156 (Ag, Au + CO).
(198) Marian, C. M. *Chem. Phys. Lett.* **1993**, *215*, 582.
(199) Post, D.; Baerends, E. J. *J.Chem. Phys.* **1983**, *78*, 5663.
(200) Ha, T.; Nguyen, M. T. *J. Mol. Struct. (THEOCHEM)* **1984**, *109*, 331.
(201) Bagus, P. S.; Hermann, K.; Bauschlicher, C. W., Jr. *J. Chem. Phys.* **1984**, *81*, 1966.
(202) Bagus, P. S.; Bauschlicher, C. W., Jr.; Nelin, C. J.; Laskowski, B. C.; Seel, M. *J. Chem. Phys.* **1984**, *81*, 3594.
(203) Bagus, P. S.; Muller, W. *Chem. Phys. Lett.* **1985**, *115*, 540.
(204) Bauschlicher, C. W., Jr. *Chem. Phys. Lett.* **1985**, *115*, 535.
(205) Avouris, P.; Bagus, P. S.; Nelin, C. J. *J. Electron Spectrosc. Relat. Phenom.* **1986**, *38*, 269.
(206) Hermann, K.; Bagus, P. S.; Nelin, C. J. *Phys. Rev. B* **1987**, *35*, 9467.
(207) Antonsson, H.; Nilsson, A.; Martensson, N.; Panas, I.; Siegbahn, P. E. M. *J. Electron Spectrosc. Relat. Phenom.* **1990**, *53*, 601.
(208) Nygren, M. A.; Siegbahn, P. E. M.; Jin, C.; Guo, T.; Smalley, R. E. *J. Chem. Phys.* **1991**, *95*, 6181.
(209) Pavao, A. C.; Braga, M.; Taft, C. A.; Hammond, B. L.; Lester, W. A. *Phys. Rev. B* **1991**, *43*, 696.
(210) Nygren, M. A.; Siegbahn, P. E. M. *J. Phys. Chem.* **1992**, *96*, 7579.
(211) Hirai, K.; Kosugi, N. *Can. J. Chem.* **1992**, *70*, 301.
(212) Schwerdtfeger, P.; Bowmaker, G. A. *J. Chem. Phys.* **1994**, *100*, 4487.
(213) Bauschlicher, C. W., Jr. *J. Chem. Phys.* **1994**, *100*, 1215. *Chem. Phys. Lett.* **1994**, *229*, 577.
(214) Barone, V. *J. Phys. Chem.* **1995**, *99*, 11659.
(215) Blitz, M. A.; Mitchell, S. A.; Hackett, P. A. *J. Phys. Chem.* **1991**, *95*, 8719.
(216) Slater, J. L.; Sheline, R. K.; Lin, K. C.; Weltner, W., Jr. *J. Chem. Phys.* **1971**, *55*, 5129.
(217) Zhou, M. F.; Andrews, L.; Li, J.; Bursten, B. E. *J. Am. Chem. Soc.* **1999**, *121*, 9712 (U+CO).
(218) Zhou, M. F.; Andrews, L.; Li, J.; Bursten, B. E. *J. Am. Chem. Soc.* **1999**, *121*, 12188 (Th+CO).
(219) Li, J.; Bursten, B. E.; Zhou, M. F.; Andrews, L. *J. Am. Chem. Soc.*, in press.
(220) Devilliers, C.; Ramsay, D. A. *Can. J. Phys.* **1971**, *49*, 2839.
(221) Rayner, D. M.; Nazran, A. S.; Drouin, M.; Hackett, P. A. *J. Phys. Chem.* **1986**, *90*, 2882.
(222) Seder, T. A.; Ouderkirk, A. J.; Weitz, E. *J. Chem. Phys.* **1986**, *85*, 1977.
(223) Zhou, M. F.; Andrews, L. *J. Phys. Chem. A* **2000**, *104*, 3915 (Fe + NO).
(224) Wang, X.; Zhou, M. F.; Andrews, L. *J. Phys. Chem. A* **2000**, *104*, 10104 (Fe + CO, NO).
(225) Edgell, W. F.; Lyford, J.; Barbetta, A.; Jose, C. I. *J. Am. Chem. Soc.* **1971**, *93*, 6403.
(226) Braterman, P. S. *Metal Carbonyl Spectra*; Academic Press: London, 1975.

(227) Sunderlin, L. S.; Wang, D.; Squires, R. R. *J. Am. Chem. Soc.* **1992**, *114*, 2788.
(228) Sunderlin, L. S.; Wang, D.; Squires, R. R. *J. Am. Chem. Soc.* **1993**, *115*, 12060.
(229) Breeze, P. A.; Turner, J. J. *J. Organomet. Chem.* **1972**, *44*, C7.
(230) Breeze, P. A.; Burdett, J. K.; Turner, J. J. *Inorg. Chem.* **1981**, *20*, 3369.
(231) Elian, M.; Hoffmann, R. *Inorg. Chem.* **1975,** *14*, 1058.
(232) Burdett, J. K. *J. Chem. Soc., Faraday Trans,* **1974**, *70*, 1599.
(233) VanOrden, S. L.; Pope, R. M.; Buckner, S. W. *Organometallics* **1991**, *10*, 1089.
(234) McDonald, R. N.; Jones, M. T.; Chowdhury, A. K. *J. Am. Chem. Soc.* **1992**, *114*, 71.
(235) McDonald, R. N.; Schmidt, M. A. *Int. J. Mass Spectrom. Ion Processes* **1992**, *117*, 171.
(236) McDonald, R. N.; Jones, M. T.; Chowdhury, A. K. *Organometallics* **1992**, *11*, 392.
(237) Ricca, A.; Bauschlicher, C. W., Jr. *J. Phys. Chem.* **1995**, *99*, 5922.
(238) McDonald, R. N.; Bianchina, E. J. *Organometallics* **1990**, *10*, 1274.
(239) Richardson, J. H.; Stephanson, L. M.; Braumann, J. I. *J. Am. Chem. Soc.* **1974**, *96*, 3671.
(240) Rynard, C. M.; Braumann, J. I. *Inorg. Chem.* **1980**, *19*, 3544.
(241) Chini, P.; Martinengo, S. *Inorg. Chim. Acta* **1969**, *3*, 21.
(242) Malatesta, L.; Caglio, G.; Angoletta, M. *Chem. Commun.* **1970**, 532.
(243) Simoes, J. A. M.; Beauchamp, J. L. *Chem. Rev.* **1990**, *90*, 629.
(244) Dunbar, R. C.; Hutchinson, B. B. *J. Am. Chem. Soc.* **1974**, *96*, 3816.
(245) Wenthold, P. G.; Gunion, R. F.; Lineberger, W. C. *J. Chem. Phys.* **1997**, *106*, 9961.
(246) Zhou, M. F.; Andrews, L. *J. Chem. Phys.* **1999**, *111*, 4230.
(247) Souma, Y.; Sano, H. *J. Org. Chem.* **1973**, *38*, 2016. Xu, Q.; Imamura, Y.; Fujiwara, M.; Souma, Y. *J. Org. Chem.* **1997**, *62*, 1594. Xu, Q.; Nakatani, H.; Souma, Y. *J. Org. Chem.* **2000**, *65*, 1540.
(248) Halle, L. F.; Crowe, W. E.; Armentrout, P. B.; Beauchamp, J. L. *Organometallics* **1984**, *3*, 1694.
(249) Schultz, R. H.; Crellin, K. C.; Armentrout, P. B. *J. Am. Chem. Soc.* **1991**, *113*, 8590.
(250) Khan, F. A.; Clemmer, D. E.; Schultz, R. H.; Armentrout, P. B. *J. Chem. Phys.* **1993**, *97*, 7978.
(251) Khan, F. A.; Steele, D. L.; Armentrout, P. B. *J. Phys. Chem.* **1995**, *99*, 7819.
(252) Sievers, M.; Armentrout, P. B. *J. Phys. Chem.* **1995**, *99*, 8135.
(253) Meyer, F.; Chen, Y. M.; Armentrout, P. B. *J. Am. Chem. Soc.* **1995**, *117*, 4071.
(254) Andrews, L. *Annu. Rev. Phys. Chem.* **1979**, *30*, 79.
(255) Bondybey, V. E.; Miller, T. A. *Molecular Ions: Spectroscopy, Structure and Chemistry*; North-Holland: Amsterdam, 1983.
(256) Knight, L. B., Jr. *Acc. Chem. Res.* **1986**, *19*, 313.
(257) Jacox, M. E.; Thompson, W. E. *Res. Chem. Intermed.* **1989**, *12*, 33.
(258) Desjardins, C. D.; Edwards, D. E.; Passmore, J. *Can. J. Chem.* **1979**, *57*, 2714.
(259) Strauss, S. H. *J. Chem. Soc., Dalton Trans.* **2000**, 1.
(260) Scott, A. F.; Wilkening, L. F.; Rubin, B. *Inorg. Chem.* **1969**, *8*, 2533.
(261) Souma, Y.; Iyoda, J.; Sano, H. *Inorg. Chem.* **1976**, *15*, 968.
(262) Rack, J. J.; Webb, J. D.; Strauss, S. H. *Inorg. Chem.* **1996**, *35*, 277. Ivanova, S. M.; Ivanov, S. V.; Miller, S. M.; Anderson, O. P.; Solntev, K. A.; Strauss, S. H. *Inorg. Chem.* **1999**, *38*, 3756.
(263) Hurlburt, P. K.; Anderson, O. P.; Strauss, S. H. *J. Am. Chem. Soc.* **1991**, *113*, 6277.
(264) Hurlburt, P. K.; Rack, J. J.; Dec, S. F.; Anderson, O. P.; Strauss, S. H. *J. Am. Chem. Soc.* **1993**, *115*, 373.
(265) Hurlburt, P. K.; Rack, J. J.; Luck, J. S.; Dec, S. F.; Webb, J. D.; Anderson, O. P.; Strauss, S. H. *J. Am. Chem. Soc.* **1994**, *116*, 10003.
(266) Rack, J. J.; Moasser, B.; Gargulak, J. D.; Gladfelter, W. L.; Hochheimer, H. D.; Strauss, S. H. *J. Chem. Soc., Chem. Commun.* **1994**, 685.
(267) Willner, H.; Schaebs, J.; Hwang, G.; Mistry, F.; Jones, R.; Trotter, J.; Aubke, F. *J. Am. Chem. Soc.* **1992**, *114*, 8972.
(268) Willner, H.; Aubke, F. *Inorg. Chem.* **1990**, *29*, 2195.
(269) Hwang, G.; Wang, C.; Aubke, F.; Willner, H.; Bodenbinder, M. *Can. J. Chem.* **1993**, *71*, 1532.
(270) Willner, H.; Bodenbinder, M.; Wang, C.; Aubke, F. *J. Chem. Soc., Chem. Commun.* **1994**, 1189.
(271) Wang, C.; Bley, B.; Balzer-Jollenbeck, G.; Lewis, A. R.; Sui, S. C.; Willner, H.; Aubke, F. *J. Chem. Soc., Chem. Commun.* **1995**, 2071.
(272) Bley, B.; Willner, H.; Aubke, F. *Inorg. Chem.* **1997**, *36*, 158.
(273) Bach, C.; Willner, H.; Wang, S.; Rettig, S. J.; Trotter, J.; Aubke, F. *Angew. Chem., Int. Ed. Engl.* **1996**, *35*, 1974.
(274) Bodenbinder, M.; Balzer-Jollenbeck, G.; Willner, H.; Batchelor, R. J.; Einstein, F. W. B.; Wang, C.; Aubke, F. *Inorg. Chem.* **1996**, *35*, 82.
(275) Van Zee, R. J.; Weltner, W., Jr. *Chem. Phys. Lett.* **1997**, *266*, 403. Knight, L. B., Jr.; Cobranchi, S. T.; Herlong, J.; Kirk, T.; Balasubramanian, K.; Das, K. K. *J. Chem. Phys.* **1990**, *92*, 2721.
(276) Barnes, L. A.; Rosi, M.; Bauschlicher, C. W., Jr. *J. Chem. Phys.* **1990**, *93*, 609.
(277) Allison, J.; Mavridis, J.; Harrison, J. F. *Polyhedron* **1988**, *7*, 1559.
(278) Mavridis, A.; Harrison, J. F.; Allison, J. *J. Am. Chem. Soc.* **1989**, *111*, 2482.
(279) Merchan, M.; Nebot-Gil, I.; Gonzalez-Luque, R.; Orti, E. *J. Chem. Phys.* **1987**, *87*, 1690.
(280) Veldkamp, A.; Frenking, G. *Organometallics* **1993**, *12*, 4613.
(281) Ehlers, A. W.; Ruiz-Morales, Y.; Baerends, E. J.; Ziegler, T. *Inorg. Chem.* **1997**, *36*, 5031.
(282) for trends in bond energies see Lupinetti, A. J.; Jonas, V.; Thiel, W.; Strauss, S. H.; Frenking, G. *Chem. Eur. J.* **1999**, *5*, 2573.
(283) Lupinetti, A. J.; Havighurst, M. D.; Miller, S. M.; Anderson, O. P.; Strauss, S. H. *J. Am. Chem. Soc.* **1999**, *121*, 11920.
(284) Lindblad, T.; Rebenstorf, B. *Acta Chem. Scand.* **1991**, *45*, 342.
(285) Lai, C.-H.; Lee, W.-Z.; Miller, M. L.; Reibenspies, J. H.; Darensbourg, D. J.; Darensbourg, M. Y. *J. Am. Chem. Soc.* **1998**, *120*, 10103.
(286) Bee, M. W.; Kettle, F. A.; Powell, D. B. *Spectrochim. Acta* **1974**, *30A*, 585.
(287) Garland, C. W.; Lord, R. C.; Troiano, P. F. *J. Phys. Chem.* **1965**, *69*, 1188.
(288) Yates, J. T., Jr.; Duncan, T. M.; Worley, S. D.; Vaughn, R. W. *J. Chem. Phys.* **1979**, *70*, 1219.
(289) Cavanagh, R. R.; Yates, J. T., Jr. *J. Chem. Phys.* **1981**, *74*, 4150.
(290) Rice, C. A.; Worley, S. D.; Curtis, C. W.; Guin, J. A.; Tanner, A. R. *J. Chem. Phys.* **1981**, *74*, 6487.
(291) Yates, J. T., Jr.; Kolasinski, K. *J. Chem. Phys.* **1983**, *79*, 1026. Paul, D. P.; Ballinger, T. H.; Yates, J. T., Jr. *J. Phys. Chem.* **1990**, *94*, 4617.
(292) van't Blik, H. F. J.; van Zon, J. B. A. D.; Huizinga, T.; Vis, J. C.; Koningsberger, D. C.; Prins, R. *J. Am. Chem. Soc.* **1985**, *107*, 3139.
(293) Wovchko, E. A.; Zubkov, T. S.; Yates, J. T., Jr. *J. Phys. Chem. B* **1998**, *102*, 10535. Zubkov, T. S.; Wovchko, E. A.; Yates, J. T., Jr. *J. Phys. Chem. B* **1999**, *103*, 5300.
(294) Wovchko, E. A.; Yates, J. T., Jr. *J. Am. Chem. Soc.* **1995**, *117*, 12577.
(295) Wovchko, E. A.; Yates, J. T., Jr. *J. Am. Chem. Soc.* **1996**, *118*, 10250.
(296) Wovchko, E. A.; Yates, J. T., Jr. *J. Am. Chem. Soc.* **1998**, *120*, 7544.
(297) Fisher, I. A.; Bell, A. T. *J. Catalysis* **1996**, *162*, 54.
(298) Ballinger, T. H.; Yates, J. T., Jr. *J. Am. Chem. Soc.* **1992**, *114*, 10074.
(299) Miessner, H. *J. Am. Chem. Soc.* **1994**, *116*, 11522.
(300) Anderson, J. A.; Rochester, C. H.; Wang, Z. J. *J. Mol. Catal. A* **1999**, *139*, 285 and references therein.
(301) Wasserman, E. P.; Moore, C. B.; Bergman, R. G. *Science* **1992**, *255*, 315.
(302) Bengali, A. A.; Schultz, R. H.; Moore, C. B.; Bergman, R. G. *J. Am. Chem. Soc.* **1994**, *116*, 9585.
(303) Serron, S.; Nolan, S. P.; Moloy, K. G. *Organometallics* **1996**, *15*, 4301 and references therein.
(304) Zecchina, A.; Areán, C. O. *Chem. Soc. Rev.* **1996**, *25*, 187.
(305) Andrews, L.; Liang, B.; Li, J.; Bursten, B. E. *Angew. Chem., Int. Ed.* **2000**, *39*, 4565.
(306) Delley, B.; Wrinn, M.; Luthi, H. P. *J. Chem. Phys.* **1994**, *100*, 5785.
(307) Jonas, V.; Thiel, W. *J. Chem. Phys.* **1995**, *102*, 8474.
(308) Berces, A.; Ziegler, T. *J. Phys. Chem.* **1995**, *99*, 11417.
(309) Scott, A. P.; Radom, L. *J. Phys. Chem.* **1996**, *100*, 16502.
(310) Jang, J. H.; Lee, J. G.; Lee, H.; Xie, Y.; Schaefer, H. F., III *J. Phys. Chem. A* **1998**, *102*, 5298.
(311) Ehleurs, A. W.; Baerends, E. J.; Bickelhaupt, F. M.; Radius, U. *Chem. Eur. J.* **1998**, *4*, 210.
(312) Hyla-Krypsin, I.; Koch, J.; Glater, R.; Klettke, T.; Walther, D. *Organometallics* **1998**, *17*, 4724.
(313) Hansford, G. M.; Davies, P. B. *J. Mol. Spectrosc.* **1994**, *168*, 540. Hansford, G. M.; Davies, P. B. *J. Chem. Phys.* **1996**, *104*, 8292.
(314) Asselin, P.; Soulard, P.; Tarrago, G.; Lacome, N.; Manceron, L. *J. Chem. Phys.* **1996**, *104*, 4427.

CR990102B